Divergent Roles of PAX2 in the Etiology and Progression of Ovarian Cancer

Ensaf M. Alhujaily

Thesis submitted to the Faculty of Graduate and Postdoctoral Studies in partial fulfillment of the requirements for a doctoral degree in Cellular and Molecular Medicine.

Department of Cellular and Molecular Medicine
Faculty of Medicine
University of Ottawa

DEDICATION

To my parents and my siblings for their love and support.

ABSTRACT

PAX2 is a transcription factor that is essential for development. Aberrant expression of PAX2 in adult tissues is associated with carcinogenesis and experimental evidence shows that PAX2 generally exhibits oncogenic properties. Although PAX2 is not expressed in normal ovaries, it is highly expressed in low malignant potential and low-grade epithelial ovarian tumors, suggesting that PAX2 induction in ovarian surface epithelium (OSE) may contribute to transformation. Herein, we provide evidence that expression of PAX2 in normal murine OSE (mOSE) cells enhances their proliferation and survival and, when combined with loss of P53, induces tumorigenicity.

In addition, OSE cells are known to gain an epithelial phenotype and express epithelial markers prior to their transformation. This study revealed that PAX2 induction in mOSE cells results in an enhanced epithelial phenotype associated with reduction of the epithelial-mesenchymal transition markers, SMA-α and COX-2. Furthermore, PAX2 inhibits the mesenchymal phenotype induced by TGF-β and reverses the TGF-β-mediated induction of both SMA-α and COX-2, in mOSE cells.

Toward tumor progression, we found that when PAX2 was expressed in murine ovarian cancer cells, it enhanced or inhibited their aggressiveness, depending on the model system. In OSE cells transformed by K-RAS and MYC, PAX2 inhibited P53 accumulation and increased the level of pERK1/2 and COX-2. In addition, PAX2 inhibited apoptotic induction in these tumors, while increasing angiogenesis, both of which are enhancers of tumor aggressiveness. However, in a murine model of high-grade serous ovarian cancer, PAX2 expression reduced tumor mass and improved animal survival, likely via reduced proliferation and metastasis. Mechanistic studies showed that PAX2 increased *Htra1* and

decreased COX-2 in those tumors. Both HTRA1 and COX-2 are novel downstrream targets for PAX2 that are identified in the current study. These results suggest that PAX2 may not act as a classical oncogene or tumor suppressor in ovarian cancer; rather, it modulates tumorigenesis differently, depending on the tumor context. The observation that PAX2 targets distinct biological and molecular pathways might help to guide future studies to different therapeutic targets in low-grade vs. high-grade cancers.

TABLE OF CONTENTS

LIST OF TABLES

LIST OF FIGURES

LIST OF ABBREVIATIONS

AdCre: Ad5CMVCre recombinant adenovirus

AdGFP: Ad5CMVeGFP recombinant adenovirus

AKT: AKT8 virus oncogene cellular homolog

ANG II: angiotensin II

ANOVA: analysis of variance

ARID1A: AT rich interactive domain 1A

AT1R: ANG II type 1 receptor

AT2R: ANG II type 2 receptor

B-RAF: v-Raf murine sarcoma viral oncogene homolog B1

BAD: BCL-2 associated agonist of cell death

bp: base pair

Brca1: breast cancer 1, early onset

ChIP: chromatin immunoprecipitation

c-myc: avian myelocytomatosis virus oncogene cellular homolog

CA125: cell surface antigen-125

Caspase: cysteine proteases with aspartate specificity

CCNE1: cyclin E1

CD31: cluster of differentiation 31

cDNA: complementary deoxyribonucleic acid

CK-19: cytokeratin-19

CO_2: carbon dioxide

COX-2: cyclooxygenase-2

CTNNB1: catenin-Beta 1

D-MEM: Dulbecco's Modified Eagle Medium

DAB: diaminobenzidine

DAPI: 4',6-diamidino-2-phenylindole

ddH2O: double-distilled water

DNA: deoxyribonucleic acid

DTT: Dithiothreitol

EDTA: Ethylenediaminetetraacetic acid

EGF: epidermal growth factor

eGFP: enhanced green fluorescent protein

EGFR: epidermal growth factor receptor

eIF: eukaryotic initiation factor

EMT: epithelial-to-mesenchymal transition

EOC: Epithelial Ovarian Cancer

EpCAM: epithelial cell adhesion molecule

ER: estrogen receptor

ERBB2: Receptor tyrosine-protein kinase erbB-2

ERK: extracellular signal-regulated kinase

FBS: fetal bovine serum

GAPDH: Glyceraldehyde 3-phosphate dehydrogenase

Grp4: groucho-related gene product 4

hBD1: human beta defensing-1

HCl: hydrochloric acid

HOX genes: homeobox genes

hr: hour

HRP: horseradish peroxidase

Htra1: High-temperature requirement A serine peptidase1

IB: immunoblotting

i.p.: intraperitoneal

IHC: immunohistochemistry

IP: immunoprecipitation

IPA: ingenuity pathway analysis

ITSS: Insulin-Transferrin-Sodium-Selenite Solution

JNK: c-Jun N-terminal kinase

K-RAS: Kirsten rat sarcoma virus

KDa: Kilo Dalton

LH: Luteinizing Hormone

LMP: low melting point

loxP: locus of X-over P1

LSD1: lysine (K)-specific demethylase 1A

MAPK: mitogen activated protein kinase

MET: mesenchymal-to-epithelial transition

min: minutes

mOSE: mouse ovarian surface epithelium

mTOR: mammalian target of rapamycin

MVD: microvessel density

NaCl: sodium chloride

NAIP: neuronal apoptosis inhibitory protein

nM: nanomolar

nmole: nano mole

OVGP1: oviduct-specific glycoprotein

PAX2: paired box gene 2

PBS: phosphate buffer saline

PCR: polymerase chain reaction

PI3K: phosphoinositide 3 kinase

PIK3CA: phosphoinositide 3 kinase catalytic subunit alpha

PMSF:phenylmethanesulfonyl fluoride

Ppia: peptidylprolylisomerase A (cyclophilin A)

pRB: retinoblastoma protein

PTEN: phosphatase and tensin homolog

Ptgs-2: Prostaglandin-endoperoxide synthase 2

Q-PCR: quantitate polymerase chain reaction

RAS: renin-angiotensin system

Rig-1: retinoic acid-inducible gene 1

RIPA: radioimmunoprecipitation assay

RNA: ribonucleic acid

S-PBS: Stockholm PBS

SDS-PAGE: sodium dedocyl sulfate-polyacrylamide gel electrophoresis

shRNA: short hairpin RNA

SMA-α: smooth muscles actin-alpha

SMAD: small body size (SMA) and mothers against decapentaplegic (1) homologs

SMAD2: SMAD family member 2

SMAD3: SMAD family member 3

Snail: snail homolog 1 (Drosophila)

SV40 TAg: semian virus 40 T-antigen

STAT3: signal transducer and activator of transcription 3

STIC: serous tubal intraepithelial carcinoma

TAE: Tris-acetate-EDTA

TBS-T: Tris-buffered phosphate with Tween-20

TGFβ: transforming growth factor beta

WT-1: Wilms tumor suppressor protein

XIAP: X-linked inhibitor of apoptosis protein

α-MEM: Minimum Essential Medium Alpha

μg: microgram

μl: microliter

μm: micrometer

μM: micromolar

ACKNOWLEDGMENTS

First and foremost I would like to send my deep and sincere thanks to my mentor, Dr. Barbara Vanderhyden. You provided guidance and direction when I lost my way (both in science and in life). Simply, you are a great human being before being a great scientist and I will always look up to you.

Many thanks to my thesis advisory committee, Drs. Lee, McKay and McBurney, who always challenged me and constantly provided countless pieces of advice.

I have been fortunate to work with some wonderful people, some of whom have become life long friends. I'd like to thank my lab advisors, Olga Collins and Elizabeth Macdonald for their expertise, and willingness to teach. Special and sincere thanks to Dr. Kenneth Garson, You were always there to answer my questions and have taught me so much; thanks for endless patience.

Thanks to my friend and labmate, Kholoud Alwosaibai, who was always there for me, no matter what! You are an awesome friend and hard to be replaced! I am so grateful to have you in my life. Thanks to Dr. Josee Coulombe for handling my nagging and craziness and for making the lab a fun place! Your cheerful spirit and beautiful smile will be always in my memory.

Finally, a special thanks to all my cheerleaders, especially my parents, my sister (Fatimah) and my brother (Khaled), who without hesitation were always there to offer support, encouragement and prayers. To my family, you are the best thing to have happened to me in this life!

INTRODUCTION

1.1 Ovarian cancer

1.1.1 Clinical features of ovarian cancer

Ovarian cancer is the most lethal gynecological malignancy in the western world and is the fifth leading cause of cancer-related deaths(2, 3). The cure rate of ovarian cancer is very low (approximately 30%) and has not improved over the past 30 years (1). Patients with ovarian cancer are rarely diagnosed when the tumors are restricted to the ovary (stage I) when treatment is successful and prognosis is very good. However, the rate of favorable prognosis drops significantly after the disease metastasizes to the pelvic organs (stage II), organs within the abdomen (stage III) or organs outside the peritoneal cavity (stage IV) (2, 4). The standard treatment for ovarian cancer includes surgical debulking followed by platinum- and taxane-based chemotherapy.

There are three basic types of ovarian cancers: epithelial ovarian carcinoma (EOC), granulosa cell tumors and germ cell tumors(3). EOCs represent more than 90% of all ovarian cancers (5). They are very heterogeneous in nature, and there are many histotypes. Serous ovarian cancers are typically cystic and/or papillary and they are morphologically no different than fallopian tube cancer. Ovarian clear cell carcinomas resemble renal clear cell carcinomas (3). In contrast, cells of mucinous ovarian cancers resemble intestinal or endocervical epithelia, while endometrioid EOCs are characterized by endometrial-like glands(6).

EOCs have been categorized into a two-tiered system based on distinct molecular

characteristics and clinical behavior (Figure 1 and Table 1) (7, 8). Type I tumors usually present at low stage, evidenced by large tumors that are confined to the ovary at diagnosis. They are generally indolent and have a good prognosis. From a histopathological point of view, type I tumors comprise low-grade serous, low-grade endometrioid, clear cell and mucinous carcinomas. These tumors are genetically stable, relative to type II, and associatedwith somatic mutations in *KRAS*, *BRAF*,*ARID1A*,*ERBB2*, *PTEN*, *PIK3CA* and/or*CTNNB1* (5). While type I patients show resistance to chemotherapy, type II patients are more chemo-responsive. Patients with type II tumors encompass 75% of all EOC cases, including high-grade serous, high-grade endometrioid, undifferentiated carcinomas and mixed mesodermal tumors (carcinosarcomas) (7, 8). Type II tumors are highly genetically unstable and harbor mutations in *TP53* in more than 95% of the cases. They also frequently display mutations in *CCNE1* and inactivation of*BRCA1/2* (9, 10).Unfortunately, they are very aggressive tumors and often diagnosed at an advanced stage (5, 11), resulting in 5-year survival rates of 35.5% and 18% for patients with stage III and IV ovarian cancer, respectively(9). This dualistic model suggests that type I and type II ovarian tumors develop independently involving different molecular pathways (6).

1.1.2 Origin of ovarian cancer

Significant contributing factors to the high mortality rate of EOCs are the lack of early detection tools and the relatively asymptomatic progression of this disease (12). Both of these factors have led to the fact that more than two-third of patients are diagnosed at latestage, which, in turn, results in not only a poor prognosis but also a poor understanding of

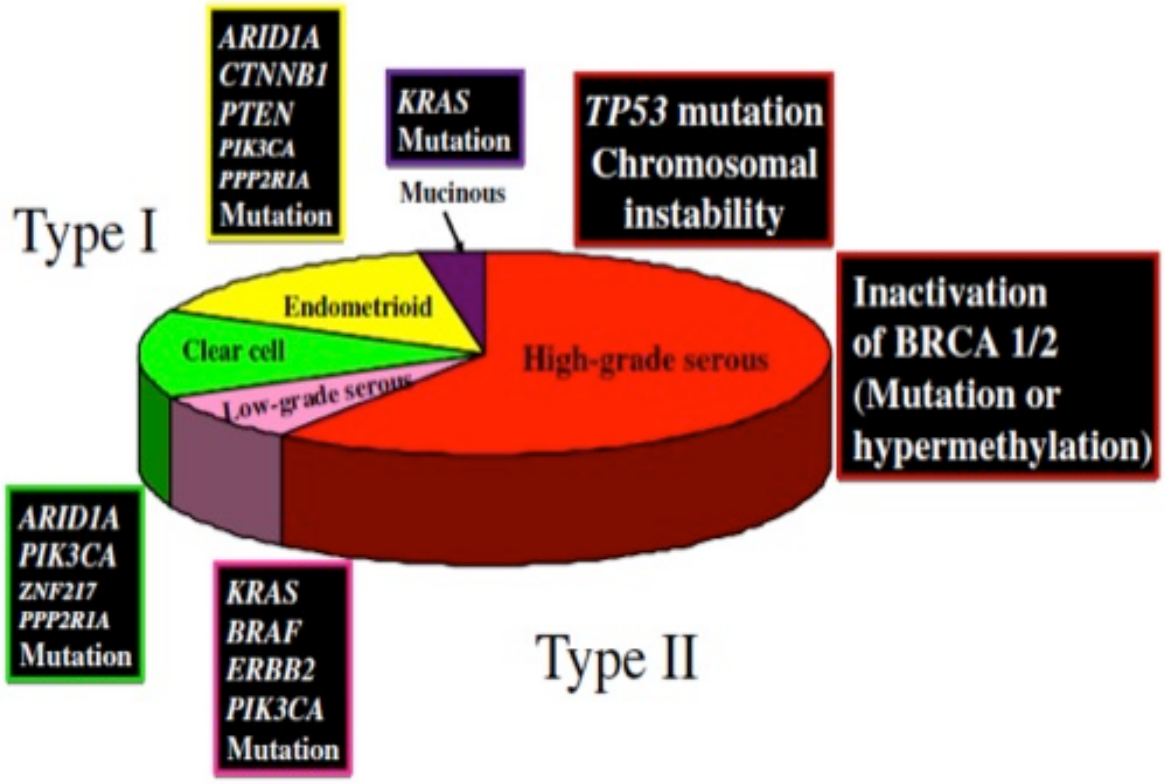

Figure 1: Prevalence of subtypes of EOCs and their associated molecular genetic changes (6).

Table1: A two-tiered system in which epithelial ovarian tumors are subdivided into low-grade and high-grade has been proposed. This system is based on biological and molecularevidence indicating that the two tumor types develop via different pathways.

Type I	**Type II**
clinically indolent	highly aggressive
low stage	advanced stage
low grade-serous	high grade-serous
low grade-endometrioid	high grade-endometrioid
clear cell, mucinous carcinoma	undifferentiated carcinoma
resistant to chemotherapy	responsive to chemotherapy
mutations in *KRAS-BRAF-ERBB2, PTEN, PIK3CA, CTNNB1*	mutations in *TP53, BRCA1, BRCA2, CCNE1*

the pathogenesis of early disease. Not only are the initial events of neoplastic transformation poorly understood, but also controversy remains regarding the cell type from which ovarian cancers arise (3, 13, 14). Until recently, it was widely accepted that most, if not all, EOCs begin in the ovarian surface epithelium (OSE) (3, 15, 16).

OSE is the single contiguous layer of flat to cuboidal mesothelium that overlies the ovaries. The cells are held together laterally by poorly developed junctional complexes andare loosely attached to an underlying basement membrane (Fig. 2A). Because they are separated from the underlying stroma by a thick collagen layer, OSE cells have poor access to metabolic exchange with thestroma and circulation. Hence, they reside in a niche where they are in an isolated and quiescent state, an ideal niche for a population of stem cells (3, 17). The evidence for highly expressed stem cell maintenance genes in the OSE indicates its potential to serve as ovarian cancer initiating cells (18-20). In addition, OSE cells are poorly differentiated with the ability to differentiate to a fibroblastic or an epithelial phenotype, depending on the environmental conditions (12, 16, 21).

The fact that OSE are incompletely committed and multipotential, provides a possible explanation for the phenotypic diversity of EOCs (16).OSE cells have been shown to lose mesenchymal characteristics and gain a columnar epithelial phenotype, which is the phenotype of epithelial tubal cells and the high-grade ovarianserous carcinoma as well (17). In addition, OSE cells have beenshown to gain this columnar phenotype as they form surface invaginations (clefts) and migrate through the stroma to form inclusion cysts (3) (Fig. 2B). Strong evidence shows that OSE cells actually undergo mesenchymal-to-epithelial

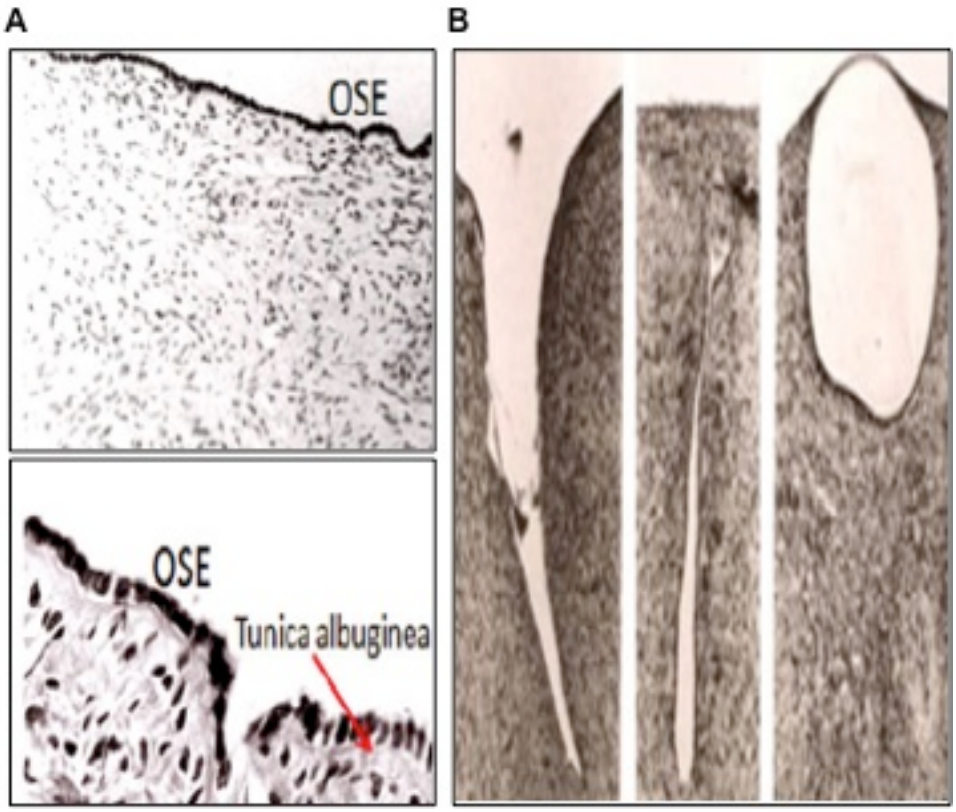

Figure 2: A: The ovarian surface epithelium (OSE) is the part of the pelvic peritoneum that overlies the ovary. The OSE is separated from the ovarian stroma by a thick collagen layer (the tunica albuginea). B: Evidence for development of an inclusion cyst from OSE. OSE-lined epithelial inclusion cyst may form through fusion of adjacent OSE-lined invaginations. Adapted from (3).

transition (MET) during formation of inclusion cysts (16, 21). The formation of inclusion cysts is thought to be a preliminary step toward ovarian carcinogenesis, as both clefts and inclusion cysts express markers such as E-cadherin and the cell surface antigen-125 (CA-125, a serum marker for epithelial cancer (22), that are not normally expressed in human OSE but are found in EOCs(3, 16). Indeed, E-cadherin expression in the human OSE is limited to the rare regions where the cells assume columnar shapes, *i.e.*, where they approach the phenotype of metaplastic epithelium and shown to be was increased in surface invaginations and particularly in epithelial inclusion cysts (23). Furthermore, forced expression of E-cadherin in human simian virus 40-immortalized OSE cells resulted in epithelial differentiation and production of CA-125 into the culture medium (24).Interestingly, dysplastic lesions and early stage ovarian cancers have been observed contiguous with normal OSE and within OSE-lined epithelial inclusion cysts (12, 25, 26).

Additional evidence that supports the idea that OSE is a source of high-grade serous ovarian carcinomas is that mesothelin, which is a specific marker of mesothelium and highly expressed in OSE, is one of the most prominent markers of high-grade ovarian serous carcinoma (27). Furthermore, OSE cells have been transformed to high-grade serous carcinoma in cultures of human OSE (28-30) and in animal models (31-33).

In addition to OSE, there are extraovarian sources that have been suggested as origins for EOCs, due to histological and molecular similarities. The most important of these extraovarian sources is the fimbria, which is at the distal end of the fallopian tube. The fimbria arein contact with the ovary and have recently been suggested to be an important origin for ovarian carcinogenesis (3, 6). The strongest evidence for the hypothesis that fimbria is a source for high-grade ovarian serous carcinomas arose when premalignant serous

tubal intraepithelial carcinoma (STIC) in the fallopian tube were found in 61% of high-grade pelvic (ovarian, fallopian tube and primary peritoneal) serous carcinoma (34). Furthermore, STICs were detected in 10-15% of fallopian tubes prophylactically removed from women with high risk of ovarian carcinoma due to germ line *BRCA1/2* mutations; the STICs morphologically resemble ovarian high-grade serous carcinoma, but no similar lesions were found in the ovaries of these women (35, 36). Importantly, both STICs and co-existing high-grade ovarian serous carcinoma harbor identical *TP53* mutations, indicating a clonal relationship between the two (37). Experimental support comes from studies showing transformation of fallopian tubes to tumors resembling human high-grade ovarian serous carcinoma using human fimbrial epithelial cells and in fallopian tube-restricted genetically modified animal models (38, 39).

Peik et al. proposed the fallopian tube as a source of high-grade ovarian serous carcinoma and suggested that occult fallopian tube carcinoma shed malignant cells that implant and grow in the ovary (40). The hypothesis implied that tumor cells are deposited on the ovarian surface by either retrograde flow or as a natural process of collecting the ovulated oocyte during ovulation where fimbriae sweep the ovarian surface(3, 40) (see Figure 3 for the proposed model). One support of this hypothesis is that inclusion cysts, considered a preliminary step toward ovarian carcinogenesis, consist of cells phenotypically similar to the secretory and ciliated cell types of the fimbrial epithelium. It was suggested that fimbrialepithelium may attach to the ovary with adhesion formation and subsequently be incorporated into the newly formed ovarian surface invaginations that proceed to form

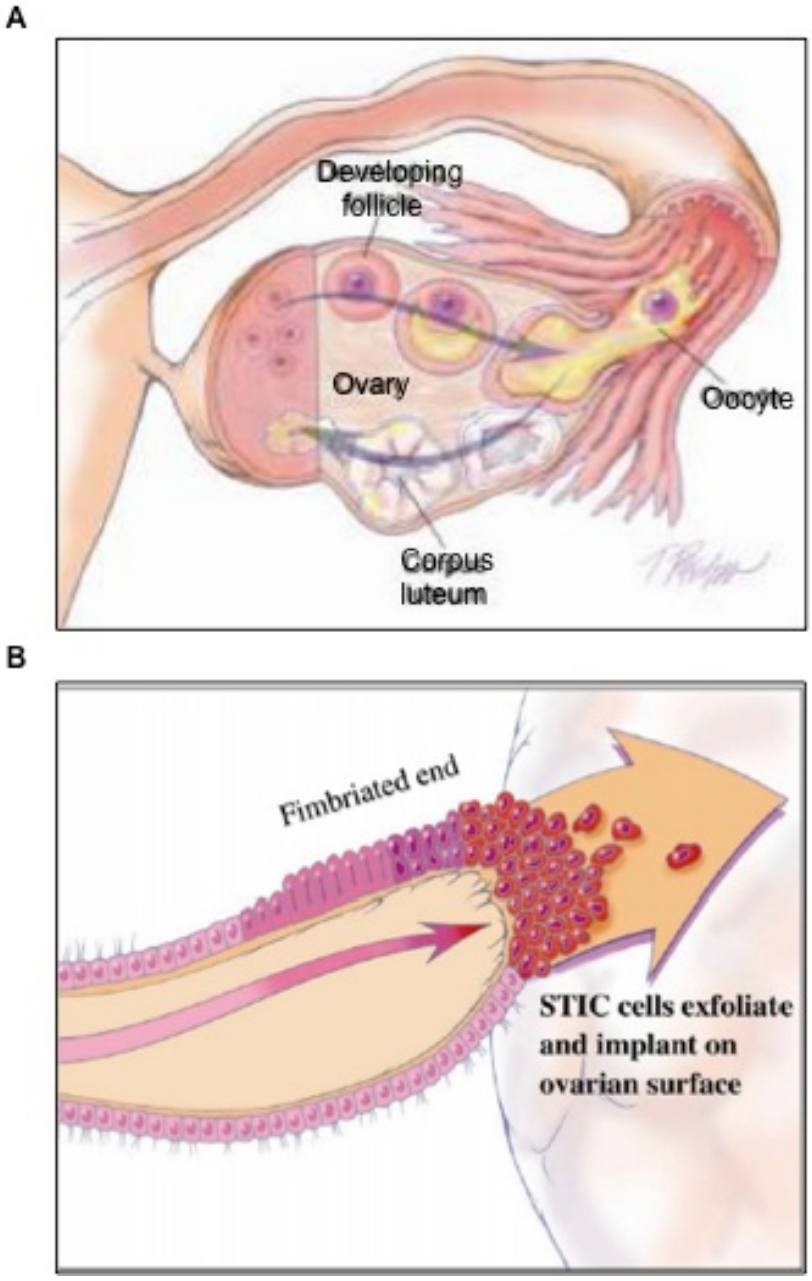

Figure 3: Proposed model for the development of ovarian carcinoma from the fallopian tube. A: Anatomical relationship of fallopian tube to the ovary showing that the fimbria envelops a portion of the ovary. At the time of ovulation, the ovarian surface ruptures with expulsion and transfer of the oocyte to the fimbria. The fimbria is in intimate contact with the ovary at the site of rupture. B. A schematic representation of direct dissemination or shedding of a serous tubal intraepithelial carcinoma (STIC) cells onto the ovarian surface, where the carcinoma cells ultimately establish a tumor mass that is presumably arising from the ovary. Adapted from (5).

inclusion cysts. Although inclusion cysts may present markers of fimbrialepithelium, this hypothesis is weakened by the ability of OSE cells to gain this columnar epithelial morphology in association with expression of markers of tubal epithelial differentiation including, E-cadherin, the epithelial cell adhesion molecule (EpCAM), cilia and oviduct-specific glycoprotein (OVGP1) (25, 41).

While the fallopian tube is thought to be a possible source of high-grade serous ovarian cancers, clear-cell and endometrioid ovarian carcinomas are hypothesized to develop from endometrioticcysts and are frequently associated with implants of endometriosis on the ovary (42, 43). Beside the morphological and molecular evidence, this hypothesis is further supported by epidemiological evidence which has shown that the protective effect of tubal ligation is most evident for endometrioid and clear-cell carcinomas because tubal ligation would prevent the endometrial tissues from reaching the ovaries (44).

1.1.3 Risk factors for ovarian cancers

A number of epidemiologic studies have evaluated a variety of risk factors for ovarian cancer, including genetic and reproductive factors (45, 46). A history of infertility, an early age of menarche and late age of menopause, conditions associated with numerous lifetime ovulations, areconsistent risk factors for ovarian carcinoma. Conversely, usage of oral contraceptives, breastfeeding and pregnancy, all of which suppress ovulation, have been correlated to reduced risk of ovarian cancers (46). These findings have led to the hypothesis that repeated ovulation is the primary non-heritable risk factor for ovarian cancer (47, 48). Ovulation is the process by which a mature oocyte, along with its attached cumulus cells, is expelled from the ovary(49). During ovulation, there is a breakdown of the collagenous

basement membrane separating the OSE from ovulating follicle and the OSE cells at the apex of the ovulating follicle undergo apoptosis, allowing release of the mature oocyte. The OSE then proliferate rapidly to close the ovulatory wound (50). Frequent cycling of this wound-repair process renders OSE susceptible to genetic aberrations (50, 51). Furthermore, as ovulation involves minor trauma, it also involves repeated exposure of the ovarian surface to inflammatory mediators, reactive oxygen species and follicular fluid, all of which are by-products of follicular rupture (48, 50, 52). Exposure of OSE cells to such agents may result in DNA damage and supports the hypothesis that repeated ovulation predisposes the OSE to neoplastic transformation (52, 53).

1.2 PAX2

1.2.1 PAX2 structure

The process of embryogenesis is tightly regulated by specific genes that are expressed in a temporal and spatial manner (54). Many such genes encode proteins with DNA binding domains such as homeobox domains, helix-loop-helix domains, zinc fingers and paired box (PAX) domains. The *PAX* family of genes encodes transcription factors and consists of 9 members in human and mice that are crucial for embryogenesis. All PAX proteins share an evolutionarily-conserved sequence of 28 amino acids called the DNA-binding PAiredboX (PAX) domain (54-56). As shown in Figure 4, they are classified into 4 subgroups according to structural similarities and the presence or absence of an octapeptide domain, a homeodomain or a partial homeodomain(57).While the octapeptide domain serves as a protein-binding motif for potential inhibitory affect on downstream targets, all PAX proteins have a C-terminal domain that is responsible for its transactivation function (58, 59).

PAX2 belongs to subgroup II of the PAX family, which have an octapeptide domain and only a partial homeodomain. The human *PAX2* gene maps to chromosome 10 (10q24-25) and consists of 12 exons, spanning 86Kb, as depicted in Figure 5 (60). Several *PAX2* exons are alternatively spliced to produce different isoforms. In humans, *PAX2* mRNAs lacking exons 6 and 10 encode the PAX2b protein, while mRNAs lacking exon 6 but containing exon 10 encode PAX2c (61). While exon 6 is included in isoforms A and E, exon 10 is excluded. Finally, there are two distinct splice acceptor sites at the 3' end of intron 11. In addition to the competing intron 11 splice acceptor sites, the inclusion or exclusion of exon 10 leads to distinct 3'terminus structures and reading frames among the transcripts. It is worth mentioning that none of the known transcripts contains all 12 coding exons of the *PAX2* gene (61, 62).*Pax2* isoforms have also been described in mouse. *Pax2*cDNAs lacking exon 10, but either containing exon 6 (PAX2a) or lacking exon 6 (PAX2b) have been described in mice (63). To our knowledge, the exact function of alternatively spliced exons has not been evaluated.

Similar to all PAX proteins, the transactivation function of PAX2 requires the serine-threonine-rich carboxyl-terminal domain (64). Phosphorylation of the transactivation domain of PAX2 enhances its transactivation ability. The activation domain of PAX2 is phosphorylated by the c-Jun N-terminal kinase (JNK) to enhance PAX2-dependent transcription (65). PAX2 also has an epigenetic function by mediating chromatin remodeling. Phosphorylated PAX2 binds to a target DNA sequence and interacts with the adaptor protein PAX Transactivation domain Interacting Protein (PTIP). PTIP recruits a histone H3 lysine 4 methyltransferase complex (H3K4) to specific DNA sites to alter the pattern of histone modifications (69). Such epigenetic mark is known to impart active or accessible

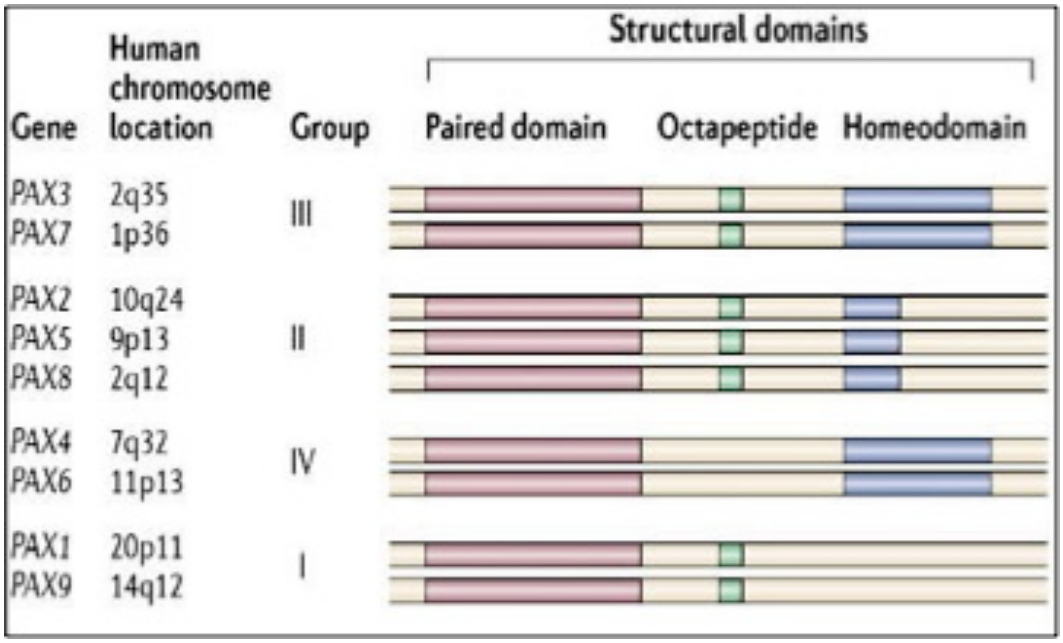

Figure 4: Classification of PAX transcription factors according to protein structure. All PAX proteins contain a transactivation domain (not shown in the figure) and a DNA-binding domain known as the paired domain. Some PAX family members also contain an additional DNA-binding homeodomain and/or an octapeptide region (66).

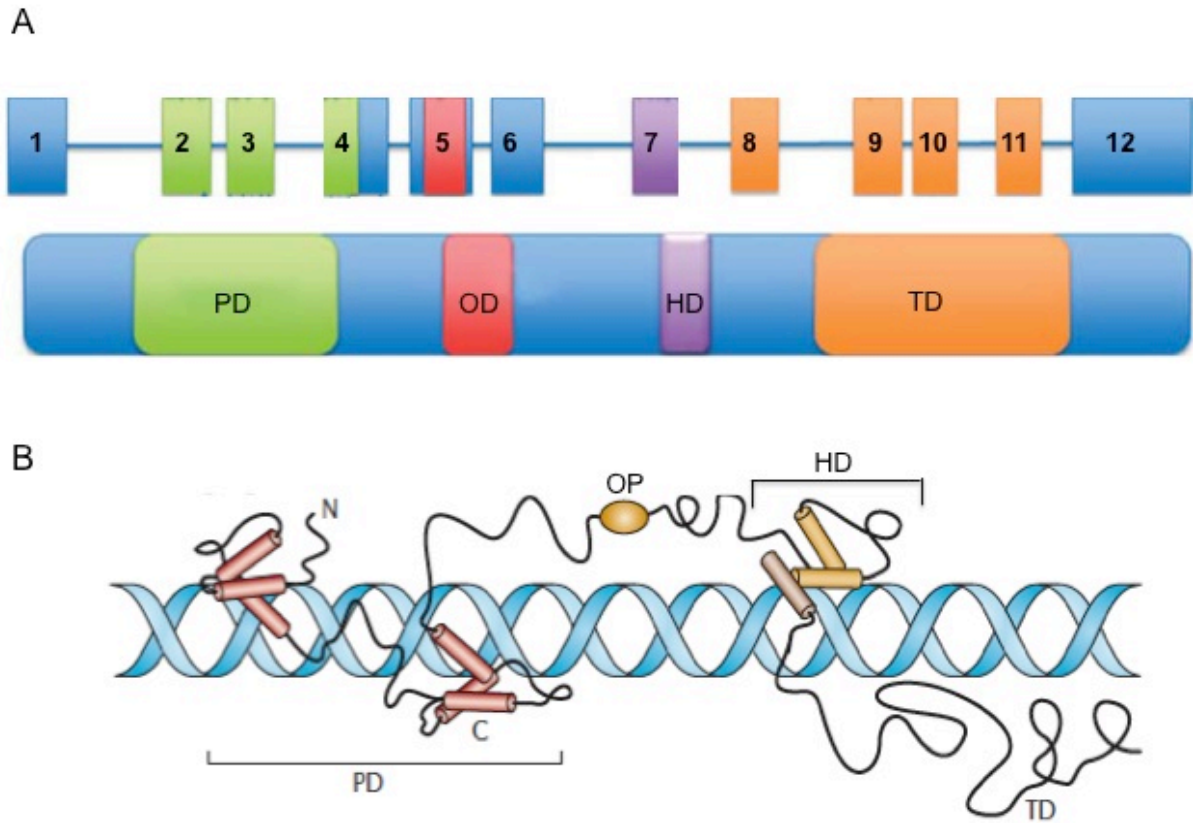

Figure 5: A:Genomic organization of the human PAX2 gene. The gene is composed of 12 exons, spanning 86Kb on chromosome 10q. Exons 2, 3 and part of 4 encode the paired domain (PD, green) of the PAX2 protein illustrated below. The octapeptide domain (OD, red), truncated homeodomain (HD, purple)and transactivation domain (TD, orange) are indicated. B: PAX2 protein containing a PD composed ofamino- and carboxy-terminal subdomains, each of which is composedof three α-helices. The third helix of each subdomain (67) is shown incontact with the major groove of DNA. An OPmotif is followed by a HD with a helix–turn–helixstructure. Finally, a carboxy-terminal TD isshown. This domain is responsible for transactivation activity (58, 68).

chromatin signatures to enable gene expression (70). On other hand, the groucho-related gene product 4 (Grg4) can completely suppress phosphorylation of the PAX2 transactivation domain and, thereby, suppresses the PAX2-dependent gene activation (71). Grg4 binding to PAX2 protein results in recruitment of the phosphatase PPM1B, which dephosphorylates the PAX2 carboxy-terminal domain and inhibits PTIP interactions(72). The PAX2-Grg4-PPM1B complex may then promote silencing byrecruiting the polycomb repressor 2 complex H4R3 and H3K27 methylation, two marks associated with gene silencing (73).

1.2.2 PAX2in developing tissues

1.2.2. a. Expression of PAX2 in development

During development, PAX proteins regulate development of several organs including the brain, eye, ear,urogenital tracts, lymphatic system, musculature, central nervous system, thymus and vertebrae (reviewed in (59). In particular, PAX2 is expressed in the developing inner ear, central nervous system and urogenital system.

Expression patterns and functional ablation experiments established the pivotal role of PAX2 in the initiation and progression of development, as well as in human diseases (58, 59). Torres and colleagues showed that *Pax2* is essential for development of all the epithelial tissues derived from the intermediate mesoderm. Homozygous *Pax2*-null mice die shortly after birth and invariably lack kidneys and ureters. In addition, the development of Müllerian ducts in females and Wolffian ducts in males is completely impaired. Both sexes completely lack the entire genital tract, as females have no uterus, oviduct nor upper vagina, whereas males lack ductuli efferentes, epididymis, vas deferens and seminal vesicles (74). Interestingly, the genital tracts were completely normal in mice with deletion or mutation of

single *Pax2*allele; however, heterozygous mutants develop renal hypoplasia, as well as defects in the eyes, ears and midbrain (74-77). Other *Pax2*mutant mouse models show that PAX2 is essential for the formation of the midbrain-hindbrain boundary, which controls the development of the midbrain and cerebellum, and homozygous mutation results in a complete depletion of the cerebellum (77, 78).

Although expression of *Pax2* is essential for kidney development, repression of *Pax2* expression during maturation of the renal tubules is required for normal development. Forced constitutive expression of *Pax2* in hemizygous transgenic mice resulted in severe kidney abnormalities including dilation and microcyst formation, and is associated with death at 1-3 days post partum (79).

1.2.2. b. Effect of PAX2 on cellular functions during embryogenesis

During embryogenesis, PAX proteins regulate the expression of genes involved in cell proliferation, cell survival, migration and cell-lineage specification (54, 59, 80).PAX2 is required for cell survival and morphogenesis in developing tissues (81-84). Although the renal hypoplasia that was observed in heterozygous mutant mice and in humans was considered a result of increased apoptosis during nephrogenesis with no changes in the proliferative rate (81, 82, 85), PAX2 expression was shown to be restricted to the proliferating cells in the developing inner ear and kidney (86, 87).

Interestingly, PAX2 expression in the nephric ducts is shown only during the MET process. Use of antisense oligonucleotides against *Pax2* in mouse kidney organ culture prevented kidney mesenchymal cell aggregation and polarization and, further, inhibited the formation of epithelium derived from this mesenchyme (88). Similarly, the complete renal agenesis found in mice with a null mutation of *Pax2*was attributed to the lack of

mesonephronic tubules, formation of which requires the nepherogenic mesenchyme to undergo epithelial transition (74). In addition, murine organ culture and embryo analyses point to a loss of epithelial cell polarity and increased mobility in kidney cells that have deleted PAX2 function (89). In summary, PAX2 appears to be critical for cell survival and MET in developing embryonic tissues.

1.2.3 PAX2 in adult tissues

1.2.3. a. Expression of PAX2 in adult tissues

Although the expression of PAX genes is attenuated as soon as the process of development is completed (55, 57), there are few exceptions. For instance, continuing expression of PAX2 has been detected in the human brain (90), retina (91) and in the putative stem cell population of the breast (84). Its expression is also retained in the female genital tract, specifically the epithelium of the endometrium, endocervix and fallopian tubes (92, 93). In addition, PAX2 is expressed in the distal tubular epithelium in adult kidneys (94).

1.2.3. b. Effect of PAX2 on cellular functions in adult tissues

Although PAX2 has been widely reported in normal adult tissues, there are gaps in the literature with respect to a direct link between PAX2 expression and function in normal adult tissue. However, the general principal role of all PAX genes is the maintenance of a stem-like state in progenitor cells (59), protection against cell death (94) and to aid organ regeneration and repair (95-97).

A recent study shows that loss of PAX2 expression in non-ciliated cells in human adult and fetal fallopian tube is associated with metaplastic differentiation and abnormal growth into multilayered epithelium (98).In adult kidneys, PAX2 function includes promoting

osmotic tolerance in renal tubular cells by protecting cells against apoptosis induced by high NaCl concentrations (94).

Recurrent expression of *Pax2*in adult tissues has been reported during tissue regeneration (95, 96, 99). For instance, PAX2 is re-expressed in prostrate following male castration in animal models (95).In a similar phenotype, renal injury results in transient re-expression of PAX2 in proximal tubular epithelium. This is accompanied by decreases in injury-induced apoptosis and trans-differentiation of renal tubule epithelia into progenitor like cells, suggesting that PAX2 plays a role in tissue regeneration (96, 99).

1.2.3. c. Defect of PAX2 in human tissues

While homozygous deletion mutation has not been reported in humans, heterozygous (frameshift) mutations resulting in haploinsufficiency have been reported in patients suffering from renal coloboma syndrome that is characterized by optic nerve colobomas, vesicouretertic reflux and hypoplastic kidney(100, 101). Some of these patients, in addition to eye and renal anomalies, have high frequency of hearing loss and defects in the central nervous system(62). Therefore, there are many similarities between renal coloboma syndrome in human and the phenotype in heterozygous *Pax2* mutant animals (68).

In patients with polycystic dysplastic kidney disease, renal dysplastic epithelia have high cell division and highly express PAX2 (102, 103). This pathology of kidney abnormalities has also been seen in transgenic mice with constitutive expression of *Pax2* (79). Since PAX2 was found to be downregulated during maturation and low level of protein is evident in collecting ducts in human (103), persistent expression of *PAX2* in human kidneys may result in enhanced proliferation and cyst growth.

1.3 PAX2 and cancer

1.3.1 PAX2 expression in cancers

Aberrant expression of PAX2 in human adult tissues has been shown primarily in cancers (reviewed in (66, 97). A comprehensive immunohistochemical analysis of 406 primary tumor tissues showed high expression of PAX2 in tumors of the brain, breast, colon, lung, ovary, prostate and in lymphoma and melanoma (104). PAX2is highly expressed in 40-53% of lobular or ductal breast (84) and 52% of prostate cancers (105), irrespective of hormone receptor status. It is also overexpressed in Kaposi's sarcoma (106), Wilms tumor (63) and in all subtypes of renal cell carcinoma, except the transitional cell carcinoma (107, 108). The expression of PAX2 has also been widely reported in ovarian carcinomas (92, 93, 104, 109-112).

As summarized in Table 2, expression of PAX2 seems to be evident in all histotypes of EOCs. PAX2 expression has been shown in 33-64% of primary serous ovarian cancers (104, 111, 112). It has also been detected in 28-43% of clear cell carcinoma of the ovaries (104, 109, 110). While Murtavoska and colleagues did not detect staining for PAX2 in endometrioid or mucinous carcinomas, Song et al. reported positive staining in 33% and 12% of endometrioid and mucinous carcinomas, respectively (104, 110). The conflicting reports on PAX2 expression does not appear only among different histotypes, but it is also controversial whether its expression correlates with the tumor grade. Using immunohistochemistry and immunoblot, Tung et al. (2009) showed expression of PAX2 in 63% (N=16) and 59% (N=17) of low-grade ovarian serous carcinomas and ovarian tumors with low malignant potential, respectively (92). In contrast, only 9% (N=263) or none of high-grade ovarian serous carcinomas showed strong staining of PAX2 in the nuclei (92,

113). This data is in conflict with that of Tong et al. (2007) where PAX2 expression was shown in immunohistochemical sections of 67% of ovarian papillary serous carcinoma (N=36) with no significant correlation to tumor grade (93). There is no clear explanation for such discrepancy). While Tong and colleagues did not indicate the antibody being used, allother investigators used the same rabbit polyclonal antibody(Invitrogen) that was raised to afusion protein containing amino acids 203-373 from the C-terminal domain of the murine PAX2 protein. Although the information provided by Invitrogen states that there is no cross-reactivity with other members of the PAX family of proteins, this antibody may cross-react with PAX5 as the peptide sequences 329 through 416 of murine PAX2 are homologous to human PAX5 (116). Furthermore, using Position-Specific Iterated BLAST (PSI-BLAST), we found that this antibody could detect all isoforms of PAX2 in humans.

It is worth noting that controversy regarding PAX2 expression in different tumor grades has been only discussed in two separate reports (Tung et al. vs Tong et al.) and many pathologists support the observation of Tung et al. as loss of PAX2 is evident in all high grade pelvic serous carcinomas, including ovarian (113-115, 117, 118).

Table 2: Expression of PAX2 in ovarian cancers.

Tumor type	Tumor subtypes	%, N	Reference
Type I	Mucinous	0%, N=5 12%, N=17	Murtacoska et al. (104). Song et al. (110).
	Clear cell	28%, N=7 43%, N=7 35%, N=26	Muratovska et al. (104). Gokden et al. (109). Song et al. (110).
	Low-grade serous	50%, N=6 63%, N=16	Tong et al. (93). Tung et al. (92).
Type II	High-grade serous	62%, N=24 9%, N=263 16%, N=56 31%, N=16	Tong et al. (93). Tung et al. (92). Roh et al. (114). Chen et al. (115).
	Endometroid	0%, N=5 33%, N=12	Murtacoska et al. (104). Song et al. (110).

1.3.2 Function of PAX2 in cancerous tissues

Although forced expression of *Pax2* in transgenic mice showed no evidence of tumor incidence(79), it has been suggested as a potential proto-oncogene given that ectopic expression of the*Pax2* gene led to tumorigenic transformation of the rat fibroblast 280 cell line when cells were injected subcutaneously into nude mice (119). Supporting evidence for the potential oncogenic role of PAX2 comes from several *in vitro* and *in vivo* analyses, as described below.

When a proto-oncogene is abnormally activated, it may drive the cells to acquire some characteristics that are considered hallmarks of cancer. These hallmarks include, but are not limited to, sustaining proliferative signals, evading growth inhibitory signals, resisting cell death, enabling replicative immortality, inducing angiogenesis and activating invasion and metastasis (120).

1.3.2. a. PAX2 and cell survival and proliferation

PAX2 expression in renal cancer is positively correlated with a higher proliferative index and metastatic stage (108). *In vitro* analyses showed that inhibition of PAX2in renal cell carcinoma, Kaposi sarcoma, colon cancer, prostate cancer, bladder cancer, endometrial carcinoma and ovarian cancer cell lines results in a decrease in the proliferative rate and/or an increase in cell death (104, 106, 107, 121-123). Additionally, human microvascular endothelial cells that exogenously express *PAX2*have enhanced cell proliferation and enhanced resistance to apoptosis, when deprived of serum or challenged with vincristine (106, 124).PAX2 not only enhanced chemoresistance to vincristine, but its inhibition in a renal cancer cell line resulted in enhanced apoptotic induction following exposure to cisplatin (125). Although PAX2 has shown to mediate the growth stimulatory effects of

estrogen or tamoxifen in endometrial cancer cell lines (123), silencing PAX2 has been shown to reverse the growth arrest induced by tamoxifen in breast cancer cell lines (126).In summary, there is discrepancy in the literature about the role of PAX2 in control of cell growth; however; most of the literature suggests an oncogenic behavior of PAX2 shown by enhanced proliferation and/or survival.

1.3.2. b. PAX2 and cell migration, invasion and angiogenesis

Some*in vitro* analyses strongly support the oncogenic behavior of PAX2 as an enhancer of cellular migration, invasion and angiogenesis (106, 124). For example, knockdown of PAX2 in Kaposi sarcoma cells resulted in a decrease in cellular motility and invasion, and inhibited the spindle shape morphology, which is characteristic of Kaposi's sarcoma cells. Similarly, PAX2 knockdown in renal tumor-derived endothelial cells made them less invasive in matrigel, less adhesive to cancer cells and less angiogenic both *in vitro* and *in vivo*. Consistent with these studies, when human microvascular endothelial cells were transfected to overexpress*PAX2*, they acquired phenotypes similar to that of tumor-derived endothelial cells, as they became proinvasive, proangiogenic and more adhesive to cancer cells (124).Thus, oncogenic potential of PAX2 may include its positive role in enhancing migration, invasion and angiogenesis.

1.3.2. c.Evaluation of PAX2 in animal cancer models

In addition to the *in vitro* analyses, PAX2 has shown oncogenic activity in several *in vivo* studies (122, 123, 125, 127). When human endometrial cancer cells overexpress PAX2, tumor growth in athymic BALB/c mice was significantly enhanced. Furthermore, silencing PAX2 attenuated the enhancement of tumor growth by estrogen or tamoxifen administration (123). Similarly, Zhang and colleagues showed that silencing PAX2 in a human

endometrioid carcinoma cell line resulted in regression of tumor volume and growth, when they were injected into nude mice. However, there was no associated difference in animals' survival (127). Knockdown of PAX2 has been shown to be inversely related to tumor volume in a colon cancer xenograft model (122). In contrast, Hueberet al. showed that expression of PAX2 is not associated with tumor volume in a renal cell carcinoma xenograft model. Nevertheless, when treated with cisplatin, tumors with knockdown of PAX2 resulted in enhanced tumor regression, suggesting that treatments targeting PAX2 might be useful in combination with cisplatin (125). Therefore, animal studies suggest that PAX2 is an enhancer for tumor progression and/or chemoresistance.

1.3.2. d. Controversial role of PAX2 in ovarian cancer

Although these different models of cancer have undoubtedly improved our knowledge of the role of PAX2 in carcinogenesis, we have no direct evidence for its contribution to ovarian tumorigenicity, especially when the available reports on PAX2 function in ovarian cancer are limited and conflicted. PAX2 has been shown to enhance and inhibit proliferation in different human ovarian cancer cell lines (104, 110). A recent study suggests that PAX2 might have both oncogenic and tumor suppressor functions in ovarian cancer cell lines. In that study, two ovarian cancer cell lines (RMUGL; mucinous and TOV21G; clear cell) with endogenous expression of PAX2 showed reduced cellular proliferation and migration when PAX2 was knocked down. In contrast, over-expressing PAX2 in two serous ovarian cancer cell lines (OVCAR-3 and OVCA-423) suppressed cell proliferation. The authors did not provide an explanation for the differential effect of PAX2, except toconclude that "PAX2 could have both oncogenic and tumor suppression functions which will depend on the genetic content of the cancer cells". However, it is worth noting that OVCAR-3 and OVCA-

432 cell lines, where PAX2 induces anti-tumor function, have mutant *TP53*(128). On the other hand, PAX2 acts as an oncogene in the wild type *TP53* cell lines (RMUGL and TOV21G) (129). This is consistent with the observation of Muratovskaet, where knockdown of PAX2 resulted in inhibition of proliferation and induction of apoptosis in the endometrioid ovarian cancer cell line IGROV-1 (104, 130), which has wild type *TP53*(131).

Therefore, it seems that the differential effects of PAX2 might be associated with the histotype of ovarian tumors (endometrioid and serous vs. clear cell and mucinous). Clear cell and mucinous ovarian tumors are categorized as type I, while the majority of endometrioid and serous are type II. It is worth mentioning that those cell lines were isolated before the two-tiered system emerged. Importantly, the differential effect of PAX2 might also be associated with certain gene mutations associated with each histotype, eg.*TP53*. Thus, PAX2 might act as a tumor suppressor in *TP53*-mutant cells. This prediction has support from a report indicating a relationship between discrete*PAX2* gene downregulation in the fallopian tube and the presence of co-existing pelvic serous cancer, where *TP53* is highly mutated (113). STICs, the early neoplastic lesion in the fallopian tube show loss of PAX2 expression (70%) in association with *TP53* mutation (90%) (114, 115). Thus, for high-grade ovarian cancers that originate in the fallopian tube, an early event toward their transformation appears to be the loss of expression of PAX2, indicating that PAX2 might have a tumor suppressor role when *TP53* is mutated.

1.3.3 Potential mechanisms that mediate PAX2 action in cancer tissues

Although PAX2 is shown to favor proliferation, cell survival, invasion and angiogenesis in different cancer cell lines (66, 97, 124), the exact mechanisms underlying its actions have not been determined. A summary diagram of some of PAX2 targets that are involvedin cancer

progression is illustrated in Figure 6. Studies report that PAX2 may promote cell proliferation, at least, through its ability to suppress transcription of *TP53*(132). In addition, PAX2 interacts with the retinoblastoma protein (pRB) and inhibits its repression of the S phase entry inducer, the retinoic acid-inducible gene 1(Rig-1)(133). In a similar trend, PAX2 knockdown in colon cancer cells resulted in a decrease in the level of cyclinD1, and inhibited the phosphorylation of its downstream target, pRB (122). Phosphorylation of pRB is critical for G1-to-S phase transition during cell cycle progression (134).On the other hand,PAX2 was suggested to control cell cycle as it positively modulates the expression of the Wilms tumor suppressor protein (WT1) (135) that is known to inhibit cell cycle entry into S phase(136). Also, PAX2 has been shown to mediate the tamoxifen-induced growth arrest and repression of the oncoprotein ERRB2 in breast cancer cell lines (126). In conclusion, PAX2 may promote cell cycle progression through inhibition of P53 expression and pRB activity. However, PAX2 has been shown to inhibit ERBB2, while activate WT1, which are, respectively, positive and negative regulators of cell cycle progression.

PAX2 seems to promote cell survival by a variety of mechanisms. One study showed that PAX2 may enhance cell survival in endothelial cells through inhibition of PTEN and, in turn, enhanced phosphorylation of AKT (124). In addition, PAX2 may antagonize apoptotic induction by decreasing the level of the proapoptotic protein, BCL-2 associated agonist of cell death (BAD)(121)and increasing the level of the neuronal apoptosis inhibitory protein, NAIP(137).PAX2has also been suggested to promote cell survival through transcriptional repression of the putative tumor suppressor human beta defensing-1 (hBD1) and inhibition of hBD1-mediated cell death(138). Interestingly, while PAX2 has been shown to repress *TP53* expression, inhibition of PAX2 has been shown to promote cancer cell death irrespective of *TP53* status (121).

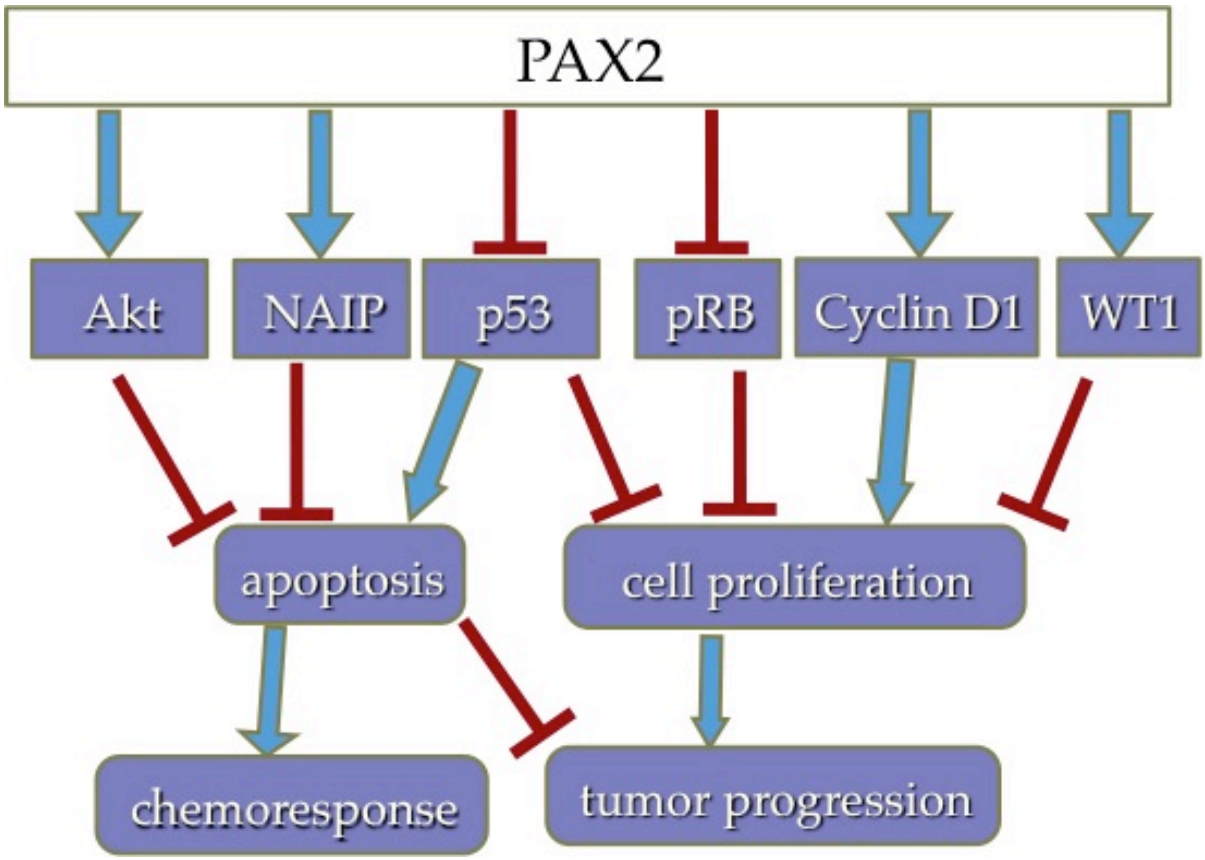

Figure 6: Schematic diagram of PAX2-induced mechanisms in cancer progression.

1.4 Modulators of PAX2 expression

While a number of factors have been shown to modulate PAX2 expression (139), a subset of these is also known to be involved in ovarian tumorigenesis. Dysfunction of the tumor suppressor gene, *TP53*, has been widely reported in ovarian cancers (140). Sood et al. demonstrated that 72% of ovarian tumors carry *TP53* mutations, 66% of which are missense mutations, while the rest (34%) carry null mutations. Tumors with null mutations are more associated with metastasis and advanced stage (stage III, IV), with no significant correlation to tumor histotypes (141). The Cancer Genomic Atlas network reported that *TP53* is mutated in almost all (96%) cases of high-grade serous ovarian cancers (10). In developing kidneys in mice, *Pax2* promoter activity is stimulated by wild type P53 and dominant negative mutant P53 inhibited this stimulation, and P53 knockdown results in downregulation of endogenous PAX2 expression. Also, chromatin immunoprecipitation (ChIP) analysis showed that P53 binds to the promoter of PAX2(142), suggesting that P53 positively regulates PAX2 expression.

Sex steroid hormones are known to be central to normal ovarian functions and estrogen plays a significant role in the etiology of ovarian, endometrial and breast carcinoma(143). Post menopausal estrogen-only hormone replacement therapy is associated with an increased risk for epithelial ovarian cancer (144). Estrogen accelerates ovarian tumor progression in an orthotopic mouse model of ovarian cancer (145). Estrogen exerts its biological activities by binding to estrogen receptors (ERα and ERβ), both of which function as ligand-dependent transcription factors(146). Tamoxifen is a classical estrogen antagonist that binds to the ERs and recruits corepressors, rather than coactivators, to the promoter regions of estrogen-

responsive genes, blocking their transcription (147). Using *in vitro* and *in vivo*models, Wu et al. (104) found that PAX2 is a crucial mediator of endometrial cancer growth that is induced by estrogen or tamoxifen. Both agents enhanced the expression of PAX2 significantly in endometrial carcinomas but not normal endometrium and this activation is associated with cancer-linked hypomethylation of *PAX2* gene. Interestingly, the study revealed that there is no typical estrogen responsive element (ERE) in the promoter region of PAX2. Nevertheless, ChIPanalysis detected the presence of ERα, but not ERβ, on the upstream regulatory region of PAX2 in endometrial cancer cells but not normal endometrial cells (123).

Angiotensin II (ANG II) belongs to the renin-angiotensin system (RAS) that classically acts through ANG II type 1 receptor (AT1R) and ANG II type 2 receptor (AT2R) (148). AT1R is highly expressed in invasive ovarian carcinoma and involved in tumor progression and angiogenesis (149). Using *in vitro*and *in vivo* models of prostate cancer, blockers of AT1R have been shown to induce antiproliferative effects mediated by reduced phosphorylation of the mitogen activated protein kinase (MAPK) and signal transducer and activator of transcription 3 (STAT3) (150).Bose et al. suggested that ANG II via AT1Rmight promote prostate tumorigenesis through upregulation of PAX2 expression and phosphorylation. This stimulatory effect was mediated by phosphorylation of ERK1/2 and STAT3 (151). While this study showed that the ANG II-induced PAX2 expression is via AT1R not AT2R, ANG II has been shown to enhance PAX2 only through AT2R in fetal renal explants (151, 152).

Another factor that is known to modulate PAX2 expression and plays a significant role in carcinogenesis is the epidermal growth factor (EGF). EGF and its associated receptor signaling have been implicated in poor prognosis of EOCs (153, 154). Ligand binding to the extracellular domain enables receptor homo- or hetero-dimerization resulting in

phosphorylation of the intracellular tyrosine kinase domain and activation of several cell signaling pathways (155, 156). These signalingpathways regulate cell growth and/or impair apoptosis by modulating the synthesis or degradation of specific proteins (157). Treatment with EGF suppresses lysosomal degradation of PAX2 in rat renal epithelial cells, resulting in a significant increase in PAX2 protein levels. Further analysis shows that PI3K and Akt but not the rapamycin-sensitive activity of mTOR arerequired for EGF to increase PAX2 and suppress lysosomal proteolysis (158).

TGF-β1, a member of the transforming growth factor superfamily (TGF-β) has been implicated in the modulation of PAX2. This cytokine is related to important biological processes such as apoptosis, cell growth, tissue regeneration and development (159). In rodent and human ovaries, TGF-β1 is detected in ovarian follicles during all stages of follicular development (160). Also, theca, granulosa and OSE cells produce the three prototypic isoforms of TGF-β (TGF-β1, TGF-β2 and TGF-β3) (160, 161). TGF-β1 signaling is transduced through the membrane type I and type II TGF-β receptors (TGF-βR I and II) (162). Both receptors are ubiquitously expressed in most cell types in the ovary, including the OSE. OSE cells could be controlled by autocrine TGF-β1 signaling (161) and/or in a paracrine manner as OSE cells come into contact with TGF-β1 that has diffused through the ovarian stroma following secretion by the granulosa or theca cells (160). In addition, OSE may be exposed to TGF-β1 that is present in the follicular fluid that is released following ovulation and follicular rupture (163). Regardless of the source, TGF-β1 is a known negative regulator of normal OSE cell proliferation (161), which may prevent the over-proliferation of OSE cells during ovulatory wound healing. Moreover, our lab has shown that TGF-β1 enhances stem cell characteristics in OSE cells (18). In advanced ovarian cancers, expression of *TGFB1* (the gene for TGF-β1) is associated with poor prognosis(164). It has been

demonstrated that TGF-β1 promotes a negative regulation of-the expression of the PAX2 protein, by reducing mRNA stability (165). In addition, exogenous TGF-β1 in a dysplastic kidney epithelial-like cell line decreased expression of PAX2. This change was associated with reduced proliferation and an induced mesenchymal phenotype, accompanied with upregulation of the mesenchymal markers alpha-smooth muscle actin (SMA-α) and fibronectin (166).

In summary, there are several factors known to regulate PAX2 expression, a subset of which are involved in the progression and/or the poor prognosis of ovarian cancers. Upregulators of PAX2 include estrogen and its antagonist tamoxifen, ANG II via the MAPK and STAT3 pathways, and EGF through the PI3K pathway (123, 151, 158). On the other hand, TGF-β1 has been demonstrated to be a negative regulator of PAX2 in renal cells (165, 166).

Rationale and hypotheses

The lack of reliable diagnostic tools and subsequently the fact that most ovarian cancer patients are diagnosed at advanced stage highlights the need for an improved understanding of the origins of ovarian cancer and how specific cellular and molecular events result in neoplastic transformation.The cell of origin of ovarian cancer is strongly debated and evidence suggests that ovarian carcinomas originate from ovarian and oviductal epithelium. Both hypotheses are based on histological and molecular markers and find support from animal experiments (3, 5).

OSE cells appear to migrate through the stroma and form inclusion cysts, which is thought to be a preliminary step toward ovarian tumorigenicity (16). Inclusion cysts may differ from OSE at the phenotypic and molecular level. For instance, OSE cells do not express PAX2, while ciliated inclusion cysts show robust induction of PAX2. PAX2 is also highly expressed in ovarian tumors of low-malignant potential and low-grade ovarian serous carcinoma, which are thought to be of ovarian origin (92). This indicates that gain of PAX2 expression in OSE cells might be an early step toward their transformation.

Pax2 is a potential oncogene, given that its expression led to transformation of fibroblast cells, as evident by tumor formation after injection in mice (119).Using different cancer cell lines, PAX2 was shown to be an enhancer of survival and/or proliferation (104, 106, 107, 121-123).***We therefore hypothesize that the induction of expression of PAX2 in ovarian epithelium is one of the early events of transformation leading to low-grade ovarian cancers, due to its positive effects on proliferation and survival.***

Although the available reports on the role of PAX2 in ovarian cancer are limited and conflicting, several *in vitro* analyses strongly support the oncogenic behavior of PAX2 as an

enhancer of cell proliferation, survival and migration in other types of cancers (104, 121, 125). In addition to the *in vitro* evidence, silencing of PAX2 in a human endometrioid and colon carcinoma cells resulted in decreased tumor volume in xenograft models (122, 127). In a renal xenograft model, knockdown of PAX2 resulted in enhanced cisplatin-induced tumor regression (125). ***We hypothesize thatPAX2 enhances ovarian cancer progression and resistance to chemotherapy.***

Specific Aims

Aim 1: To identify the biological consequences of PAX2 expression in normal ovarian epithelial cells.

Aim 2: To identify the downstream targets of PAX2 in normal ovarian epithelium.

Aim 3: To identify the role of PAX2 on ovarian tumor promotion.

Aim 4: To identify upstream regulators of PAX2.

Significance

The role of PAX2 in ovarian cancer pathogenesis is unclear considering a model of acquired expression in OSE developing into inclusion cysts or low grade cancer and a model of loss of expression in early lesions of the fallopian tube. This confusion regarding the role of PAX2 in the pathogenesis of ovarian cancer led us to more closely examine the role of PAX2 in the initiation of ovarian cancer. Clarifying the biological consequences of PAX2 overexpression in normal tissues, along with identifying its downstream signaling, will help

to explain its potential oncogenic role. In addition, exploring its role in ovarian cancer progression will allow us to determine if PAX2 is a potential target for cancer therapy.

METHODS

2.1 Cell lines and cell culture

Two independent populations of mOSE cells were isolated from randomly cycling, 6-week-old FVB/N female mice and named M0505 and M1102. For each primary culture, ovaries from 10–20 mice were individually dissected. The ovaries were rinsed twice with phosphate-buffered saline (PBS; Hyclone Laboratories, Logan, Utah), then incubated in 0.25% trypsin/PBS (0.5 ml/ovary; Invitrogen, Burlington, ON) in a 15ml Falcon tube at 37°C and 5% CO_2 for 30 min to remove the mOSE layer. Serum was then added to inactivate the trypsin, and the tube was agitated gently by hand to remove the mOSE cells from the ovaries. The supernatant containing the mOSE cells was centrifuged at 1000 rpm for 5 min, and the cells were resuspended in the mOSE medium (see below) and plated for subsequent culture.

Another independent culture of mOSE cells (named mOSE-fxp53) was obtained from *Trp53*$^{ploxP/loxP}$ mice [FVB;129-Trp53^{tm1Brn}], which are homozygous for *p53* alleles bearing *loxP* sites in introns 1 and 10 of the *p53* gene (Mouse Models of Human Cancers Consortium Mouse Repository, National Cancer Institute, Rockville, MD, USA). Infection with the recombinant adenovirus Ad5CMVCre (AdCre; Vector Development Laboratory, Houston, TX) results in the loss of functional P53 by excision of exons 2-10 (the resultant cell line was named p53$^{\Delta 2\text{-}10}$-mOSE).

In this study, two murine cancer models were used. The first model was obtained upon long-term passage of the M0505 cells, leading to the emergence of spontaneously transformed cells, which are referred to as STOSE (31). The second murine ovarian cancer cell line (RM cells) was derived from mOSE cells obtained from Immortomice which harbor

a temperature-permissive SV40 T-Antigen transgene. Following TAg-induced immortalization, the cells were maintained at a non-permissive temperature and transduced with retrovirus constructs to achieve expression of mutant *K-Ras*($KRAS^{G12D}$) and *Myc*(167).

The above mentioned cell lines were of murine origin and therefore were not authenticated by standard STR profiling, however, STOSE, derived from the FVb/n M0505 cell line were shown to be tumorigenic in the FVb/n strain and hence syngeneic with this strain. RM cells showed expression of the genetically programed oncogenes RASG12D, MYC and the SV40 large T-antigen (at permissive the permissive temperature) confirming their identity.

All of the above cell lines were maintained in mOSE media, which consists of HyClone® Minimum Essential Medium Alpha (α-MEM; Thermo Fisher Scientific Inc., Waltham, MA) supplemented with 10% v/v heat-inactivated fetal bovineserum (FBS; PAA Laboratories Inc., Etobicoke, ON), 2mM L-glutamine (Gibco, Burlington, ON), 2μg/ml epidermal growth factor(Roche, Indianapolis, IN), 5 U/ml of penicillin and 0.005 mg/ml of streptomycin solution (Sigma-Aldrich; St. Louis, MO), 0.1 μg/ml of gentamicin (Invitrogen), and 1 μg/mlof insulin-transferrin-sodium-selenite solution (ITSS; RocheDiagnostic, Laval, QC).

Human embryonic kidney 293T cells (HEK 293T cells), mouse embryonic fibroblasts (NIH 3T3 cells) and human ovarian cancer cell lines (OVCAR-3 and OVCA-432) were purchased from the American Type Culture Collection (ATCC, Manassas, VA). NIH 3T3 cells and HEK 293T cells were cultured in HyClone® Dulbecco's Modified Eagle Medium (D-MEM)/High Glucose (Thermo Fisher Scientific Inc.) supplemented with 10% FBS (PAA Laboratories Inc.), 0.005 mg/ml of streptomycin solution (Sigma-Aldrich) and 0.1 μg/ml of gentamicin (Invitrogen). OVCAR-3 and OVCA-432 were maintained in α-MEM supplemented with 10% FBS, 0.005 mg/ml of streptomycin solution (Sigma-Aldrich) and 0.1

μg/ml of gentamicin (Invitrogen).

All cells were plated on tissue-culture plates (Becton-Dickinson, Franklin Lakes, New Jersey) and grown at 37°C with 5% CO_2.

2.2 Infection

The murine *Pax2* cDNA was cloned from the murine oviduct. When the gene product was sequenced, it was found to correspond to Pax2-b variant. This product was used to generate a lentivirus expression vector (WPI-Pax2-IRES-eGFP, hereafter PAX2; Yong Tang, unpublished data; Fig. 7). It is worth noting that there are no reported specific functions for different isoforms of PAX2.

The empty vector, pWPI (Addgene plasmid 12254) was used as a control. Lentiviral vectors were prepared by co-transfection of vector plasmids (pWPI; Addgene plasmid 12254 or pWPI-Pax2; Yong Tang, unpublished data), packaging plasmid pCMVR8.74 (Addgene plasmid 22036) and the ecotropic envelope expression plasmid, pCAG-Eco (Addgene plasmid 35617) into 293T cells. PAX2 or WPI virus recovered from the supernatant of transfected 293T cells was filtered through a 0.45 μM filter and then used to infect target cells. Infected cells were passaged at least 3 times and the pooled population of infected cells was sorted for GFP expression by fluorescence-activated cell sorting (Beckman Coulter, Inc. Mississauga, ON). Both the WPI and PAX2 integrated proviruses harbor *loxP* sites in both 5' and 3' LTRs allowing the deletion of the vector encoded genes following expression of Crerecombinase. Deletion of both GFP and *Pax2* was achieved by treating PAX2-expressing cells with the AdCreand sorting them for GFP-negative cells (referred to as PAX2+Cre). Except for the mOSE-fxp53 cells, infections were done twice for each cell

line. Both replicates of infected cells presented the same results.

2.3 Cell proliferation assay

mOSE cells were plated at a density of 2×10^5 cells/ml in 12-well plates, while 1×10^5 cells of $p53^{\Delta2\text{-}10}$-mOSE, STOSE and RM cells were plated in 6-well plates. Detached and attached cells were collected and viable cells were counted using a Vi-CELL XR Cell Viability Analyzer (Beckman Coulter, Inc.) at the indicated time points. Cells were plated in duplicatefor each experiment, and each experiment was done in triplicate.

2.4 Cell survival assay

For survival analysis, cells were plated as described above for the proliferation assay. Twenty-four hours after plating, cells were starved by washing with PBS and refreshing with media supplemented only with antibiotics. After 48 hrs in starvation conditions, cell viability was measured using a Vi-CELL XR Cell Viability Analyzer. Cells were plated in duplicat for each experiment, and each experiment was done in triplicate.

For cisplatin treatment, 1×10^4 cells were plated in 96-well plates. The next day, 12.5, 25 and 50µg/ml of cisplatin was added to the media. After 48hrs of exposure to cisplatin, 20µl of Alamar Blue (Sigma-Aldrich, St. Louis, MO) was added and the cells incubated, protected from light, for 2 hrs at 37°C. Absorbance was measured using a Fluoroskan Ascent FL fluorometer (Thermo Scientific, Milford, Massachusetts). Cells were plated in triplicate for

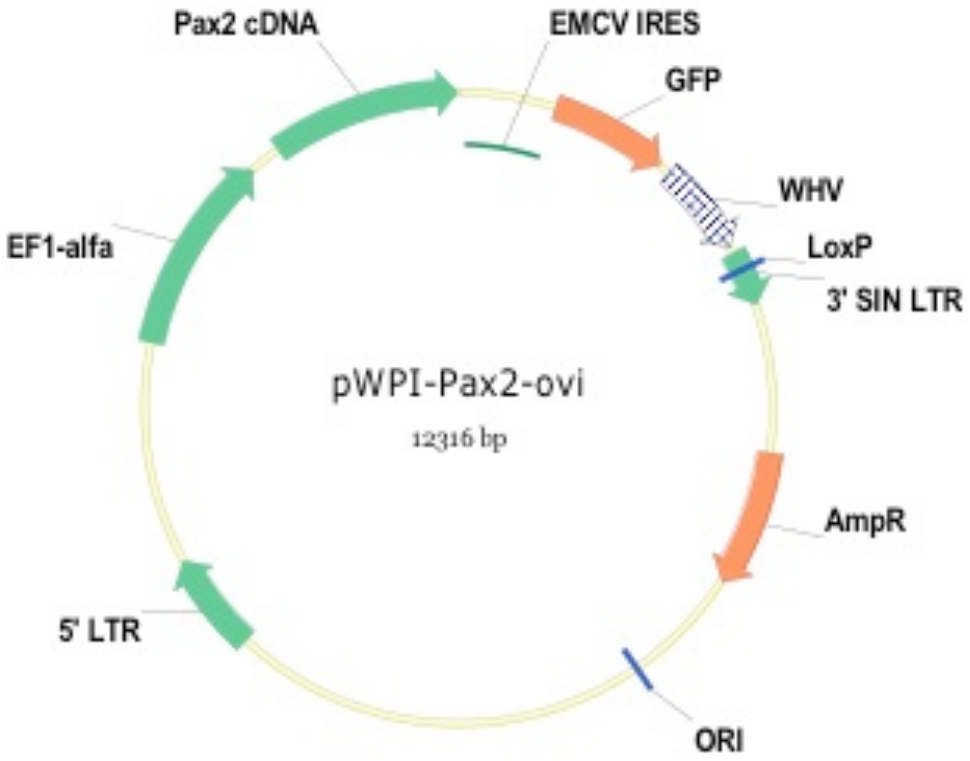

Figure 7: Schematic presentation of the PAX2 lentivirus vector, showing the PAX2-IRES-eGFP transcript expressed from the EF1-a promoter. The *Pax2*cDNA, corresponding to the pax2-b variant, was cloned from the murine oviduct. The loxP site indicated in the pWPI-Pax2-IRES-eGFP vector map is present in both the 5' and 3' LTRs in the integrated virus such that treatment with Crerecombinase leads to excision of the PAX2-IRES-eGFP expression cassette.

each experiment, and each experiment was done in triplicate.

2.5 Colony formation in soft agar assay

After releasing the cells from adherent cultures using trypsin, a single cell suspension was achieved by passing cells through a 40-µm cell strainer (Becton-Dickinson). In a 6-well plate, a base agar layer was made of 1.5 ml of 1:1 mixture of 2X D-MEM medium containing 20% FBS and 1.5% ultra pure low melting point (LMP) agarose (Life Technologies). The layer was solidified at 4°C and warmed to 37°C at least 15 minutes prior to the addition of the top layer. The top layer solution (1ml) consisted of an equal volume-mixture of 2X D-MEM medium containing 20% FBS, 1.2% LMPagarose and $1X10^5$ cells in single cell suspension. This layer was solidified at 4°C and then incubated at 37°C for the indicated periods of time. Colonies were visualized using the EVOS XL imaging system (Life Technologies Inc., Burlington, ON) and counted using ImageJ software.Cells were plated in duplicate for each experiment, and each experiment was done in triplicate.

2.6 Estrogen treatment

OVCA432 and OVCAR3 cell lines were seeded at the appropriate concentration in10 cm dishes (Corning Inc., Corning, NY) to reach r about 50% confluence after 48hrs. Then, they were treated with either 100 nM of estrogen (Sigma-Aldrich, St. Louis, MO) or the vehicle control, Ethanol. After 4 and 24 hrs of treatment, the cell lysates were used for protein and RNA analysis.

2.7 Migration assay

Migration assays were performed utilizing Radius™ 24-Well Cell Migration Assay (Cell

Biolabs, Inc; San Diego, CA) following the manufacturer's instructions. The Radius cell culture plate contains a carefully defined non-toxic, biocompatible hydro gel [Radius Gel spot 0.68 ± 0.014 mm in diameter] centralized at the bottom of each well. After plating 1×10^5 cells/well for all mOSE cell lines and 0.5×10^5 cells/well for STOSE and RM cells, the cells were allowed to attach and grow. At 0 hours, when the cells reached 90-100% confluence, the Radius Gel was removed, allowing migratory cells to move into the cell free area and close the gap. The wound-healing process was monitored carefully through 48hrs. At the endpoint, cells were stained with DAPI and pictures were taken using the EVOS XL imaging systemand by fluorescent microscopy (Axioskop 2 MOT plus, Zeiss, Thornwood, NY)using the Axiovision software (Allied High Tech Products, Rancho Dominguez, CA). Cells were plated in duplicate for each experiment, and each experiment was done in triplicate.

2.8 PCR: confirmation of DNA recombination

After the cells were released from adherent cultures using trypsin, the reaction was stopped using FBS-supplemented media. Cells were then centrifuged and washed with PBS. After removing the PBS, the pellets were kept at -80°C for RNA or DNA extraction. Genomic DNA was extracted using QIAamp DNA Blood Mini Kit (Qiagen) following the manufacturer's protocol. Genotyping for the $p53^{flox/flox}$and $p53^{\Delta 2\text{-}10}$ alleles was performed on genomic DNA using primers p53int1 forward [F](5' CAC-AAA-AAA-CAG-GTT-AAA-CCC-AG 3') and primers p53int1 reverse [R](5' AGC-ACA-TAG-GAG-GCA-GAG-AC 3') to yield a 288 bp band for wild-type p53 or a 370 bp band for the floxed sequences. To detect the presence of the *LoxP* site in exon 10, we used primers for p53int10 F (5′ AAG-GGG-TAT-GAG-GGA-CAA-GG 3′) and p53int10 R (5′ GAA-GAC-AGA-AAA-GGG-GAG-GG

3′), which yield a 431 bp or a 584 bp fragment for wild type and floxed sequences, respectively. For detection of Cre-mediated excision of exons 2–10 of p53 (named $p53^{\Delta 2\text{-}10}$), primers p53int1 F and p53int10 R were used, yielding a 612 bp product. Remaining unrecombined sequence following Cre exposure was detected using primers p53int1 F and p53int1 R or primers p53int10 F and p53int10 R.

The PCR reactions were prepared in 20 µl volumes consisting of: 1µg of genomic DNA, 1X PCR buffer, 2.5 mM $MgCl_2$, 0.1 mMdNTPs, 1nmole of forward and reverse primers and 0.05 U/µlTaq (Life Technologies Inc.). PCR conditions were as follows: 94ºC for 5 min; 30 cycles of 94ºC for 30 sec, 60ºC for 30 sec, and 72ºC for 60 sec, followed by 72ºC for 10 min. Samples were then analyzed by gel electrophoresis on 1.0% agarose gels in Tris-acetate-EDTA (168) buffer.

2.9 Gene expression analysis

2.9.1 Q-PCR

RNA was extracted from cell pellets, either fresh or stored at -80ºC, using an RNeasy Mini Kit (Qiagen) following the manufacturer's instructions. After the RNA was quantified, cDNA was made by reverse transcriptase PCR (RT-PCR) from 1000 ng of RNA using the OneStep RT-PCR Kit (Qiagen). Gene expression was determined by relative quantitative PCR (Q-PCR) and performed on an ABI 7500 FAST qRT-PCR machine (Applied Biosystems) using the SsoFast gene expression Master Mix (Bio-rad) following the manufacturer's instructions. The real-time thermo-cycler program was 95°C for 10 min, followed by 40 cycles of 95°C for 10 sec and 60°C for 30 sec. Primer pairs to amplify murine *Pax2* (forward [F], 5′-GGC-ATC-TGC-GAT-AAT-GAC-ACA-3′; reverse [R],5′-

GGT-GGA-AAG-GCT-GCT-GAA-CTT-3′), *Htra1* (F,5′-CAT-CTA-GCA-AAG-CCA-AAG-AGC-3′; R, 5′-ACT-GTC-CGT–TGA-TGC-TGA-TG-3′), *Trp53* (F,5′-ACG-CTT-CTC-CGA-AGA-CTG-G-3′; R,5′-AGG-GAG-CTC-GAG-GCT-GAT-A-3′), and *Ppia* (F,5′-AGG-GTG-GTG-ACT-TTA-CAC-GC-3′; R,5′-GAT-GCC-AGG-ACC-TGT-ATG-CT-3′) were designed using OligoPerfect primer design software (Invitrogen). Expression of *Ppia* mRNA was used as the endogenous control.

2.9.2 Microarray analysis

Microarray analysis was performed on independent duplicates from M0505+WPI, M0505+PAX2 and M0505+PAX2+Cre. cDNA was prepared as describedabove and whole genome expression was determined using the Affymetrix Gene Chip Mouse Gene 1.0 ST platform. Genes were annotated using T4-MEV software (Dana Farber Cancer Institute, Boston) and linear fold change was determined from robust multiarray-average (RMA) normalized expression values. Dr. Euridice Carmona (l'Université de Montréal, Montréal, QC, Canada) used Ingenuity Pathway Analysis software (IPA; ngenuity Systems, Qiagen) to determine functionally relevant clusters of differential gene expressionwith a fold change cutoff of 2 and P value of <0.05. Gene function was inferred using Gene Ontology (GO) terms, and GO enrichment was determined using R package GOstats.

2.10 Protein analysis

2.10.1 Immunofluorescence

In a 6-well flat-bottomed plate, glass cover slips (Fisher Scientific) were placed into each well and 0.5-1X10^5 cells were plated in each well. After 48-72 hrs, the cells were washed with PBS and then fixed with 4% paraformaldehyde (Sigma) buffered in PBS for 15 min at

37°C. Prior to immunofluorescent staining, the cells were permeabilized with PBS+0.2%Triton X-100 (Sigma) for 15 min. Subsequently, they were blocked for 30 min with PBS+3% normal goat serum. After blocking, the cells were incubated with the mouse PAX2 antibody (Santa Cruz) at a dilution of 1:200 in PBS over night. The cells were then blocked with PBS+5% normal goat serum (Sigma) for 30 min. After that, they were incubated with Alexa Fluor 488 Goat anti-mouse IgG (10 μg/ml) (Molecular Probes, Carlsbad, CA) protected from light for one hour. The cells were then mounted to a microscope slide with 4',6-diamidino-2-phenylindole (DAPI) mounting media (Vector Laboratories, Burlingame, CA) and analyzed under fluorescent microscopy (Axioskop 2 MOT plus, Zeiss) using the Axiovision software.Control experiments were done in parallel in which primary antibody was omitted.

2.10.2 Western Blot Analysis

Proteins were extracted from cell lines using M-PER mammalian lysis buffer (Thermo Scientific) containing 1X protease and phosphatase inhibitors (Halt™ protease inhibitor cocktail kit and Halt™ phosphatase inhibitor cocktail kit, Pierce, Rockford, IL, USA) and 1 mM of phenylmethanesulfonyl fluoride (PMSF; Sigma-Aldrich). To extract proteins from tissues, tissues were homogenized in the radioimmunoprecipitation assay (RIPA) buffer (50 mMTris-HCl, pH 7.6, 100 mMNaCl, 5 mM EDTA, 0.4% [v/v] NP-40, 10% [v/v] glycerol) containing protease inhibitor cocktail and PMSF. Protein concentration was measured using a Bradford Protein Assay Kit (Bio-Rad Laboratories, Mississauga, ON) and a Beckman DU® 640 Spectrophotometer (Beckman Coulter Inc.). Protein samples (40μg) were separated on 4-12% Bis-Tris pre-cast polyacrylamide gels (Invitrogen). Using Trans-Blot® Turbo™ Transfer System (Bio-Rad Laboratories), proteins were transferred to a nitrocellulose

membrane (Hybond C Extra, Amersham, Oakville, ON). Blocking was carried out with 5% milk in Tris-buffered phosphate with Tween-20 (TBS-T). For all subsequent immunoblotting, antibodies were diluted to the appropriate concentration in 5% milk in TBS-T. Blots were incubated for 2 hrs at room temperature or overnight at 4ºC with the following primary antibodies: mouse monoclonal PAX2 (1:20,000, Santa Cruz, Dallas, Texas), mouse anti-P53 (1:1000, Cell signalling, Beverly, Massachusetts), rabbit anti-COX-2 (1:1000, Abcam, Cambridge, UK), rabbit anti-EGFR (1:1000, Cell Signalling), rabbit anti-AKT (1:1000, Cell Signalling), rabbit anti-pAKT (1:1000, Cell Signalling), rabbit anti-ERK1/2 (1:1000, Cell Signalling), mouse anti-pERK1/2 (1:1000, Santa Cruz), mouse anti-SMA-α (1:200, Abcam), mouse anti-TAg (1:500, Santa Cruz), mouse GAPDH (1:10 000, Abcam) and mouse β-actin (1:50 000, Sigma-Aldrich). Then, blots were incubated with the corresponding anti-rabbit or anti-mouse horseradish peroxidase-conjugated secondary antibodies (1:5000; Cell Signalling). Visualization of protein bands was performed using the ECL Plus western blotting detection system (Amersham) and blots were imaged on a FluorChem E gel documentation system (ProteinSimple, Santa Clara, CA).

2.10.3 Immunohistochemistry (IHC)

Paraffin sections were deparaffinized in xylene and rehydrated in ethanol according to standard protocol. High temperature antigen retrieval was performed using sodium citrate buffer (pH 6; Antigen Unmasking Solution; Vector Laboratories) in a pressure cooker (Tender Cooker; Nordic Ware). Endogenous peroxidase activity was blocked using 3% hydrogen peroxide in Stockholm PBS (S-PBS). PAX2 and CD31 expression was visualized with a rabbit anti-PAX2 antibody (1:1000, Abcam) and a rabbit anti-CD31 antibody (1:100). Primary antibodies were diluted in S-PBS and incubated at room temperature for 1 hr.

Following 3 washes (5 min each) in S-PBS, sections were incubated with Dako Envision system-HRP labeled polymer anti-rabbit antibodies (K4003, Dako Canada, Burlington, ON) for 30 minutes. Detection was performed using diaminobenzidine (111) as a substrate (0.2% DAB, 0.001% H_2O_2; Sigma-Aldrich). Slides were counterstained with Harris hematoxylin, dehydrated and mounted with Permount (Fisher Scientific). Images were obtained with the ScanScope CS system and ImageScope software (Leica Microsystems Inc. Concord, ON). Control experiments were done in parallel in which primary antibodies were omitted.

2.10.4 Immunoprecipitation and immunodepletion

Immunoprecipitation and immunodepletionwere done using PureProteome™ Magnetic Beads protein G beads (EMD Millipore (Canada) Ltd, Etobicoke, ON). For immunoprecipitation, 400 μg of proteins were incubated with the indicated antibodies overnight at 4°C with rotation. Immunoprecipitates were washed three times with TBS-T. Samples were eluted by boiling beads in 2X SDS-PAGE sample buffer containing 50 mM DTT for 10 min. The supernatant was subjected to SDS-PAGE and western blotted for the target proteins.

The immunodepletion procedure for tumor and tissue samples was done to remove the host immunoglobulins and it was repeated at least twice for each sample. Protein lysates were incubated with the PureProteome™ Magnetic Beads protein G beads on a rotator for 2 hrs at room temperature. Samples were then centrifuged and supernatants were kept at -80°C until further analysis was needed.

2.11 Animal experiments

Animal experiments were performed in accordance with the Canadian Council on Animal Care's *Guidelines for the Care and Use of Animals* under protocols approved by the

University of Ottawa Animal Care Committee. Severe combined immunodeficient (SCID) and FVB/N mice were obtained from The Jackson Laboratory. Cells (1×10^7 in 500 μL PBS) were injected into the peritoneal cavity of SCID or FVB/N mice using a 25-gauge needle (Becton-Dickinson). Animals that were injected with cells were monitored for disease progression and were euthanized when they reached humane endpoints or when the experiment reached a predetermined termination date. The humane endpoints included 15% weight gain, tumor ulceration, and/or abdominal distension. Necropsies were performed at endpoint and tumors were either fixed in 10% buffered formalin for 24hrs, paraffin embedded and sectioned at 5μm for histological analysis, or were snap-frozen for RNA or protein analysis.

2.12 Statistical analyses

Based on the number of conditions tested, a Student t-test or an ANOVA with a Tukey post-test was used to determine statistical significance ($P < 0.05$). All data are presented as the mean ± standard error of the mean. Kaplan–Meier survival curves were compared using a Log-rank test and significance was also inferred at $P<0.05$. Statistical analyses were carried out using GraphPad Prism software (GraphPad, La Jolla, CA).

RESULTS

3.1 PAX2 and tumorigenicity

3.1.1 PAX2 is expressed in the Fallopian tube and uterus, but not in the ovaries of mouse tissue

Although PAX2 expression has been widely reported in the developing reproductive tract in mice (74), there is no report showing PAX2 expression in murine adult female reproductive tract. Therefore, we started the study by looking at PAX2 expression in the female reproductive system, with special considerationof the ovaries. By IHC staining, PAX2 was expressed in the epithelial cells of the murine oviduct and uterus, but not the ovary (Fig. 8), similar to its reported expression in the human reproductive tract (92, 93).

3.1.2 PAX2 enhances proliferation in mOSE cells

To investigate the biological consequences of PAX2 induction in normal mOSE cells, we used three independent isolations of mOSE cells placed in primary culture (M0505, M1102 and mOSE-fxp53). Forced expression of PAX2 proteins was achieved by lentiviral infection and confirmed by immunoblotting and immunofluorescence (Fig. 9A and B). In addition, PAX2 expression in the infected cells was confirmed by qPCR anaylsis, in comparison with murine oviductal epithelium (Fig.10).

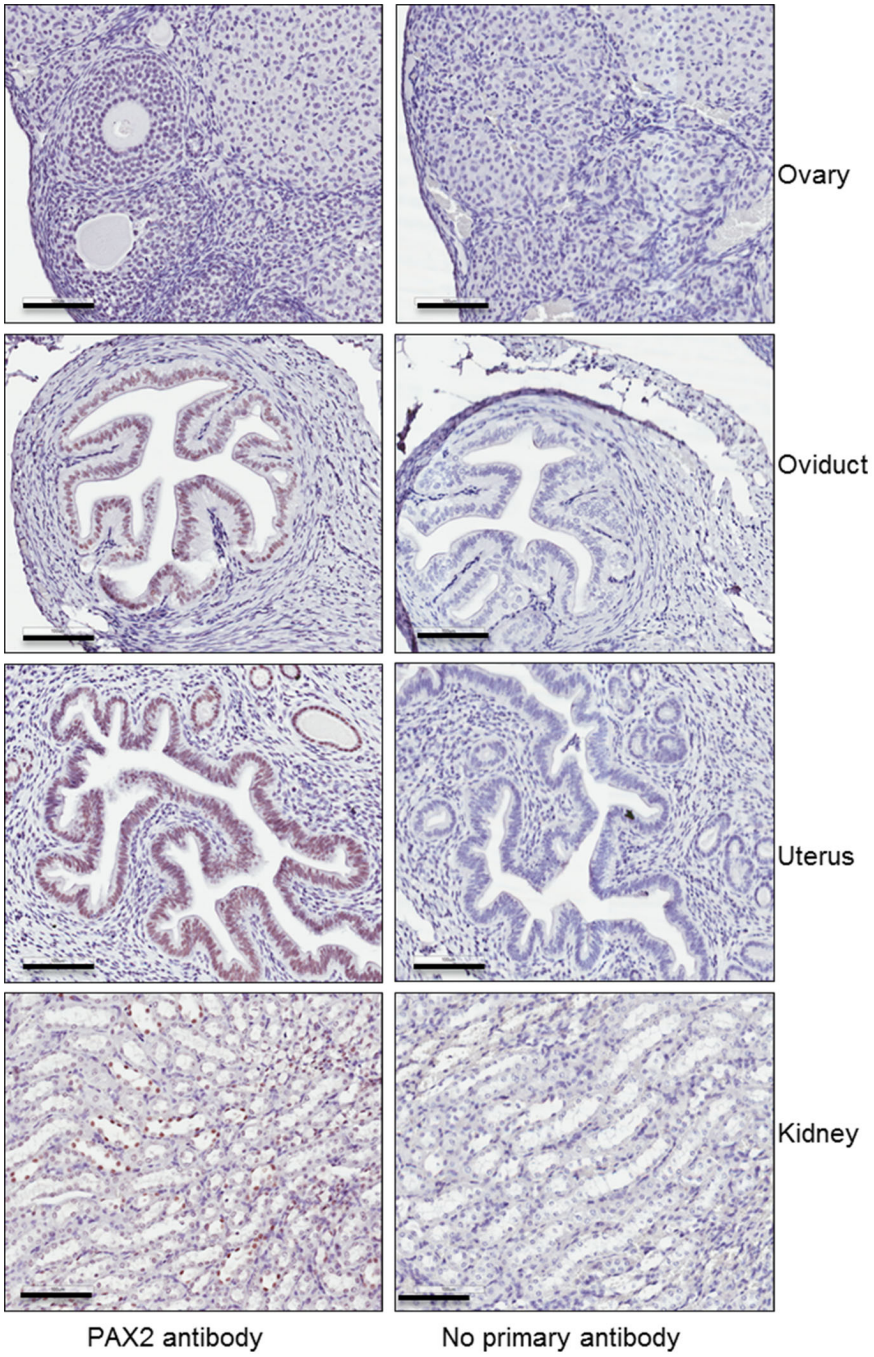

Figure 8: IHC analysis shows that PAX2 is expressed in the epithelium of the murine oviduct and uterus, but not in the ovary. Kidney is shown as a positive control. Scale bar is 100 μm.

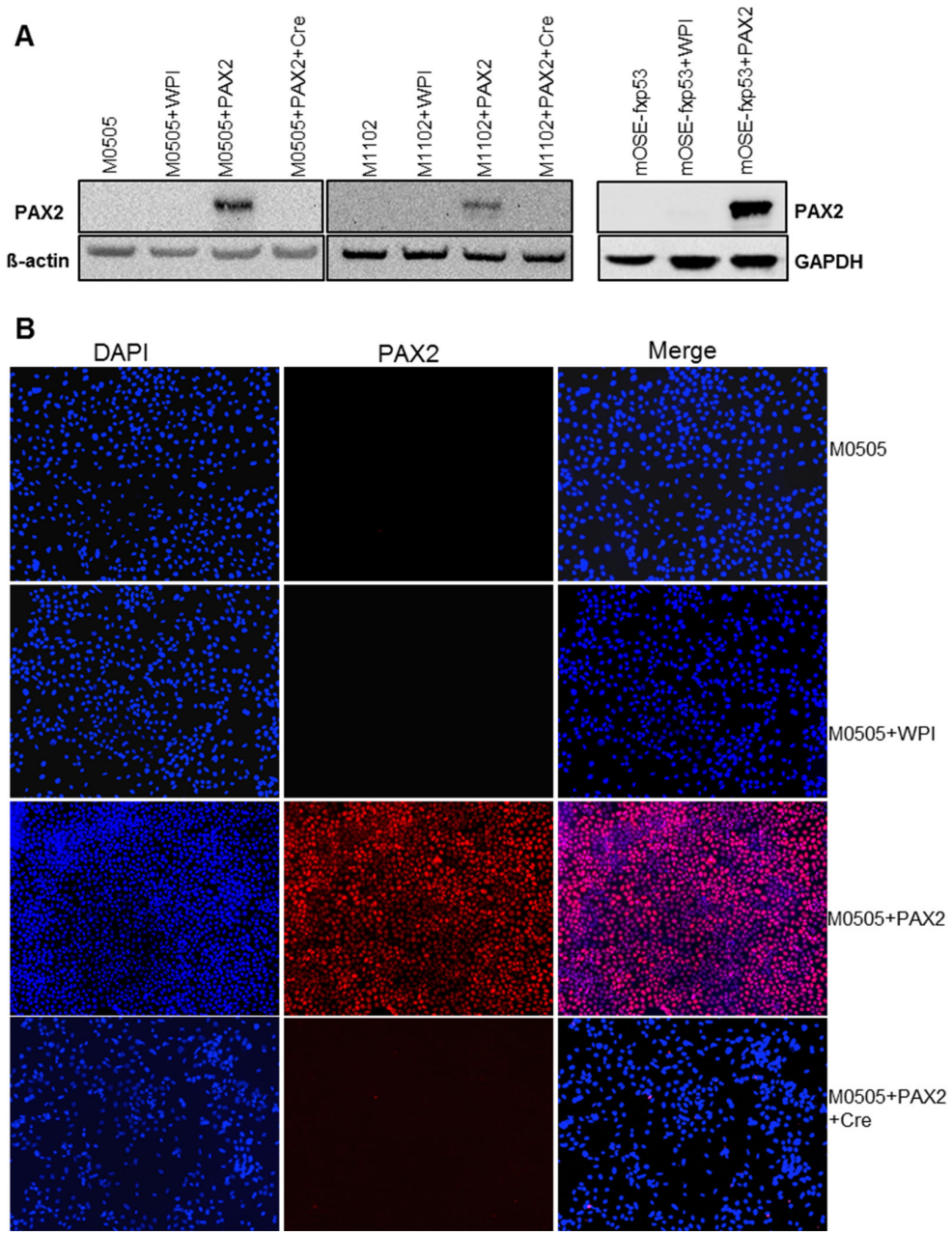

Figure 9: Expression of PAX2 in mOSE cells. (A) Western blot analysis to detect PAX2 expression in three lines of mOSE cells, each line transduced with vector (WPI) or a PAX2 expression vector (PAX2). In two cell lines, the PAX-transduced cells were subsequently treated with AdCre for cre-mediated deletion of the lentiviral provirus (PAX2+Cre). (B) Immunofluorescence of the M0505 cells showing expression of PAX2 in transduced cells, and with subsequent loss of PAX2 after AdCre infection.

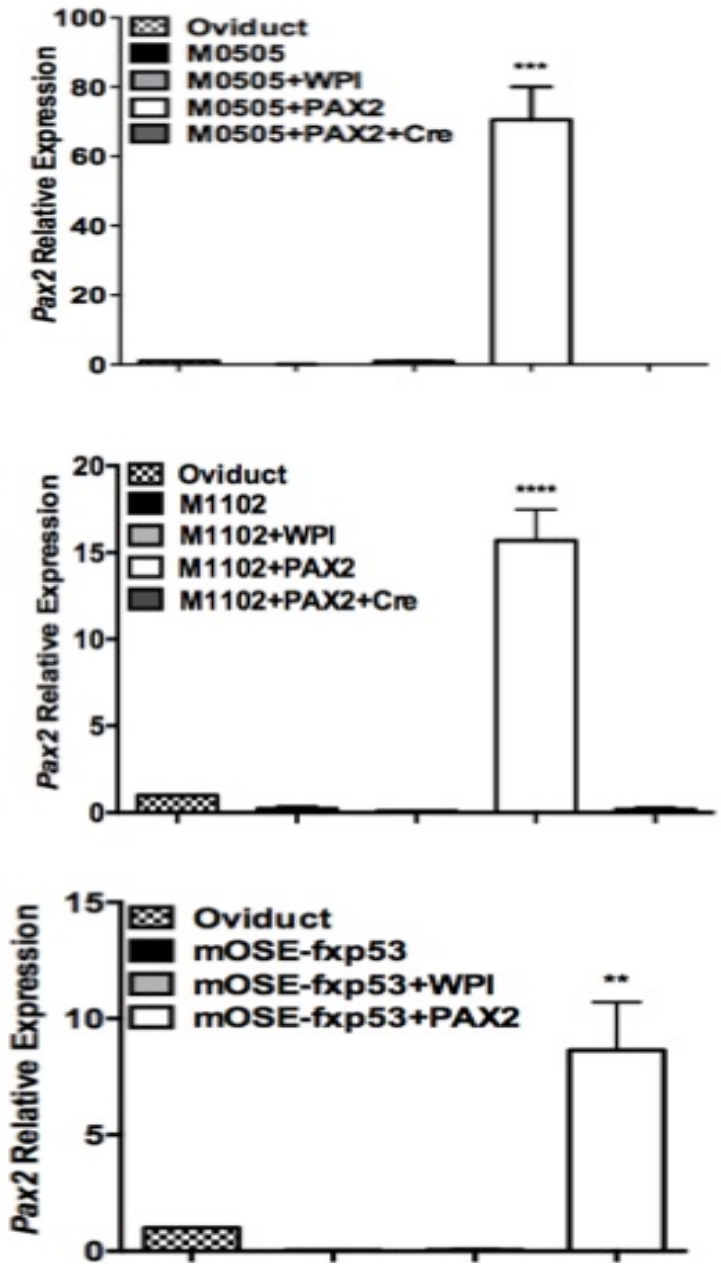

Figure 10: Induced expression of PAX2 in mOSE cells, as shown by qPCR analysis. The level of the forced expression is compared to endogenous expression of PAX2 in oviductal cells.

In all three mOSE cell lines, PAX2 significantly enhanced cell proliferation (Fig. 11A), without changes in their viability (Fig. 11B). When control cells were deprived of growth factors (starvation conditions), their proliferation was significantly inhibited, but PAX2 overcame this inhibition in all three cell lines, at least partially, supporting the notion that PAX2 has this characteristic of a potential proto-oncogene (Fig. 12A).

3.1.3 PAX2 enhances survival in mOSE cells

Since PAX2 was suggested to be a proto-oncogene and since the failure to initiate cell death following exposure to apoptotic stimuli is another feature of cancer cells as identified by Hanahan and Weinberg (120), we investigated the effect of its expression on survival of normal mOSE cells. To determine the effect of PAX2 on cell survival, cells were challenged by deprivation of growth factors, and the percentage of viable cells was normalized to viability of cells that were supplemented with growth factors. Only a limited decrease in cell viability (14-18%) was observed in the parental lines as seen in Fig. 12B. Expression of PAX2 enhanced survival significantly, albeit modestly, in M0505 cells, with a similar trend for enhanced survival in PAX2-expressing M1102 and mOSE-fxp53 cells as compared to non-expressing controls ($p=0.0725$ and $p=0.0593$, respectively; Fig. 12B).

In addition, exposure to the DNA-damaging agent, cisplatin, for 48hrs resulted insignificant decrease in number and viability of mOSE cells in a dose-dependent manner(Fig. 13). PAX2 expression in those cells resulted inno changes in cell number (Fig. 13A), buta significant increase in cell viability, confirming that it shares this characteristic of survival enhancement with other oncogenic proteins (Fig. 13B).

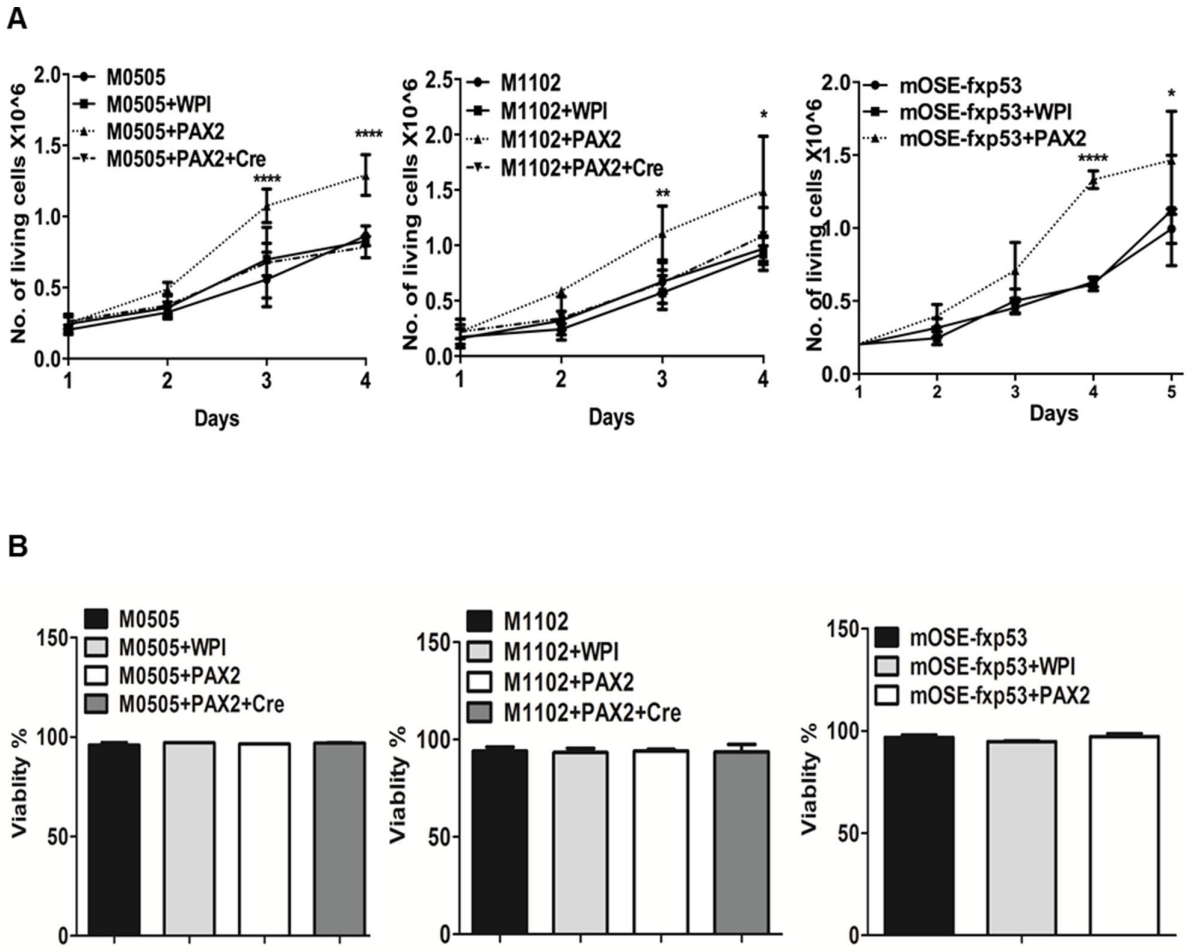

Figure 11: PAX2 enhances proliferation in normal mOSE cells. Expression of PAX2 increases the proliferation rate significantly (A) but did not change survival (B) in M0505, M1102 and mOSE-fxp53 cells when cells are grown in complete media for up to four days, as indicated.B: Percentage of viable cells (with and without PAX2 expression), showing that PAX2 has no effect on cells viability under normal growth conditions. Viability and viable cell number was calculated using trypan blue exclusion. Analyses were done using two-way ANOVA. All experiments were performed at least three times, each time in duplicate. *p<0.05, **p<0.01, ***p<0.001, ****p<0.0001.

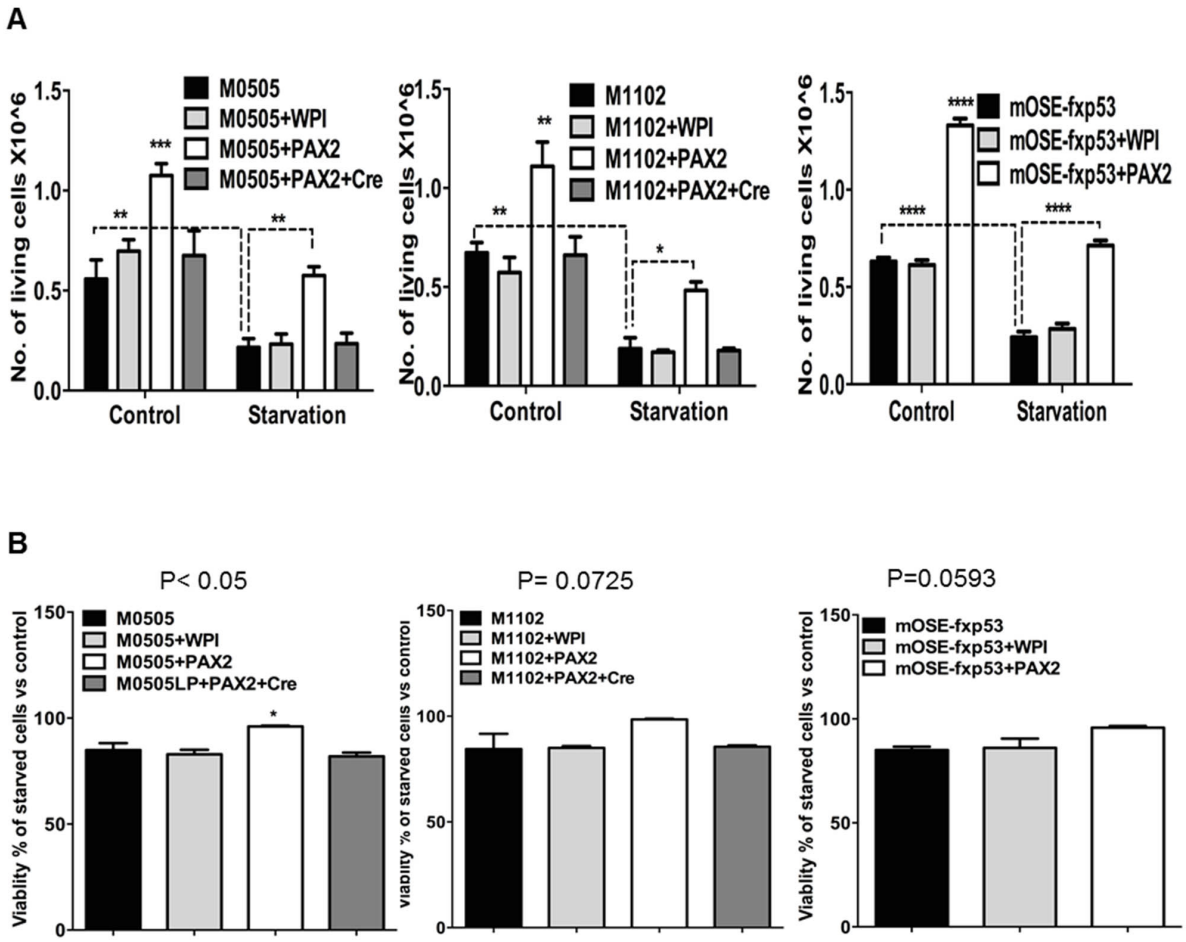

Figure 12: PAX2 enhances growth signals independency in mOSE cells. A: Expression of PAX2 increases the proliferation rate significantly in M0505, M1102 and mOSE-fxp53 cells when cells are grown in growth factor and serum free starvation media. Cells were grown in culture for up two days (M0505 and M1102) or three days (mOSE-fxp53). B: Percentage of viable cells after growth factor withdrawal (48hrs for M0505 and M1102; 72hrs for mOSE-fxp53). PAX2 modestly enhances survival of growth factor-deprived M0505 cells ($p<0.05$). Similar effects were observed in M1102 and mOSE-fxp53 cells, although the differences did not reach significance ($p= 0.0725$ and $p=0.0593$, respectively).Viability and viable cell number was calculated using trypan blue exclusion. Analyses were done using two-way ANOVA. All experiments were performed at least three times, each time in duplicate. *$p<0.05$, **$p<0.01$, ***$p<0.001$, ****$p<0.0001$.

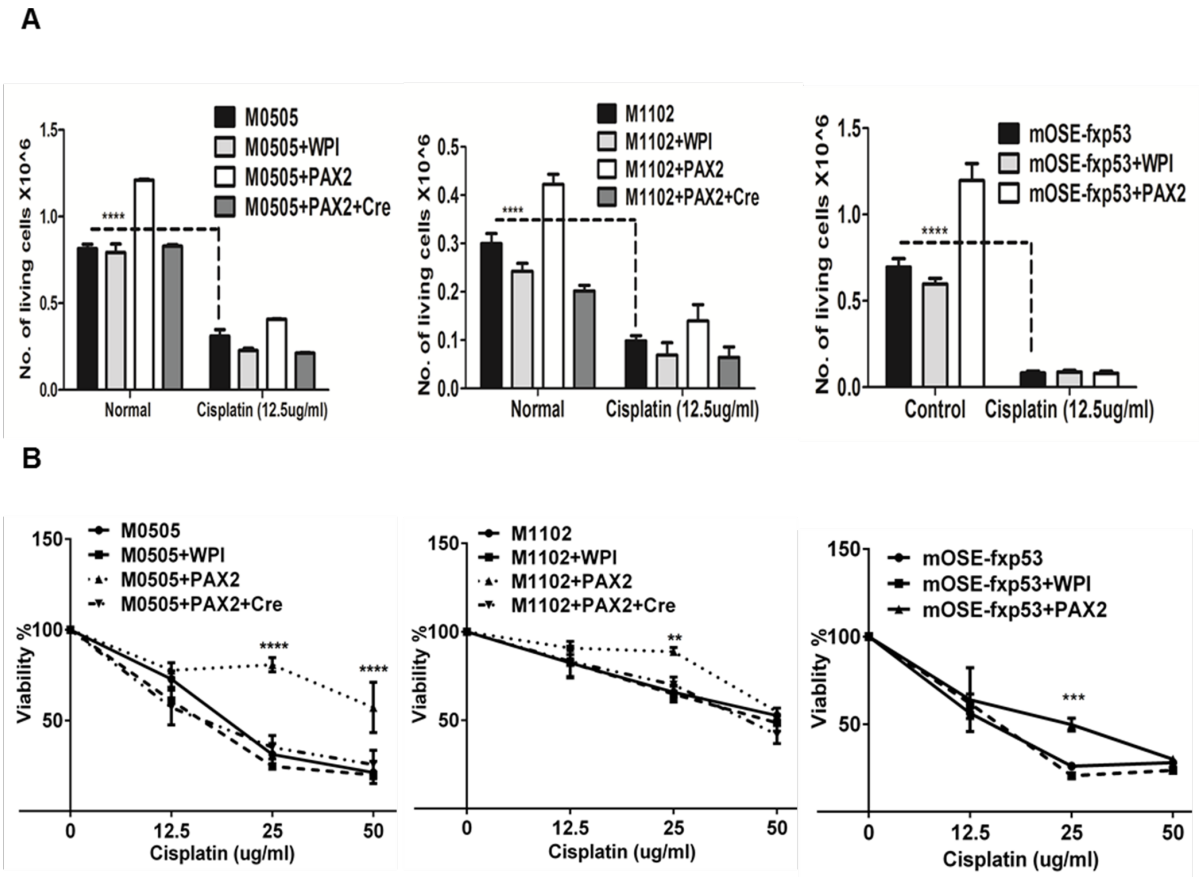

Figure 13: PAX2 enhances survival in normal mOSE cells following treatment with cisplatin. A: PAX2 expression in mOSE cells did not affect the number of proliferating cells following cisplatin treatment. Viable cell number was calculated using trypan blue exclusion. B: PAX2 induction in mOSE cells enhances resistance to cisplatin. Cells were exposed to the indicated concentration of cisplatin for 48hrs and cell viability was measured using Alamar Blue assay. All experiments were performed at least three times, each time in triplicate. Analysis was done using two-way ANOVA (*p<0.05, **p<0.01, ***p<0.001, ****p<0.0001).

3.1.4 PAX2 inhibits p53 induction by cisplatin

Since our results showed that PAX2 enhances resistance to cisplatin and it has been shown previously that PAX2 has a binding site in the first exon of *Trp53* in murine cells (132), we investigated the effect of PAX2 on cisplatin-induced P53. Exposure to cisplatin increased P53 accumulation significantly in two different mOSE cell lines (Fig. 14A). Thecisplatin-induced increase in P53 was significantly suppressed in PAX2-expressing cells, reaching only 40% of the levels induced in control cells (Fig. 14A and B). However, PAX2 expression did not change the levels of *Trp53* transcripts (Fig. 14C), indicating that PAX2 affects the translation and/or stabilization of P53, but not the transcription of *Trp53*. It is worth mentioning that sequencing of *Trp53* in M1102 and M0505 showed that both cell lines have no evident mutations in*Trp53*.

3.1.5 PAX2 enhances the epithelial morphology in mOSE cells

In human, the OSE cells are poorly differentiated cells and they undergo MET as a prerequisite for their neoplastic transformation (16). In mouse, mOSE cells show cuboidal epithelial morphology (Fig. 15A). Interestingly, forced expression of PAX2 induced a more distinct epithelial morphology (Fig. 15A). In addition, PAX2-expressing cells appeared more compact as they grow in epithelial nests and are more strongly attached than their counterparts. Diameter analysis shows that PAX2-expressing cells are smaller than the vector control cells (Fig.15B). The change in morphology and reduced size suggests that PAX2 might activate a MET program in mOSE cells. Taken together, the results so far indicate that the changes resulting from a gain of PAX2 expression are in accordance with the early events associated with OSE transformation.

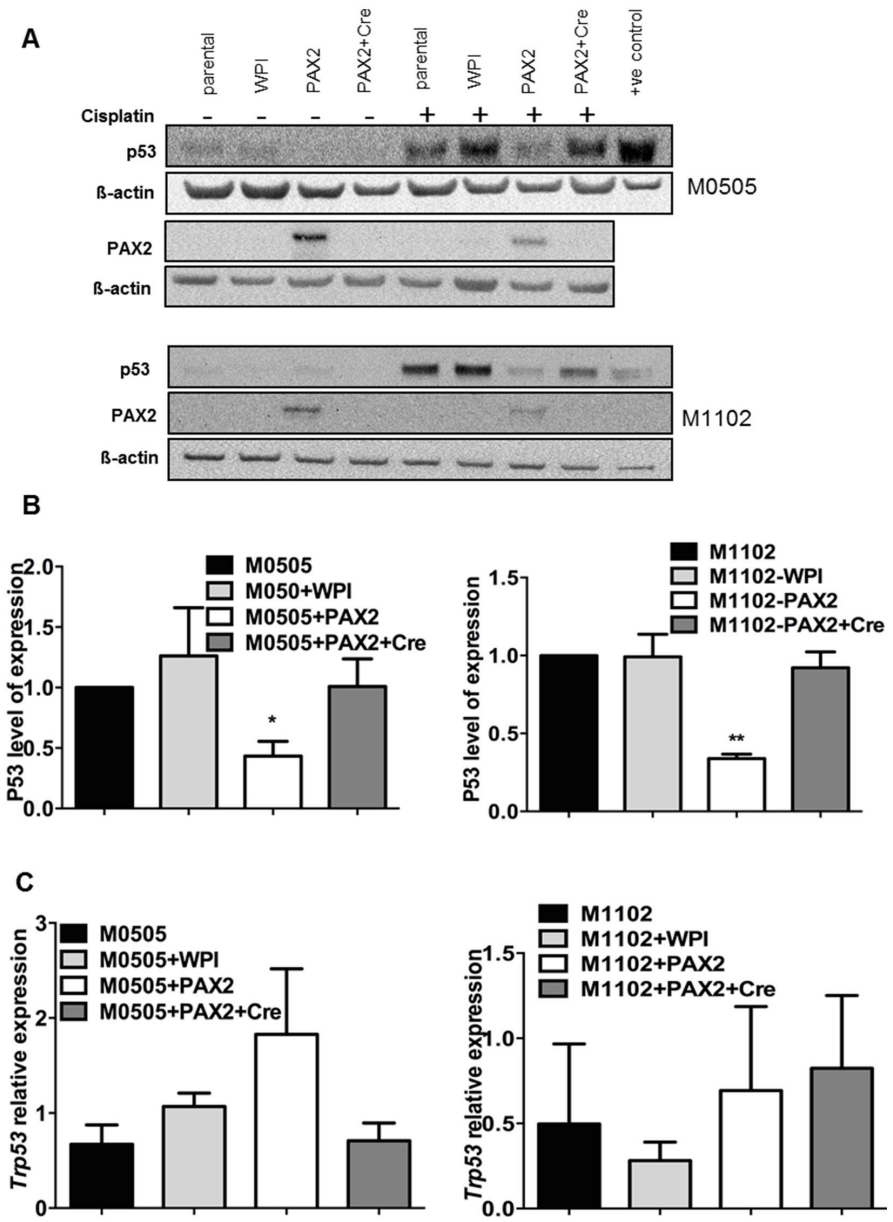

Figure 14: PAX2 inhibits cisplatin-induced P53 in mOSE cells. Control mOSE cells (parental, WPI, PAX2+Cre) and PAX2-expressing cells were treated with 12.5µg/ml of cisplatin for 48hrs. A: Western blot analysis was done for P53 in M0505 and M1102 cells before and after cisplatin treatment. The last lane is protein lysate from mouse embryonic fibroblasts (+ve control) that was collected 4hrs after exposure to UV (10 joules for 5 seconds). B: Histograms represent densitometric analysis of the induced P53 levels that were normalized to β-actin (N=3). Level of P53 in cisplatin-treated cells was analyzed using one-way ANOVA. *$p<0.05$, **$p<0.01$. C: *Trp53* mRNA levels, as determined by Q-PCR are similar in PAX2-expressing mOSE cell lines and their relevant controls.

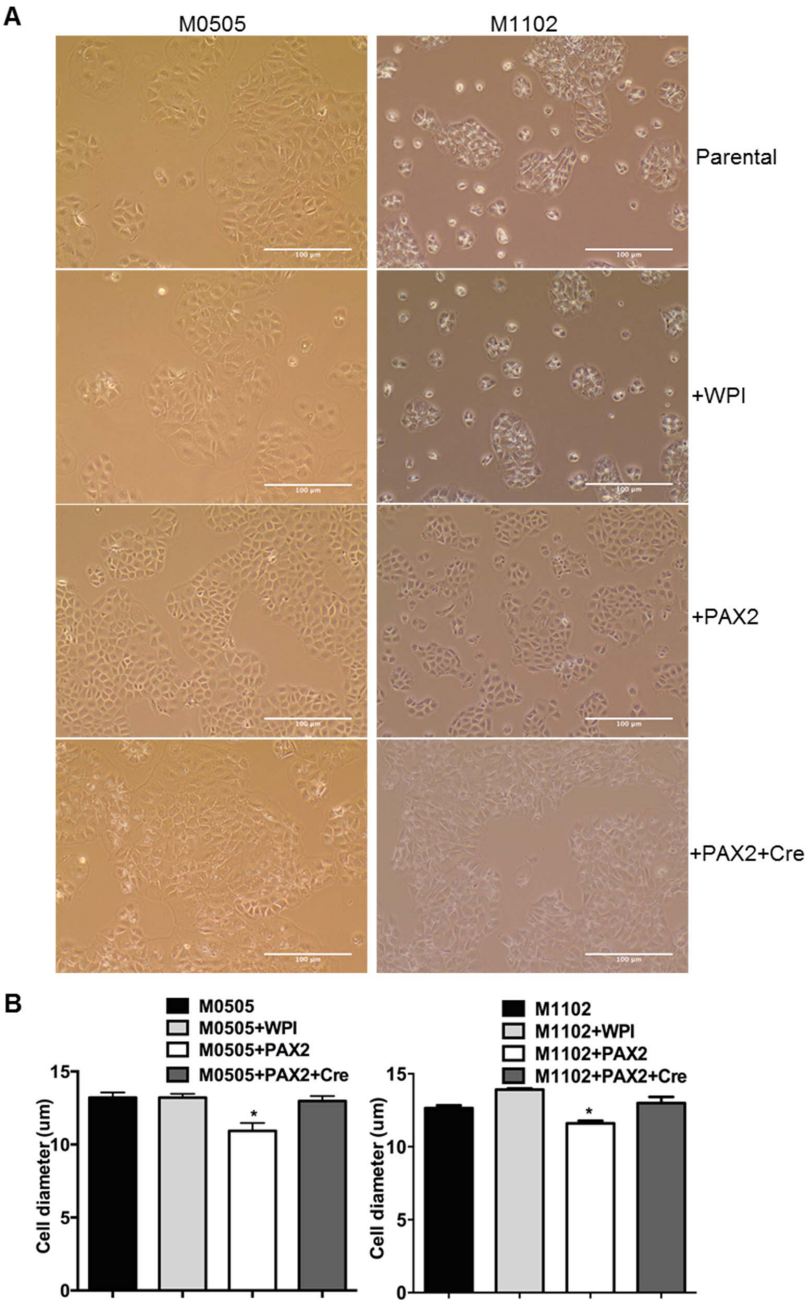

Figure 15: A: PAX2 induces more epithelial morphology in mOSE cells (M0505 and M1102). Pictures were taken using an EVOS microscope (scale bar is 100 µm). B: PAX2-expressing mOSE cells are smaller than the vector-transducedcontrol cells. Diameter was measured using the Vi-CELL XR Cell Viability Analyzer. Measurements were taken from 3 different passages from 2 independently derived sets of cell lines.

3.1.6 PAX2 deregulates cancer-associated pathways in mOSE cells

To better understand the role of PAX2 in mOSE cells, whole genome microarray analysis was performed on M0505+PAX2 and compared to M0505+WPI and M0505+PAX2+Cre transcripts. Changes were considered relevant only when a 2-linear-fold difference or more was evident between transcript levels in the PAX2-expressing cells compared with transcripts in both WPI and PAX2+Cre cells. Using these criteria, there were 41 genesupregulated and 58 genes downregulated in PAX2-expressing cells. Ingenuity Pathway Analysis (IPA) showed changes in genes involved in cancer and cellular growth, predicting an activation of cancer-associated functions (hyperplasia and tumor size) and cell proliferation (Fig.16). Table 3lists the top 10 most highly upregulated and downregulated genes in the PAX2-expressing cells compared to the two control cell lines. Many of these genes have been previously reported to be involved in tumor growth and progression, which highlights the prominent role of PAX2 in cancer initiation and development (Table 4). However, whether the identified targets are direct targets for PAX2 is unclear.

3.1.7 PAX2 exhibits oncogenic properties in normal mOSE cells

To determine if PAX2 induction in mOSE might facilitate oncogenic transformation, SCID mice were injected intraperitoneally (i.p.)with 10^7 cells of M0505+WPI, M0505+PAX2 (6 mice per group) or M1102+PAX2 (5 mice). At 114 days post-injection, not sufficient for transformation of ovarian epithelial cells.

Our data clearly show that PAX2 overexpression alone does not cause transformation.In consideration of the multiple hit theory of carcinogenesis (177), we investigated the possibility that PAX2 might need a second “hit” to initiate oncogenesis.

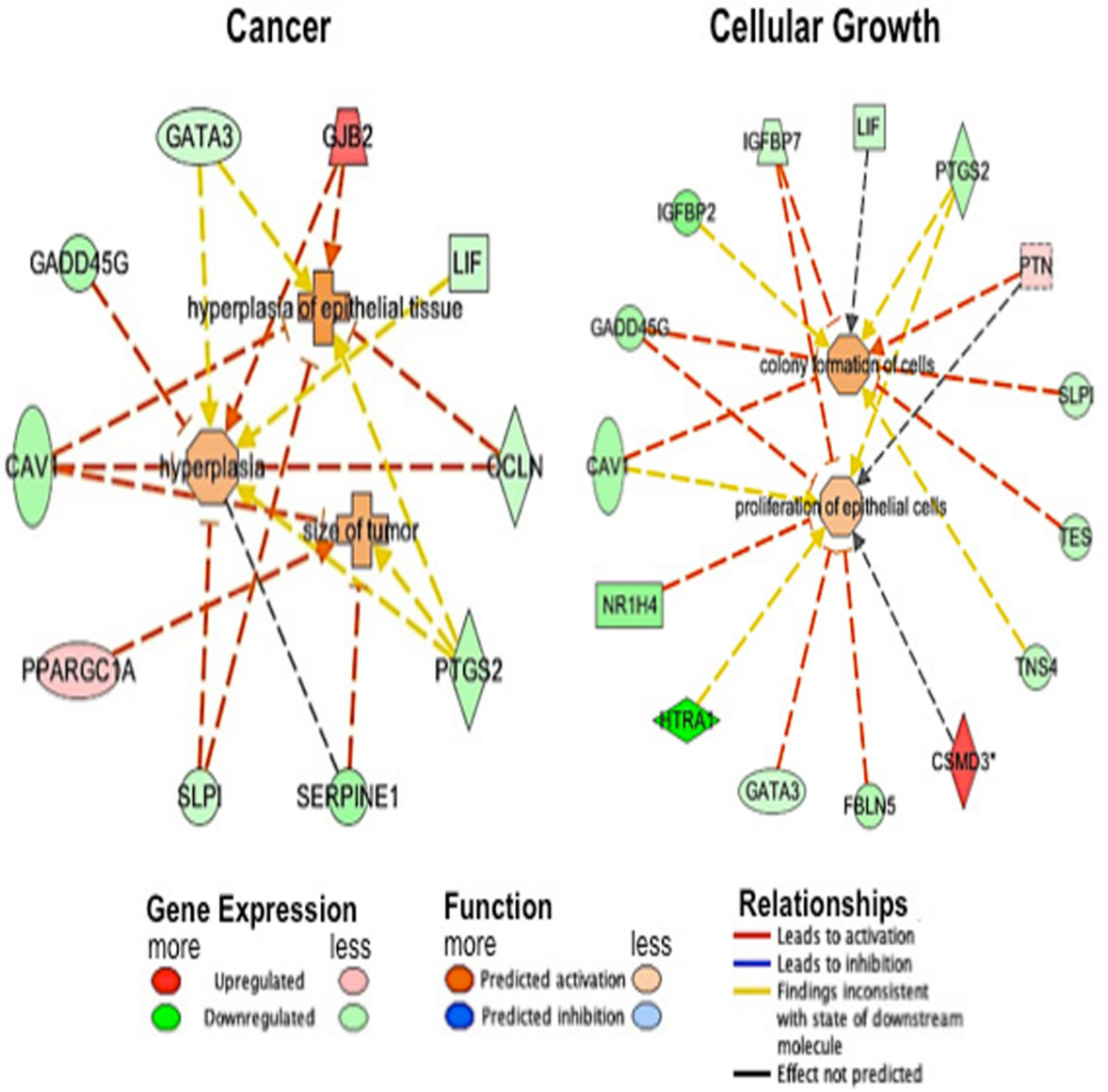

Figure 16: Ingenuity Pathway Analysis (IPA) showing that genes regulated by PAX2 expression are associated with cancer and cellular growth. IPA database was used to assign genes to biological functions and determine functions that were enriched, based on statistical significance. The relationships (lines between regulators) and the nodes (genes) are color-coded based on the predicted relationship as indicated in the legend.

Table 3: The top 10 genes upregulated and downregulated by PAX2 in MO505 cells, as shown by microarray analysis, and their known relationships to ovarian tumorigenesis.

Gene	Exp. Value[1]	Relationship to ovarian cancer
Opcml	11.071	Epigenetically inactivated in epithelial ovarian cancers(169)
Csmd3	9.178	None
Gjb2	7.790	Highly expressed in ovarian cancer cell line(170)
Mboat2	4.342	None
Adcy2	4.260	None
Chst1	4.218	None
Wasf3	3.754	None
Syt9	3.604	None
Serpina3n	3.429	None
Npas2	3.299	None
Htra1	-9.45	Downregulated in ovarian cancers(171, 172)
Gpr115	-7.511	None
Igfbp2	-4.753	Overexpressed in EOC and correlated with tumor stage(173)
Nr1h4	-4.347	None.
Vgll3	-4.305	Downregulated in ovarian cancer tissues(174)
Serpin 1	-3.984	Highly expressed in ovarian tumors(175)
Npn2	-3.962	None
Acta2	-3.676	Prognostic factor associated with progression-free survival in ovarian cancer patients(168)
Anxa3	-3.555	Upregulation is correlated with enhanced drug resistance of ovarian cancer patients (176)
Gadd45g	-3.468	None

[1] Exp. Value denotes Expression Value indicated as fold change, as compared to M0505+WPI and M0505+PAX2+Cre.

Table 4: Functional analysis of genes that were changed in M0505+PAX2 cells compared to M0505+WPI and M0505+PAX2+Cre and are involved in tumor growth and progression.

Diseases or Functions Annotation	p-Value	Molecules
progression of tumor	5.38E-06	ANXA3,CAV1,GATA3,IGFBP2,PTGS2,SEMA3E,SERPINE1
hyperplasia of epithelial cells	1.21E-05	CAV1,GATA3,GJB2,OCLN,SLPI
Serousadenocarcinoma	2.61E-05	ADCY2,IGFBP2,MUM1L1,NPAS2,OCLN,PPAP2A,SLPI
ovarian adenocarcinoma	5.36E-05	IGFBP2,MUM1L1,OCLN,PPAP2A,PTGS2,SLPI
epithelial ovarian cancer	2.91E-04	IGFBP2,MUM1L1,OCLN,PPAP2A,PTGS2,SLPI,TES
hyperplasia of cells	2.91E-04	CAV1,GATA3,GJB2,LIF,OCLN,PTGS2,SLPI
serous ovarian carcinoma process	3.42E-04	IGFBP2,MUM1L1,OCLN,PPAP2A,SLPI
Malignantovarianneoplasm	4.36E-04	IGFBP2,MUM1L1,OCLN,OPCML,PPAP2A,PTGS2,SERPINE1,SLPI,TES
invasion of tumor	9.61E-04	CAV1,PTGS2,SERPINE1,SLPI
size of tumor	1.20E-03	CAV1,PPARGC1A,PTGS2,SERPINE1
growth of tumor	1.74E-03	FBLN5,FCGR3A,FIGF,IGFBP2,LIF,OLR1,PTGS2,SERPINE1
Metástasis	2.21E-03	ACTA2,CAV1,FIGF,HTRA1,IGFBP2,IGFBP7,PTGS2,PTN SERPINE1,TES
mucinous ovarian cancer	4.67E-03	IGFBP2,SLPI
clear cell ovarian carcinoma	6.88E-03	IGFBP2,SLPI
proliferation of epithelial cells	1.56E-04	CAV1,CSMD3,FBLN5,GADD45G,GATA3,HTRA1,IGFBP7,NR1H4,PTGS2,PTN
proliferation of tumor cell lines	2.61E-03	CAV1,EGR2,FBLN5,GADD45G,HSPB8,IGFBP2,IGFBP7,ITGA7,LIF,NR1H4,PTGS2,PTN,SERPINE1,SLPI,TAB3,TES

animals were sacrificed and none had developed tumors, indicating that *Pax2* expression is

Null mutations in *TP53* have been found in (24%) of ovarian cancers (141). In addition, a previous report shows that deletion of P53 in mOSE cells is not tumorigenic, although it sensitizes the cells to neoplastic transition (32). To determine if PAX2 combined with P53 deficiency is sufficient to promote tumorigenicity, we generated mOSE cells lacking functional P53 ($p53\Delta^{2-10}$-mOSE) (Fig. 17A). Confirmation of deletion of P53 was done by genotyping and western blot analysis on lysates from cells treated with cisplatin, as seen in Figure 17B. Although lack of P53 in mOSEcells is not tumorigenic (32), $p53\Delta^{2-10}$-mOSEshow anchorage-independent growth by forming colonies in soft agar (Figure 17C) and have enhanced proliferation and survival, as compared to normal mOSE cells (Fig. 17D).While inactivation of P53 enhances mOSE cell proliferation, expression of PAX2 in P53-null cells further increases proliferation (Fig. 18A and B). However, when cells were exposed to cisplatin or cultured under growth factor deprivation conditions, PAX2 did not improve the survival of P53-null mOSE cells (Fig. 18C), which indicates that PAX2 may enhances survival and cisplatin resistance in a P53-dependent manner. Moreover, PAX2 did not result in any phenotypic changes of the $p53^{\Delta 2-10}$-mOSEcells (Fig. 19).

To test the effects of PAX2 in P53-null cells, SCID mice were injected with either $p53^{\Delta 2-10}$-mOSE+WPI or $p53^{\Delta 2-10}$-mOSE+PAX2 cells (4 animals/group). As seen by others (32), P53 deficiency was not sufficient to initiate tumorigenicity since there was no evidence of tumors in the $p53^{\Delta 2-10}$-mOSE+WPI group. However, two mice injected with PAX2-expressing $p53^{\Delta 2-10}$-mOSE cells developed tumors, reaching endpoint after 51 and 151 days. Animals that did not develop tumors were kept for six months and then sacrificed and confirmed to have no macroscopic evidence of tumor. Although the number of animals is small, this data indicates that loss of P53 confers oncogenic potency to PAX2 in mOSE cells.

3.1.8 PAX2 has contradictory effects on ovarian tumor progression

Although PAX2 has been suggested to enhance tumor progression in different cancer models (122, 127), a recent study has provided evidence to indicate that PAX2 may play a dual role in terms of invasiveness of ovarian cancer cell lines (110). To investigate this further, PAX2 was expressed in two murine ovarian cancer models generated in our lab (31, 167). The RM model was derived from immortalized mOSE cells transduced with retrovirus constructs to achieve ectopic expression of the mutant *K-Ras*($KRAS^{G12D}$) and *Myc*(167). Activating mutations in K-RAS, or one of its downstream mediators, B-RAF, are present in two-thirds of low-grade serous ovarian carcinomas (178). Overexpression of c-MYC has been found in about 70% of ovarian cancers (179). When RM cells are injected into nude mice, they form highly aggressive, poorly differentiated tumors (Fig. 20), with a median survival of 23.3±1.7 days (167). The STOSE model mimics high-grade serous ovarian cancers and arose spontaneously from long term culture of the M0505 cells (31). Intraperitoneal injection of STOSE cells into SCID and syngeneic FVB/N mice produced tumors resembling, at both the molecular and histotype levels, human high-grade ovarian serous carcinoma (31).

Expression of *Pax2* in both cell lines (Fig. 21A) resulted in different effects on proliferation, enhancing cell proliferation in RM cells, but not in STOSE cells (Fig. 21B). However, PAX2 induction in RM and STOSE cells did not change their viability (Fig. 21C). When the cancer cells were deprived of growth factors, PAX2 had no effect on their survival, neither their proliferation rate (Fig. 22A). However, when cells were exposed to cisplatin, PAX2 modestly enhanced chemosensitivity, shown by reduced viability, in STOSE cells, but not in RM cells (Fig. 23). To confirm our observation that PAX2 can enhance apoptosis

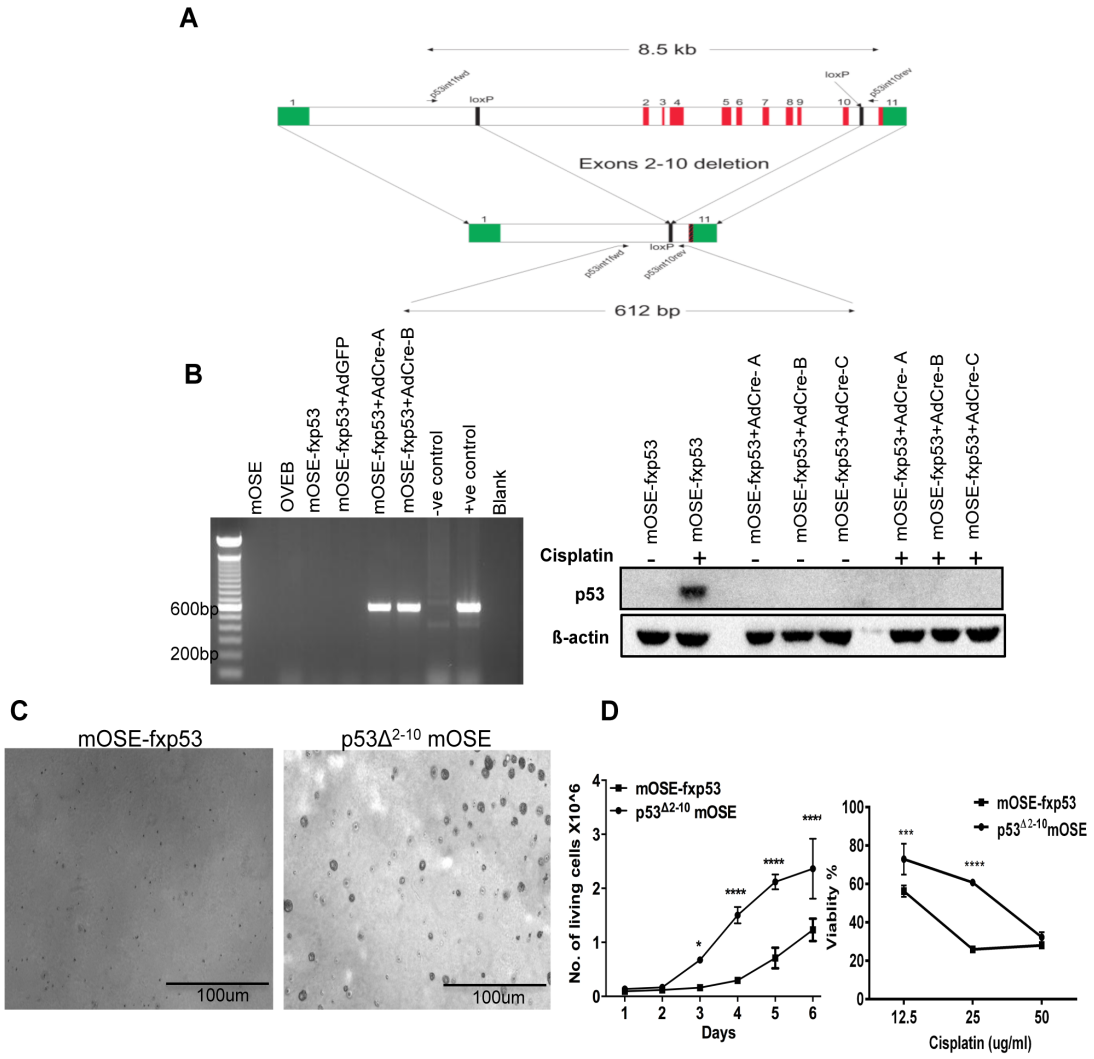

Figure 17: A: Schematic of the *loxP*-flanked *Trp53* gene before (top) and after (bottom) cre-mediated recombination. Exons are shown in green (non-coding) or red (coding). The location of *loxP* sites is indicated. B: Deletion of p53 was shown by recombination of the gDNA (left) and by western blot (right) of cellular proteins before and after treatment with cisplatin. mOSE-fxp53+AdCre-A, -B and –C show recombination at 1 week (A), 1 month (B) or 4 months (C) after removal of AdCre. C: Deletion of *Trp53* in mOSE cells resulted anchorage-independent growth as assessed by colony formation in soft agar (1.5% agarose). D: Deletion of *Trp53* in mOSE cells also resulted in increased proliferation (left) and enhanced survival during treatment with cisplatin (right).Viable cell numbers were calculated using trypan blue exclusion, while cispatin-sensitivity assay was done using the Alamar Blue assay. Analysis was done using two-way ANOVA. All experiments were performed at least three times, each time in triplicate. *p<0.05, ***p<0.001, ****p<0.0001.D: Deletion of *Trp53* in mOSE cells also resulted anchorage-independent growth as assessed by colony formation in soft agar (1.5% agarose).

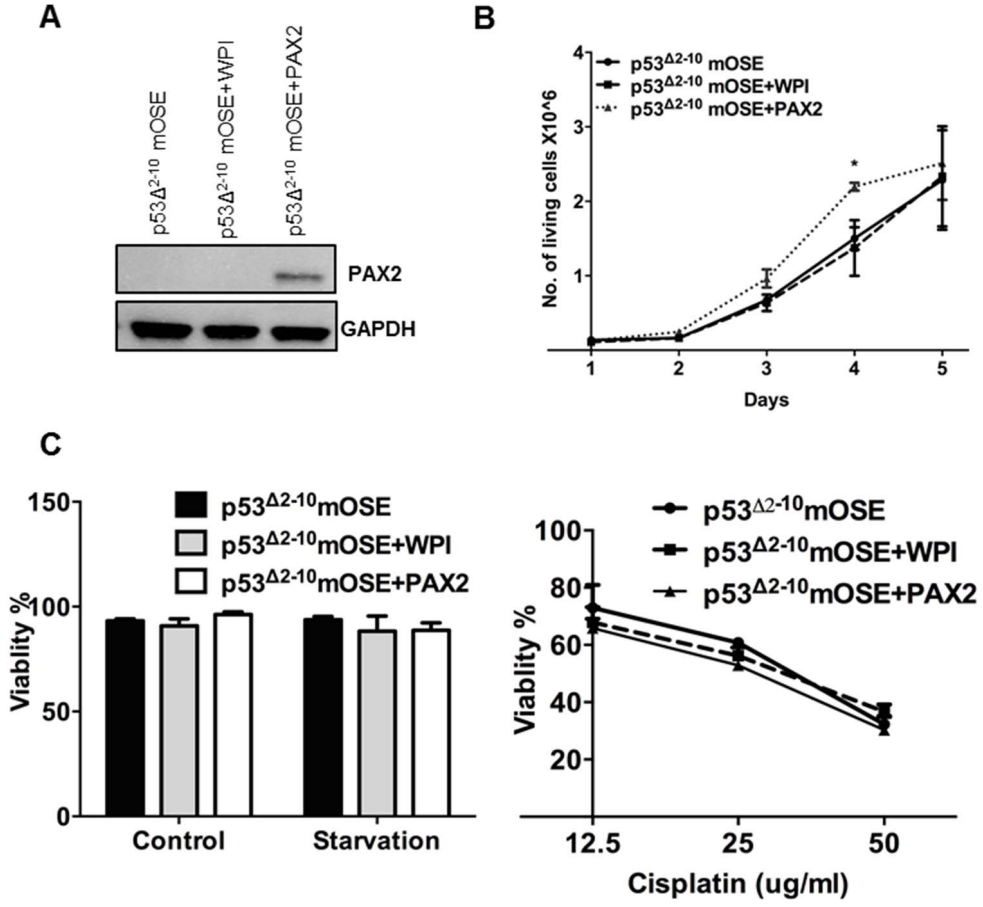

Figure 18: Expression of PAX2 in p53-null cells (A) enhanced proliferation (B) but had not impact on survival (C). For proliferation assays, cells were grown in culture for up to 4 days. Cell viability was determined using trypan blue exclusion. When cells were exposed to the indicated concentrations of cisplatin for 48hrs, cell viability was measured using Alamar Blue assay. Analysis was done using two-way ANOVA. All experiments were performed at least three times, each time in triplicate. *$p<0.05$, ****$p<0.0001$.

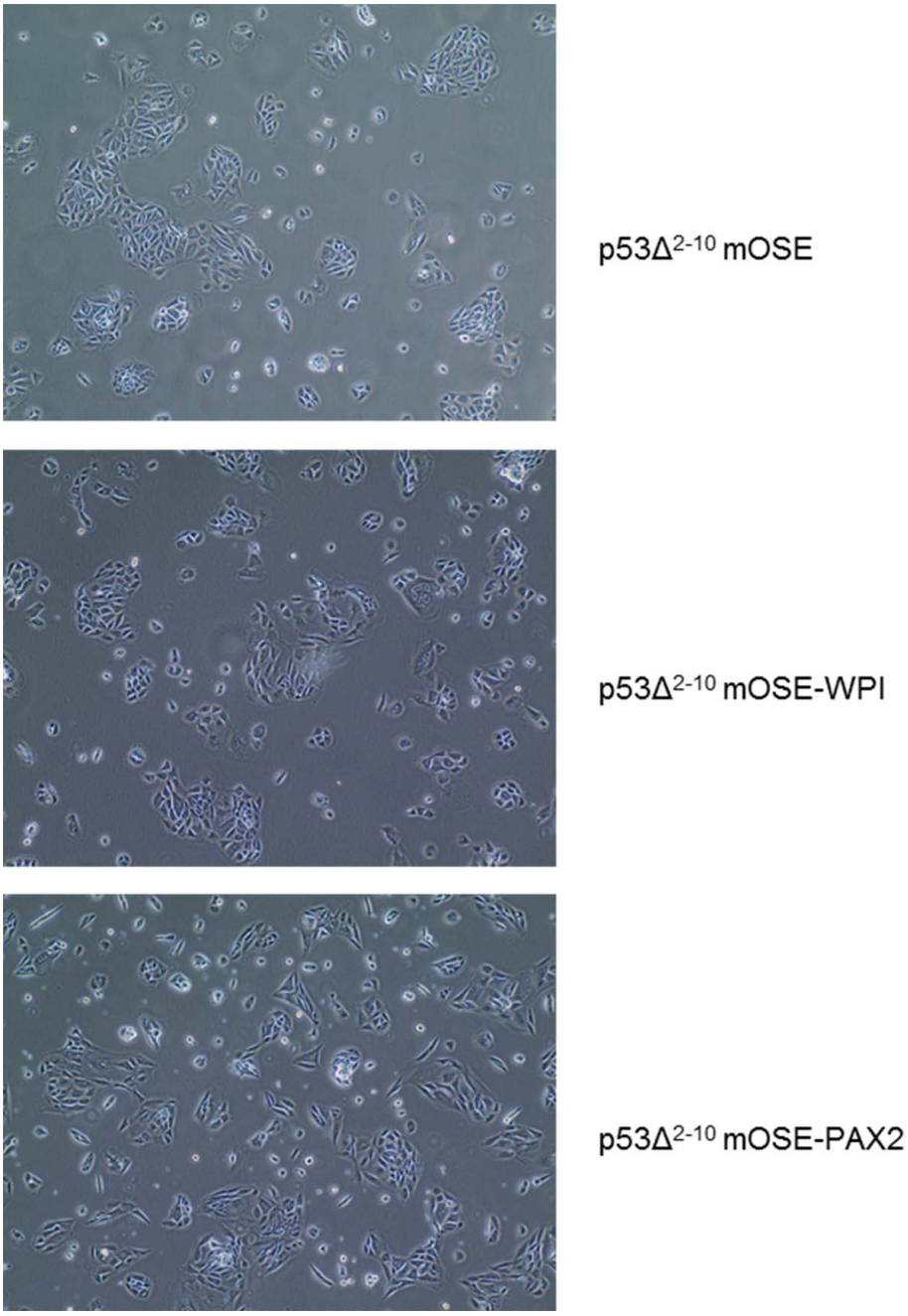

Figure 19: Expression of PAX2 in p53-null did not change cellular morphology.Pictures were taken using an EVOS microscope

induction by cisplatin, we treated STOSE cells for 48 hrs with 12.5μg/ml of cisplatin and protein were analyzed for cleaved caspase-3. As seen in Figure 23C, PAX2 enhanced abundance of cleaved caspase-3, but not P53, indicating that PAX2 activates the apoptotic machinery in STOSE cells in a P53-independent manner. It is also worth noting that when the *Trp53* gene in STOSE cells was sequenced (exons 2, 5-11), no mutation was detected.

Interestingly, PAX2 induction did not result in any phenotypic changes in both cancer cell lines (Fig. 24). Nevertheless, PAX2 reduced the number and size of colonies produced in soft agar by STOSE cells, while only a decrease in the colony size was evident in the RM model (Fig. 25A and B).

To determine the role of PAX2 on ovarian tumor progression, RM+WPI and RM+PAX2 cells were injected i.p. into 20 SCID mice per group, while STOSE+WPI, STOSE+PAX2 or STOSE+PAX2+Cre were injected i.p. into FVB/N mice (10 animals per group). To control for any potential differences due to mouse strain, STOSE+WPI and STOSE+PAX2 cells were also injected into SCID mice (4 per group). Animals were sacrificed when they reached a loss of wellness endpoint. Surprisingly, the effect of PAX2 on tumor progression was drastically different between the two tumor models, with accelerated tumor progression in RM-injected animals (median survival 11 vs. 16 days, $p<0.0001$; Fig. 26A). In contrast, the survival of immunocompetent animals injected with STOSE+PAX2 was significantly longer (median 74.5 days) than the survival of those injected with STOSE+WPI or STOSE+PAX2+Cre (median survival 27.5 and 32 days; Fig. 26B). Similar results were observed in SCID mice injected with STOSE cells, as the median survival of PAX2-expressing vs. control tumors was 59 vs. 26.5 days, $p=0.0062$ (Fig. 26B).

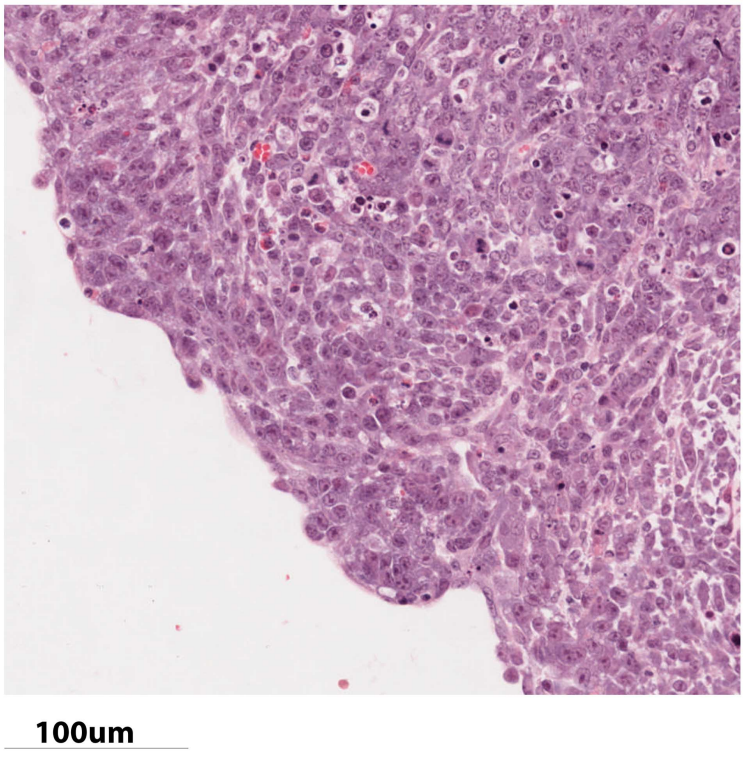

Figure 20: RM cells form poorly differentiated tumors in nude mice. Hematoxylin and eosin staining of an RM tumor formed in a nude mouse. Scale bar is 100µm.

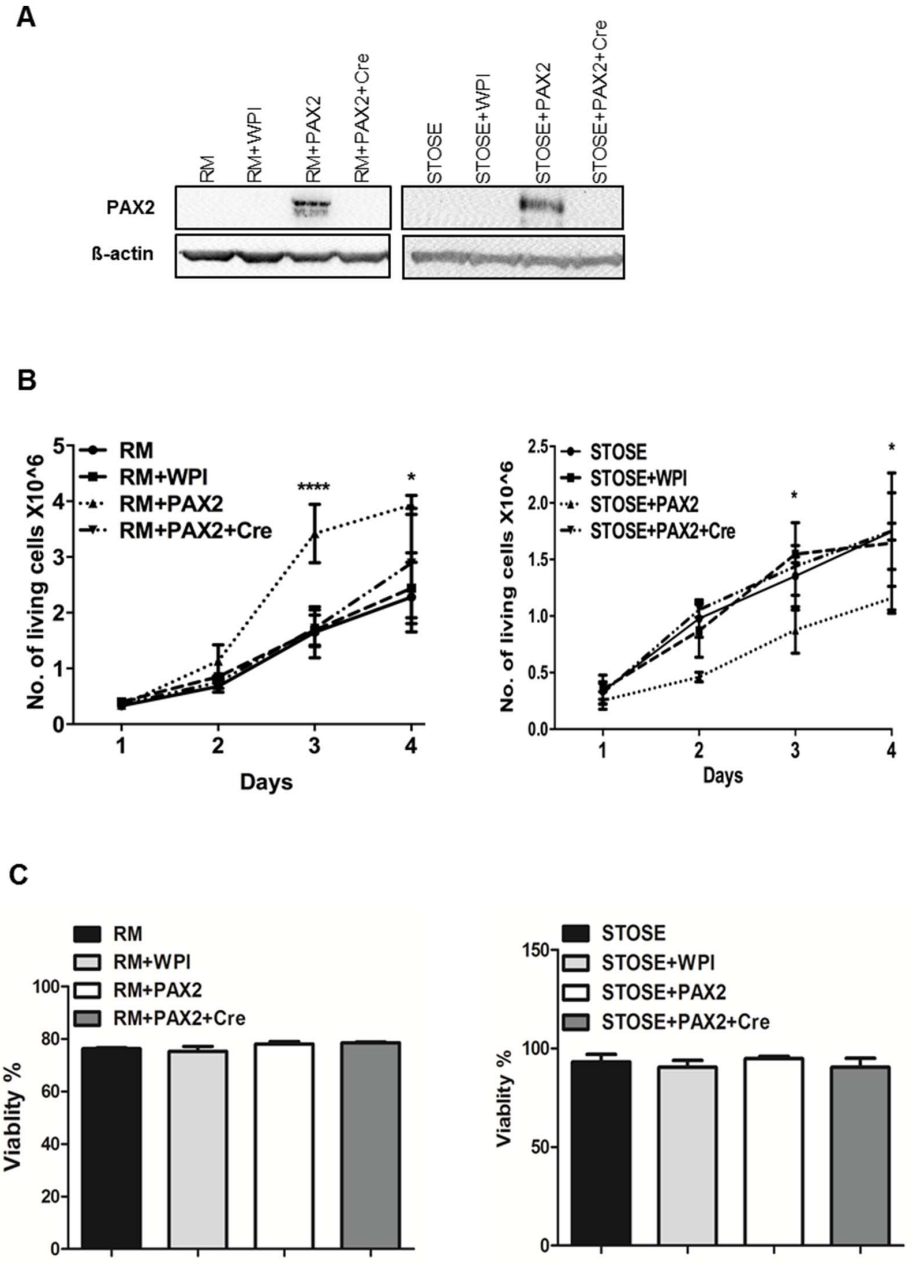

Figure 21: The effect of PAX2 on proliferation and survival in RM and STOSE cell lines. A: Western blot analysis shows induced expression of PAX2 in RM and STOSE cell lines. B: Growth curve analysis of cells, with and without PAX2, grown in culture for 3 days. C: Viability assay of RM and STOSE cells before and after forced expression of PAX2. Both viable cells number and viability percentage were assessed using Tryban Blue exclusion test.All experiments were done at least 3 times, each in duplicate and analysis was done using two-way ANOVA.

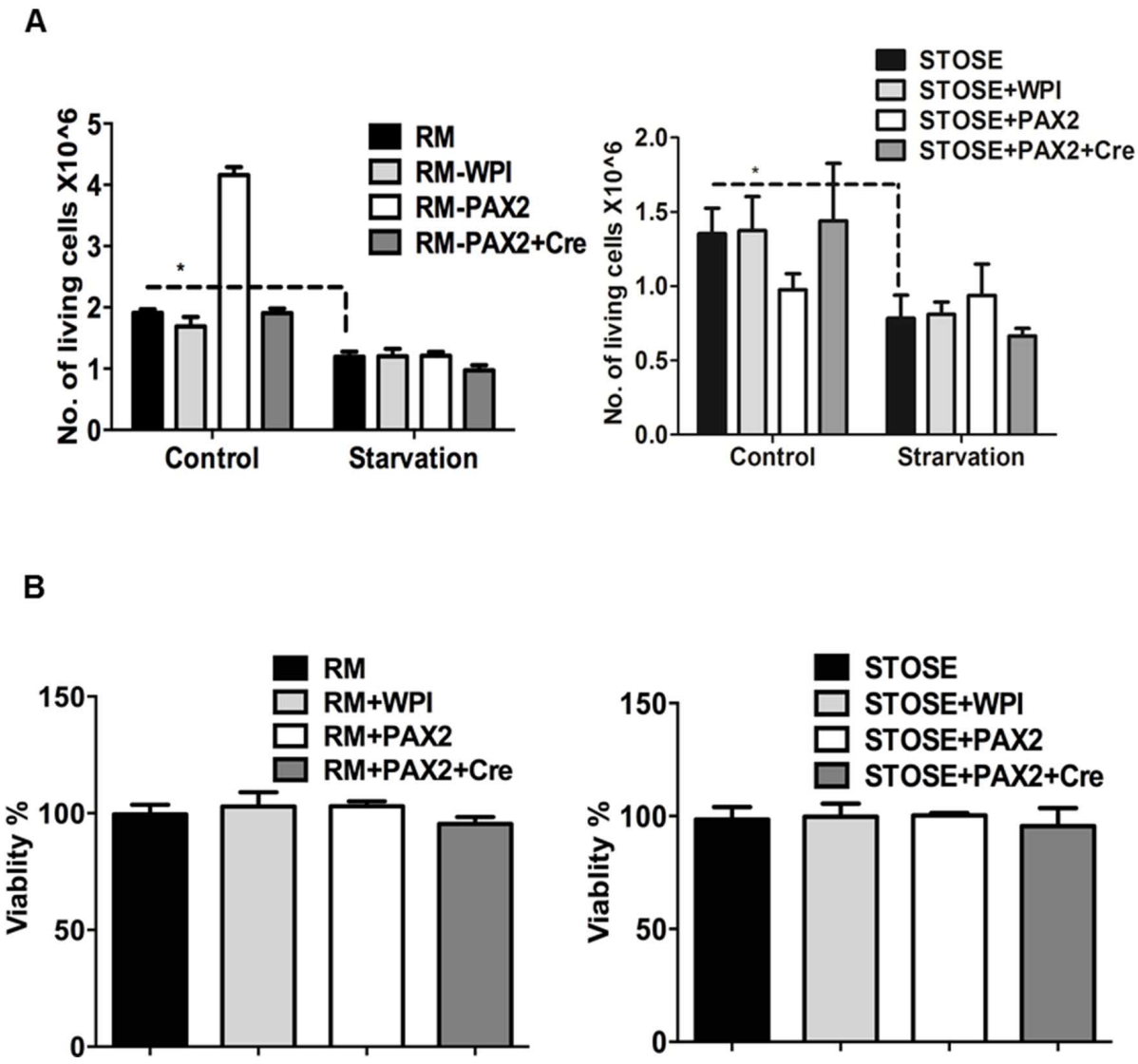

Figure 22: Growth and viability analysis of cells when they were deprived of growth factors. Viable cell number was calculated using trypan blue.All experiments were done 3 times, each in duplicate and analysis was done using two-way ANOVA.

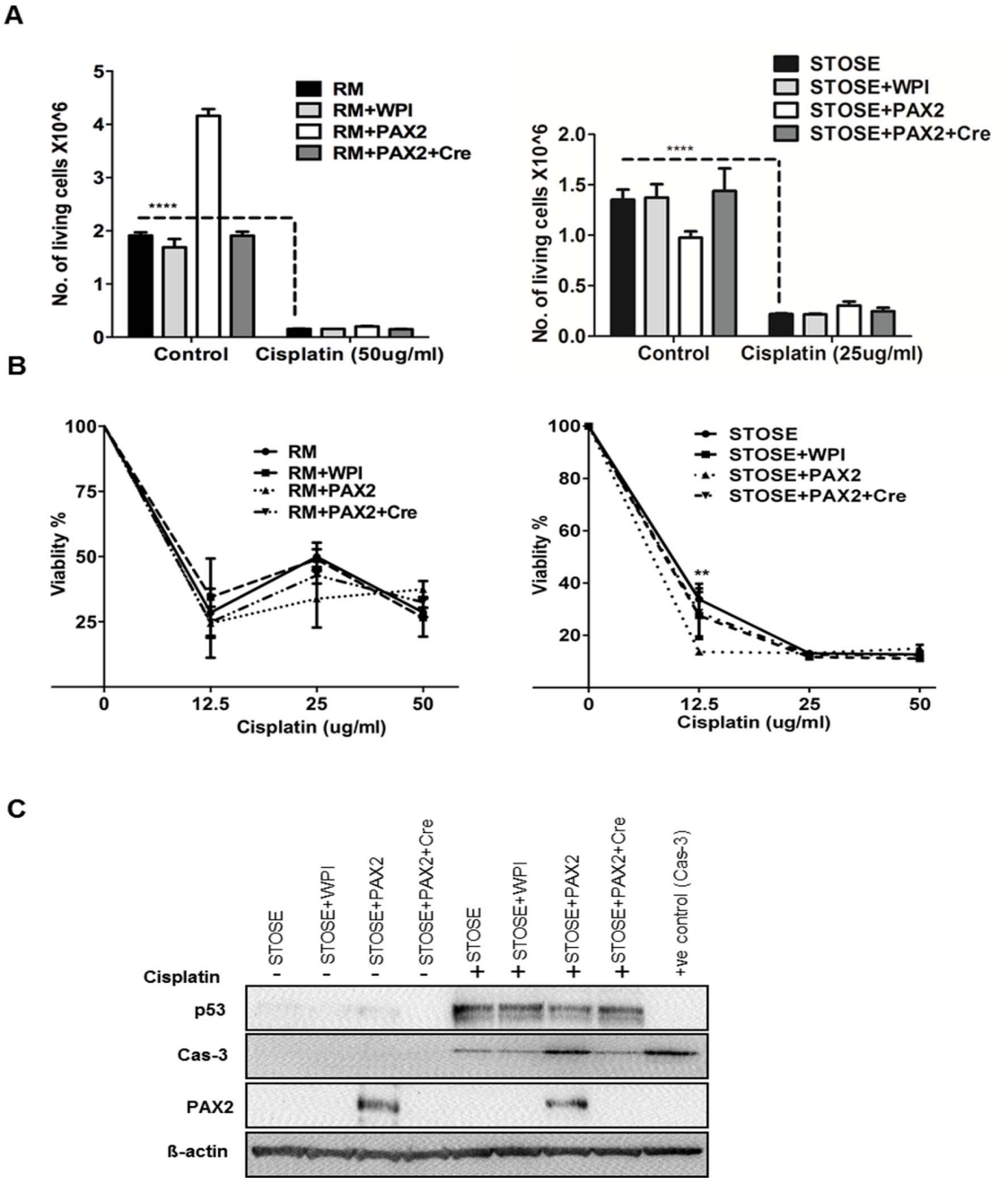

Figure 23: Growth curve and viability analysis of cells when they were they are exposed to cisplatin. A: Viable cell number was calculated using trypan blue, following 48hrs exposure to 50ug/ml of cisplatin. B: Cells were exposed to the indicated doses of cisplatin for 48hrs and cell viability was measured using Alamar Blue Assay. Analysis was done using two-way ANOVA,,**p<0.01, ****p<0.0001. All experiments were done 3 times, each in duplicate. C: Western blot analysis shows increased level of cleaved caspase-3 in the cisplatin treated STOSE expressing PAX2. Cells were treated with 12.5µg/ml of cisplatin for 48hrs.

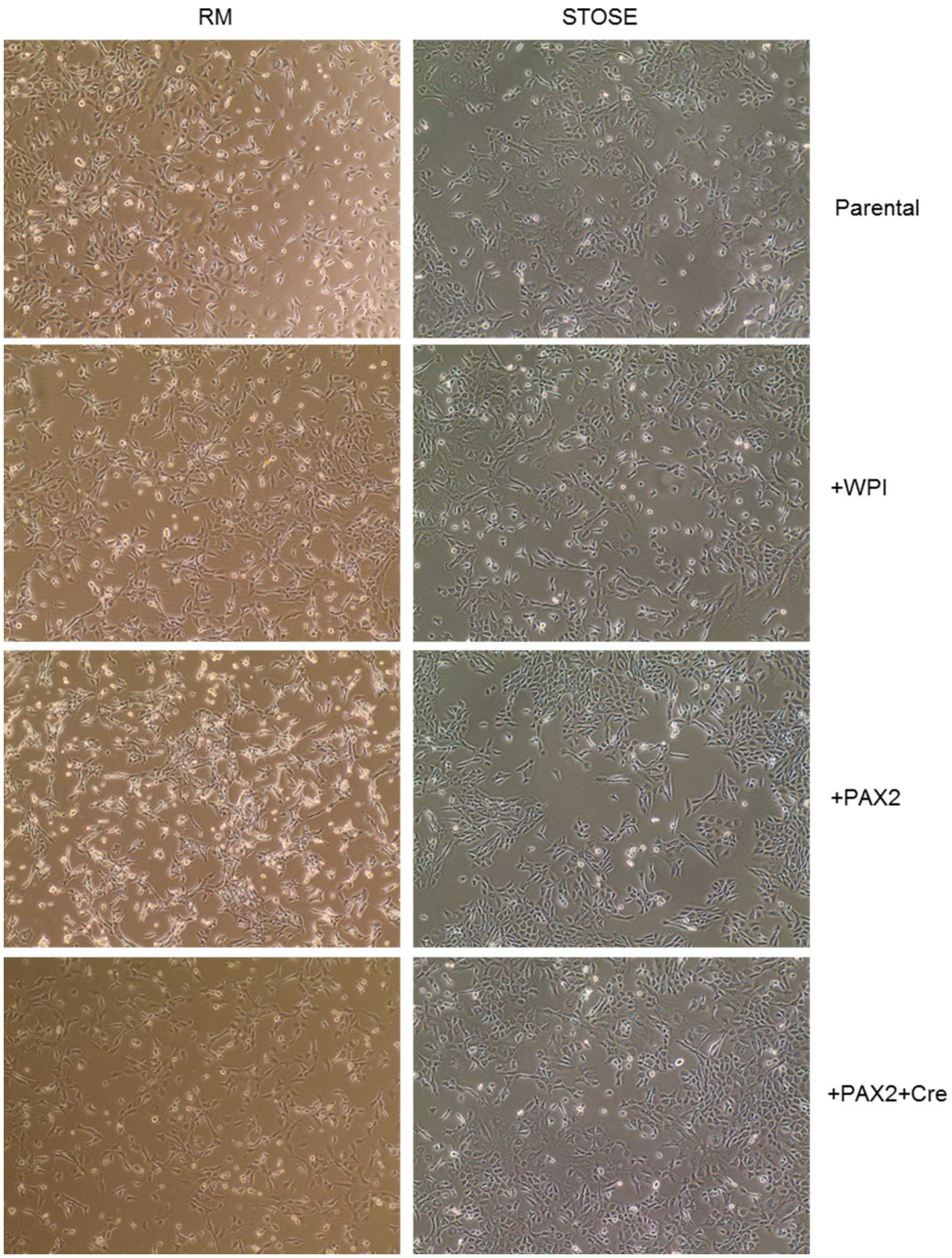

Figure 24:PAX2 expression results in no changes in the morphology of RM and STOSE cells.Pictures were taken using an EVOS microscope.

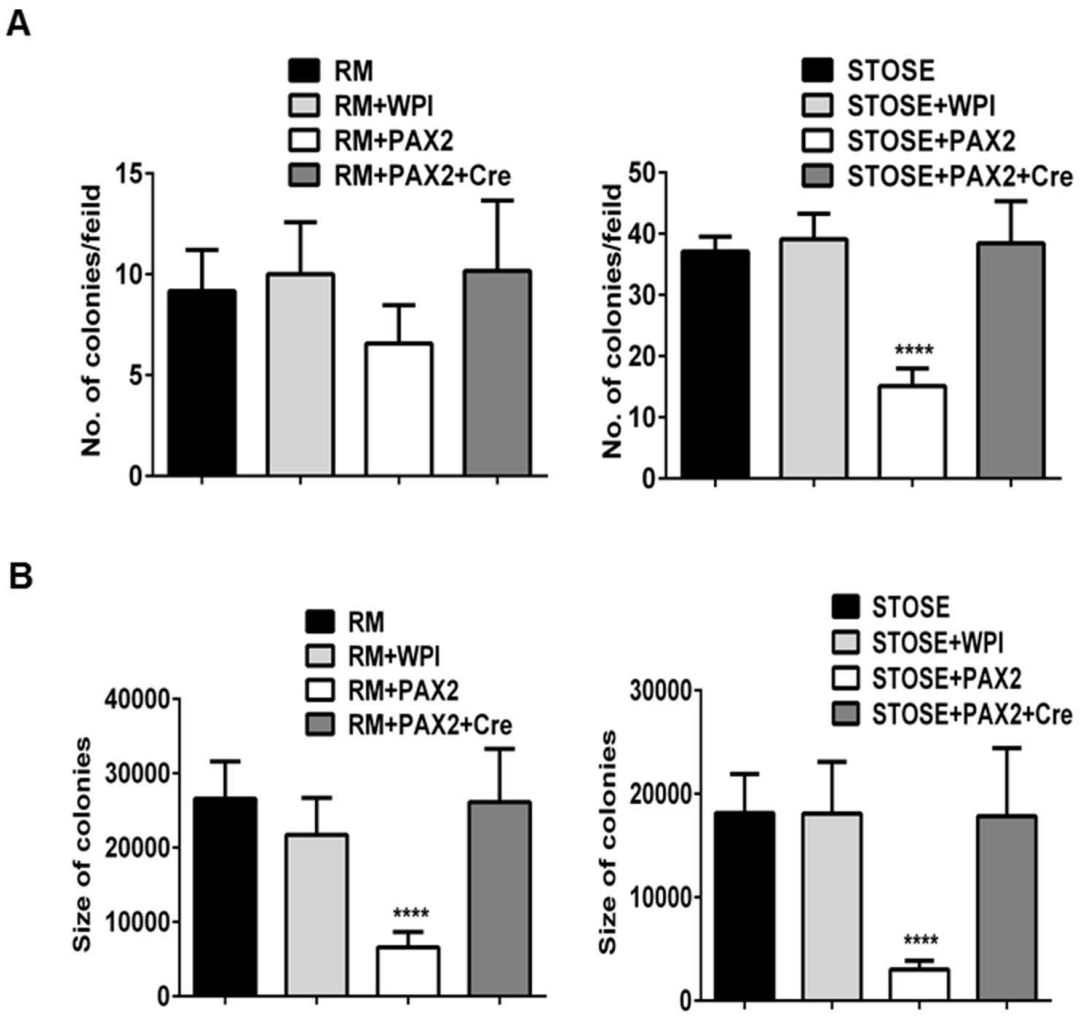

Figure 25:PAX2 induction results in a decrease in the number (STOSE cells; as seen in A) and size (STOSE and RM; as seen in B) of colonies in soft agar (1.5 % agarose).Analysis was done using one-way ANOVA,**p<0.01, ****p<0.0001.

Animals injected with RM cells were sacrificed due to large tumor burden, and there was no difference in tumor burden among animals. By contrast, all animals injected with STOSE cells reached their endpoint due to large volumes of bloody ascites, and no difference was observed in ascites volume among different groups. Dissemination in the peritoneal cavity was evident in all animals and tumor sites included peritoneum, pancreas, liver, intestine, diaphragm, uterus and ovaries. Most tumors consolidated with the intestine. However, STOSE+PAX2 tumors were mainly restricted to the abdominal wall with limited dissemination into the mesentery and showed significantly smaller tumor burden ($p= 0.0005$; Fig. 26C). All tumors were stained by hematoxylin and eosin and tumor histotypes were examined by Dr. ManijehDaneshmand (Pathologist, University of Ottawa). There was no difference in the histology among each group (Fig. 27). The data indicate that PAX2 may affect progression of ovarian cancer positively or negatively, depending on the tumor context.

3.1.9 PAX2 ablates P53 in RM tumors but not STOSE tumors

To understand why PAX2 enhanced progression of RM tumors while it inhibited progression of STOSE tumors, and given the fact that PAX2 inhibits P53 induction in normal mOSE cells, we examined the effect of PAX2 on P53 in both tumor types. Protein analysis shows that PAX2 completely inhibited P53 accumulation in RM tumors (Fig. 28A), while STOSE tumors (with or without PAX2) did not show stable levels of P53 (Fig. 28C). The inhibition of P53 was observed at the mRNA level in RM tumors only (Fig. 28Band D). Furthermore, RM+PAX2 tumors have reduced apoptosis as shown by the lack of cleavage of caspase-3 (Fig. 28A), suggesting that PAX2-expressing RM tumor cells were not being

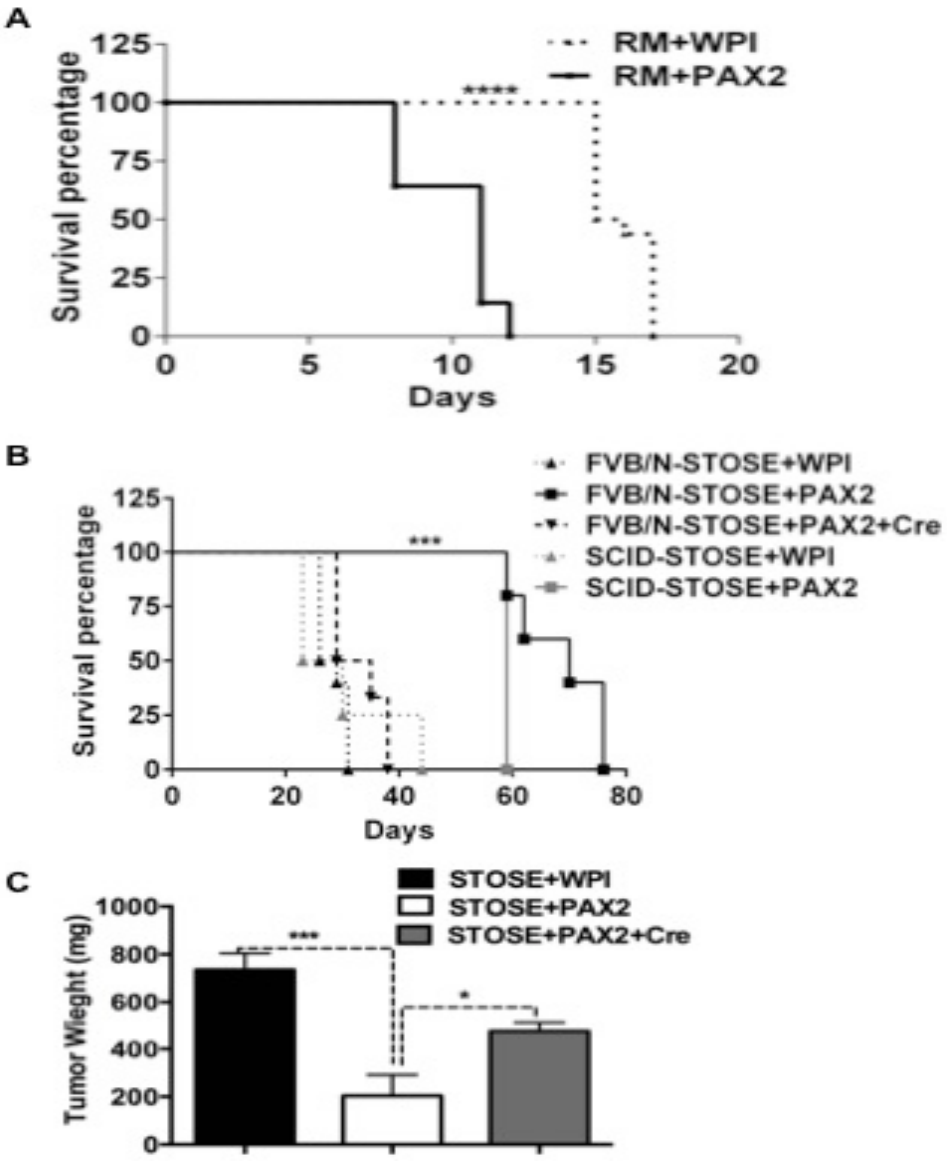

Figure 26: PAX2 accelerates tumor progression by RM cells but slows tumor progression by STOSE cancerous cells. A. Kaplan-Meier curve showing survival of SCID animals injected with 10^7 RM+WPI or RM+PAX2 cells (20 mice per group). B: Survival of FVB/N mice or SCIDs after injection with 10^7 STOSE+WPI, STOSE+PAX2 or STOSE+PAX2+Cre cells (10 mice per group). C: Masses of tumors, that were taken when the animals reached endpoint, from STOSE-PAX2 cells were significantly less than tumors originating from STOSE+WPI or STOSE+PAX2+Cre cells. **p<0.01, ***p<0.001, ****p<0.0001.

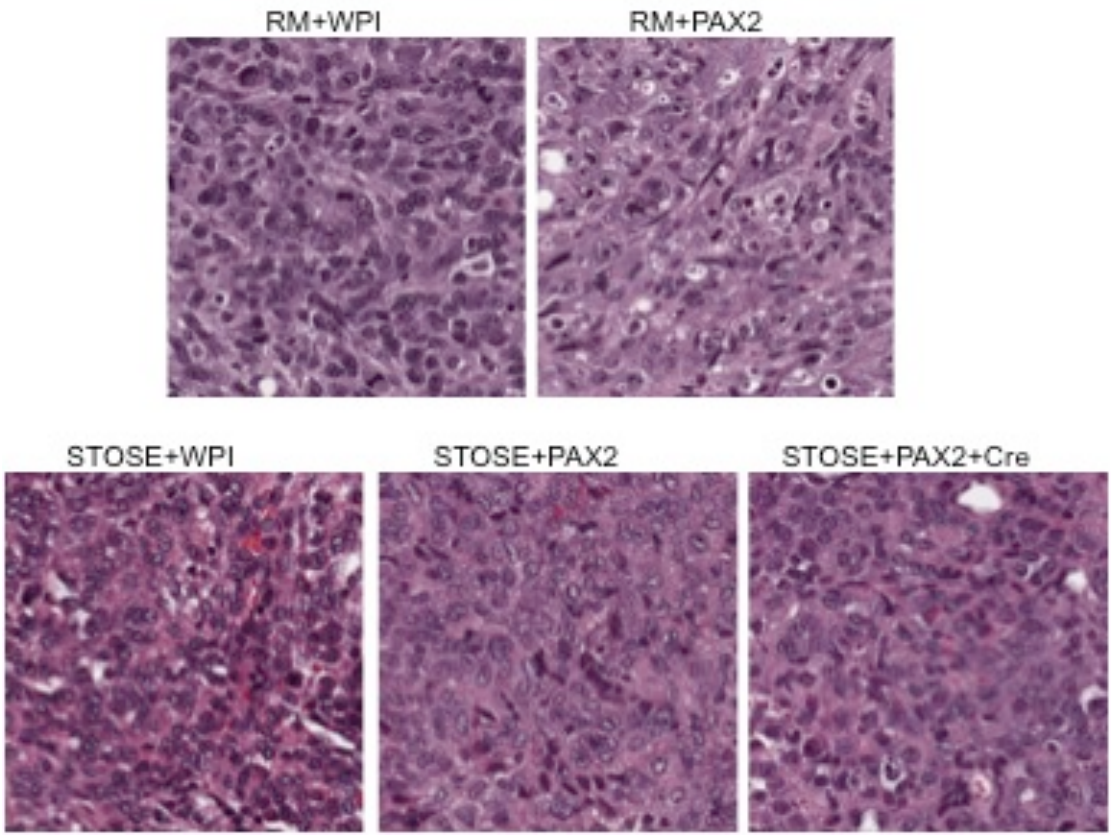

Figure 27: PAX2-expressing tumors have similar morphology to tumors that do not express PAX2. Hematoxylin and eosin staining shows RM and STOSE tumors to be poorly differentiated. Images are 1000μm by 1000μm.

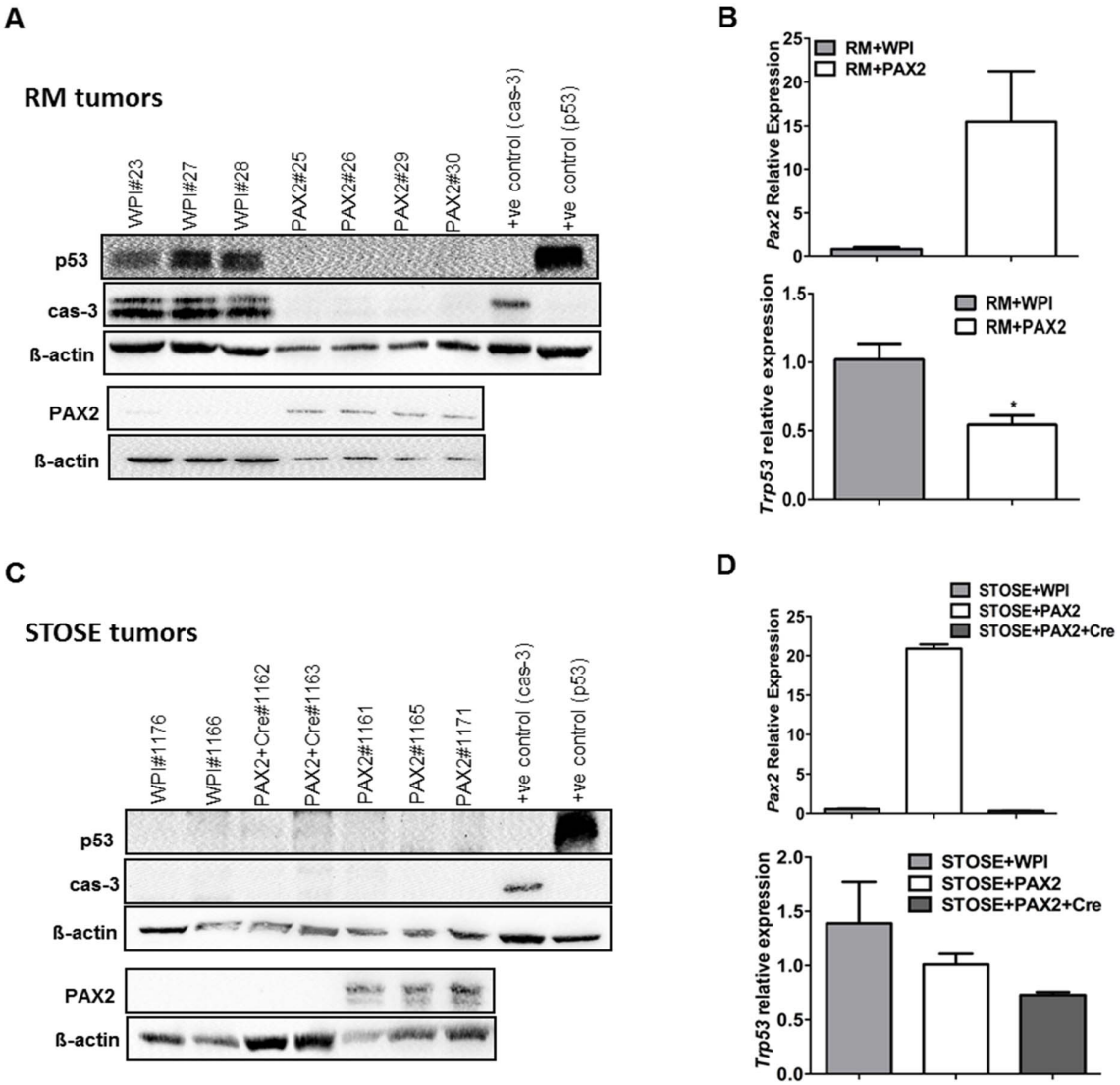

Figure 28: PAX2 resulted in inhibition of P53 accumulation in RM tumors. A: Expression of PAX2 abolished P53 accumulation as detected by western blot. Numbers identify different animals. Control lanes include a positive control for cleaved caspase-3 (cas-3) (p53-deficient mOSE cells treated with 25µg/ml cisplatin for48hrs) and a positive control for P53 expression (M1102 treated with 12.5µg/ml cisplatin for 24hrs). B: Histograms represent mRNA analysis of *Pax2* (top) and *Trp53* (bottom) in RM-WPI and RM+PAX2 tumors, as determined by Q-PCR. C: Western blot analysis of STOSE tumors showing no P53 accumulation. D: mRNA analysis shows expression of *Pax2* (top*)* in STOSE+PAX2 tumors, as compared to tumors taken from animals injected with either STOSE+WPI or STOSE+PAX2+Cre. The bottom histogram shows no significant changes in *Trp53* transcripts among the tested tumors Analysis was done using t-test (RM tumors) and one-way ANOVA (STSOE tumors) (*$p<0.05$).

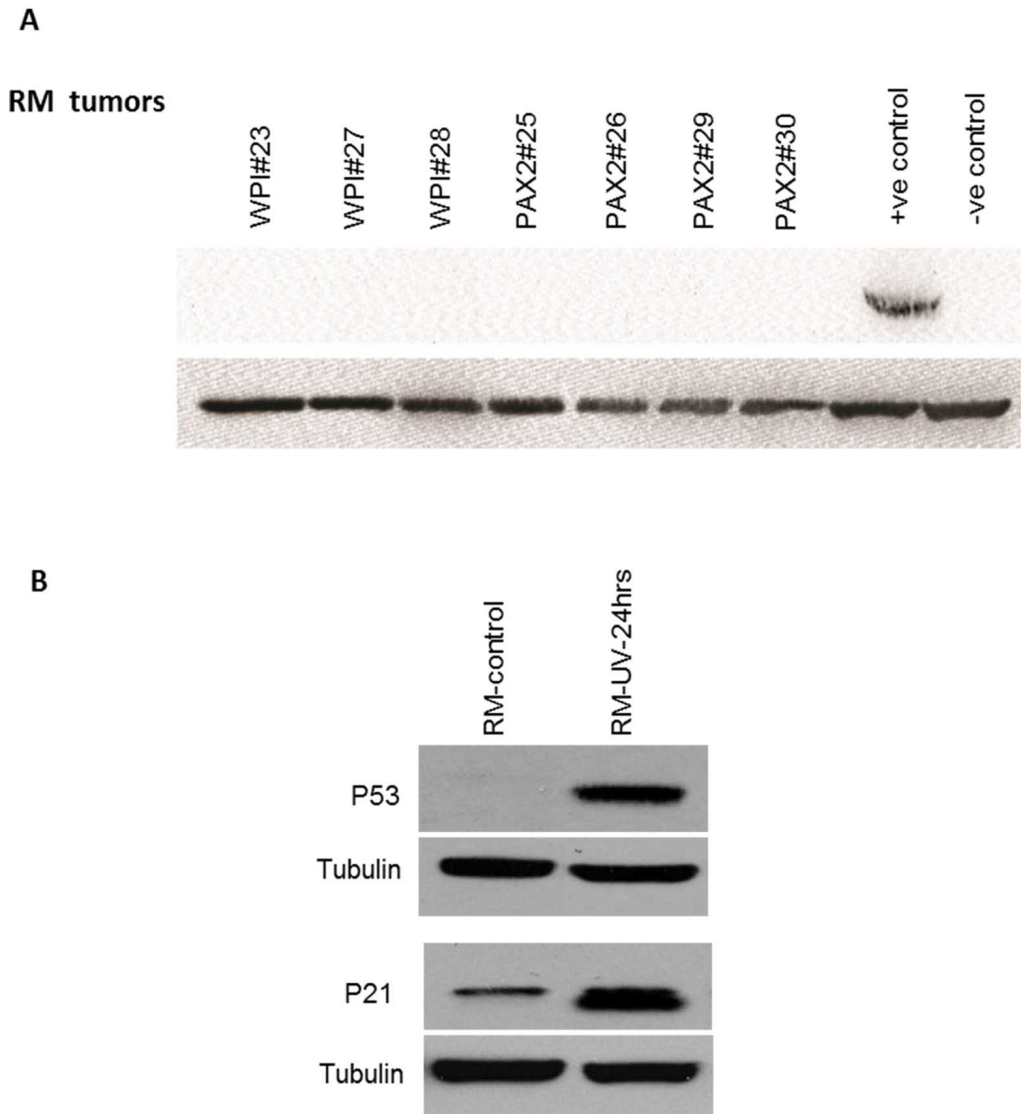

Figure 29: TAg expression and P53 status in RM tumors and cells, respectively.
A:Western blot analysis show the lack of TAg expression in RM tumors, lysate from 293T cells was used as positive control, while lysate from MDA-MB231 cells was used as negative control. B: Western blot for RM cells that were treated with 20 joules of UV and lysates were collected after 24hrs, showing induced expression of P53 and , its downstream target, P21.Figure 29B courtesy of Desheng Yao

eliminated by apoptosis. This may suggest a mechanism for more rapid tumor progression and shorter survival compared to the non-expressing RM tumors.

Since stable expression of P53 was noticed in RM tumors, we thought to examine if this stabilization is a result of TAg-induced inactivation of P53, as the cells of origin is immorto-mOSEthat have the SV40 large T-antigen (at permissive temperature of 32°C). Western blot analysis shows that RM tumors have no TAg expression (Fig. 29A) and the RM cells showed induced expression of P53 and its downsteam target P21, when the cells were exposed to UV (Fig. 29B). Since the experiment was done under non-permissive temperature, this indicates that might have active P53.

Because loss of P53 could result in enhanced proliferation, we examined the proliferative rate of tumors by Ki-67 staining. As seen in Figure 30, the pixel positivity for Ki-67 was no different in RM+WPI and RM+PAX2 tumors. On the other hand, STOSE+PAX2 tumors showed less positivity indicating a lower proliferative rate as compared to STOSE+WPI tumors. Although the difference in staining positivity between STOSE+PAX2 and STOSE+PAX2+Cre did not reach significance, there was a strong trend indicating that deletion of PAX2 restored the higher proliferation rate of STOSE+PAX2+Cre cells ($p=0.0571$).

3.1.10 PAX2 targets different pathways in different tumor contexts

To identify targets dysregulated by PAX2 in different tumors, we used the microarray analysis to search for genes involved in ovarian cancer progression that might help to identify different pathways induced by PAX2. The gene most down-regulated by PAX2 in the mOSE microarray was High-temperature requirement A serine peptidase1 (Htra1) (See

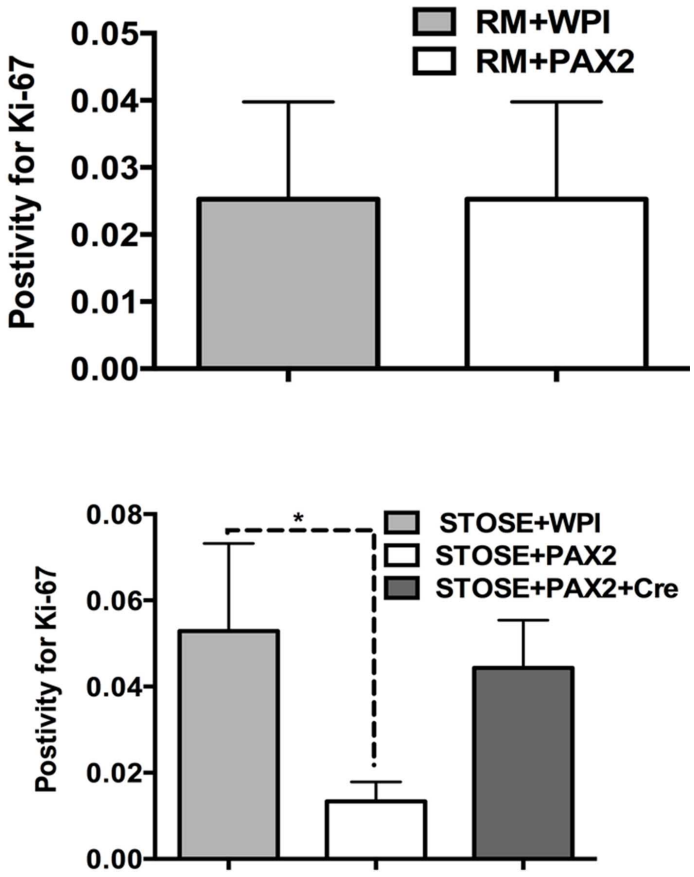

Figure 30: IHC analysis of tumors for Ki-67 staining positivity is represented on histograms (RM tumors; up, STOSE tumors; down). Analysis was done using t-test for RM tumors and one-way ANOV A for STOSE tumors.

Table 3). Htra1 is a potential tumor suppressor gene that was found to be downregulated in ovarian cancers (171, 172). It has been shown to enhance sensitivity to cisplatin in ovarian cancer cell lines by targeting XIAP for degradation (180). Furthermore, downregulation of Htra1 resulted in enhanced peritoneal dissemination of ovarian cancer cells in a xenograft study, mediated through enhancement of EGFR phosphorylation and activation of the AKT and MAPK 44/42 (ERK1/2) pathways (181).

As seen in Figure 31A, although PAX2 induced a significant reduction in the level of *Htra1* transcripts in M0505 cells, this effect was only partially reversed when PAX2 was deleted. Like mOSE cells, *Htra1* was downregulated in RM cells when PAX2 was expressed. In contrast, in STOSE there was no decrease in *Htra1* when PAX2 was expressed, but rather a trend to increased levels of *Htra1* ($p=0.0884$; Fig. 31A) that was reversed upon deletion of PAX2. This led us to further identify the downstream targets of *Htra1*. HTRA1 has been associated with EGFR activity (181), but western blot analysis showed no EGFR expression in RM tumors. In our hands, we were never able to detect phosphorylated AKT by western blot. However, when AKT was immunoprecipitated, immunoblotting showed induction of Ser473-phosphorylated AKT only in RM tumors that express PAX2. However, RM tumors expressing PAX2 with reduced *Htra1* expression showed a robust dual phosphorylation of ERK1/2 at Tyr202 and Thy204 (Fig. 31B). Interestingly, in contrast, STOSE tumors expressing PAX2 and elevated *Htra1* expression failed to induce phosphorylation of ERK1/2 (Fig. 31B).

The results indicate that induction of AKT and ERK1/2 phosphorylation shown in RM tumors is not by activation of the EGF1R. However, PAX2 has shown previously to activate AKT pathway through dwonregulation of PTEN(124). Therefore, the effect of PAX2 on PTEN level in RM tumors was investigated. Interestingly, PAX2 expressing tumors showed

lower level ofPTEN, as shown in Figure 32, explaining the activation of both AKT and ERK1/2 pathways.

Prostaglandin-endoperoxide synthase 2 (*Ptgs-2* or cyclooxygenase-2, *Cox-2*), was downregulated by PAX2 expression in M0505 mOSE cells and IPA analysis showed its involvement in several pathways related to tumor progression, hyperplasia and ovarian cancer (Figure 16and Table 4). Aberrant upregulation of *Ptgs2* has been reported in ovarian tumors and is associated with tumor progression in animal studies (182, 183).

COX-2 levels were significantly higher in RM+PAX2 tumors (5.7 fold); however STOSE+PAX2 tumors expressed much lower levels of COX-2 (0.14 fold), compared to controls (Fig. 33). Interestingly, as the expression of PAX2 leads to differential effects on tumor progression, it also leads to differential regulation of both *Htra1* and *Cox-2* that is dependent on the tumor cell context. A previous xenograft study showed that treatment with the selective COX-2 inhibitor, celecoxib, suppressed ovarian tumor growth accompanied with reduction in the tumor microvessel density (MVD) (182). To investigate whether PAX2 induction resulted in changes in the MVD of the tumors, we used IHC analysis for the vascular endothelial marker (CD 31). We selected 3-4 different tumor blocks from each type of tumor and analyzed 5 random areas from each tumor for the pixel positivity (see Fig. 34A). As seen in Fig. 34A and B, PAX2-RM tumors show a significant increase in the MVD, as compared to PAX2-non-expressing tumors. However, there is no difference in the MVD among STOSE tumors (with and without PAX2). These data indicate that in the RM tumor model, PAX2 may enhance angiogenesis, and therefore progression, through the induction of COX-2.

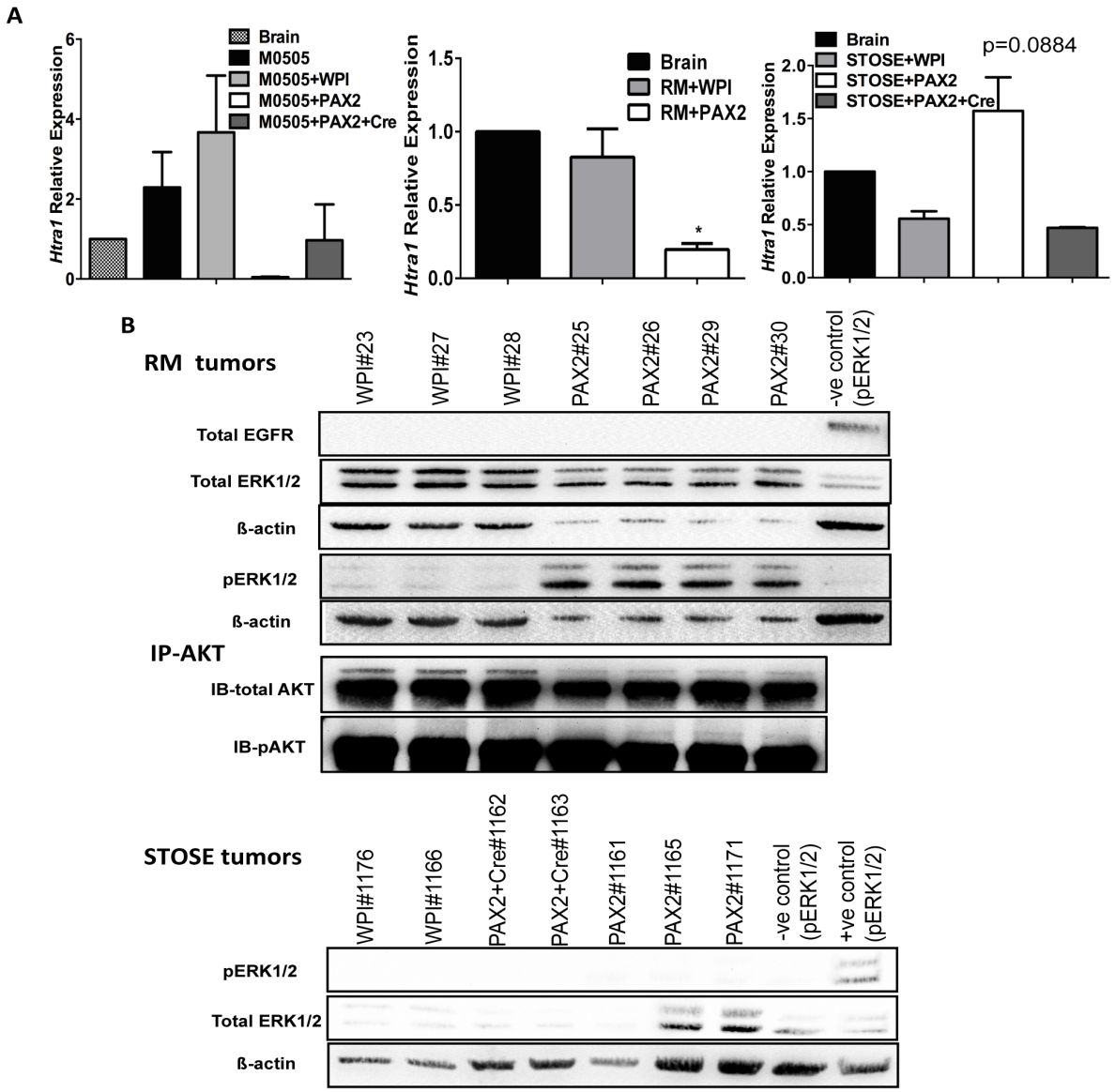

Figure 31: Signalling induced by PAX2 tumors differs in different tumor model systems. A: PAX2 resulted in a significant reduction in *Htra1* at the RNA level in mOSE cells and RM tumors, but not STOSE tumors. Analysis was done using t-test (RM tumors) and one-way ANOVA (STSOE tumors) (*$p<0.05$). B: Western blot analysis shows PAX2-associated phosphorylation of ERK1/2 at Thr 202 and Tyr 204 in RM tumors, but not in tumors originating from STOSE cells. Positive controls for EGFR (SCC25 cells) and pERK1/2 (EGF treated SCC25 cells) are shown. The negative control is SCC25 cells treated with both EGF and the EGFR inhibitor, Erlotinib 10μM. Immunoblot detection of phosphorylated AKT at Ser 437 or total AKT was done following immunoprecipitation for AKT in RM tumors.

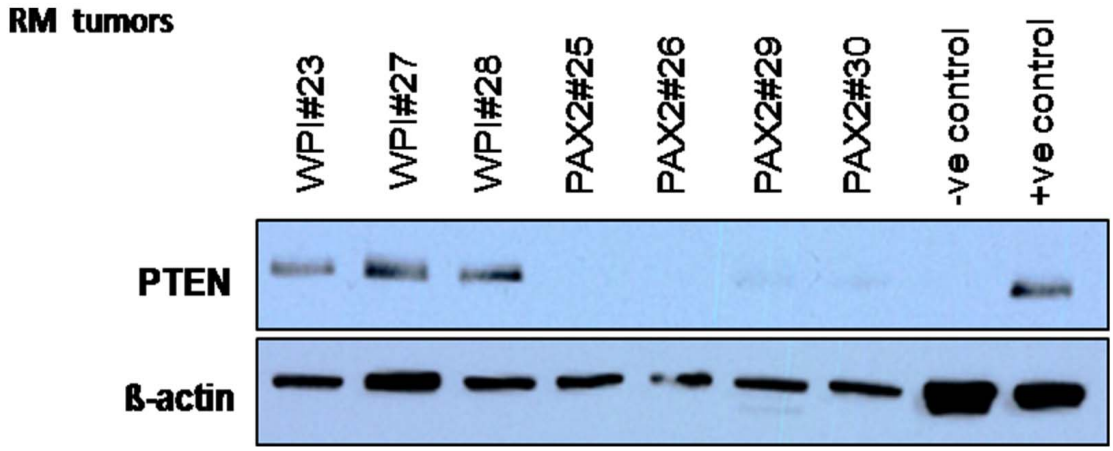

Figure 32: PAX2 expression results in dwonregulation of PTEN in RM tumors, as shown by western blot analysis. The –ve control lane is showing lysate from U57MG glioblastoma cells, while the +ve control is lysate from the same cells following infection with doxcyclin-inducible PTEN construct.

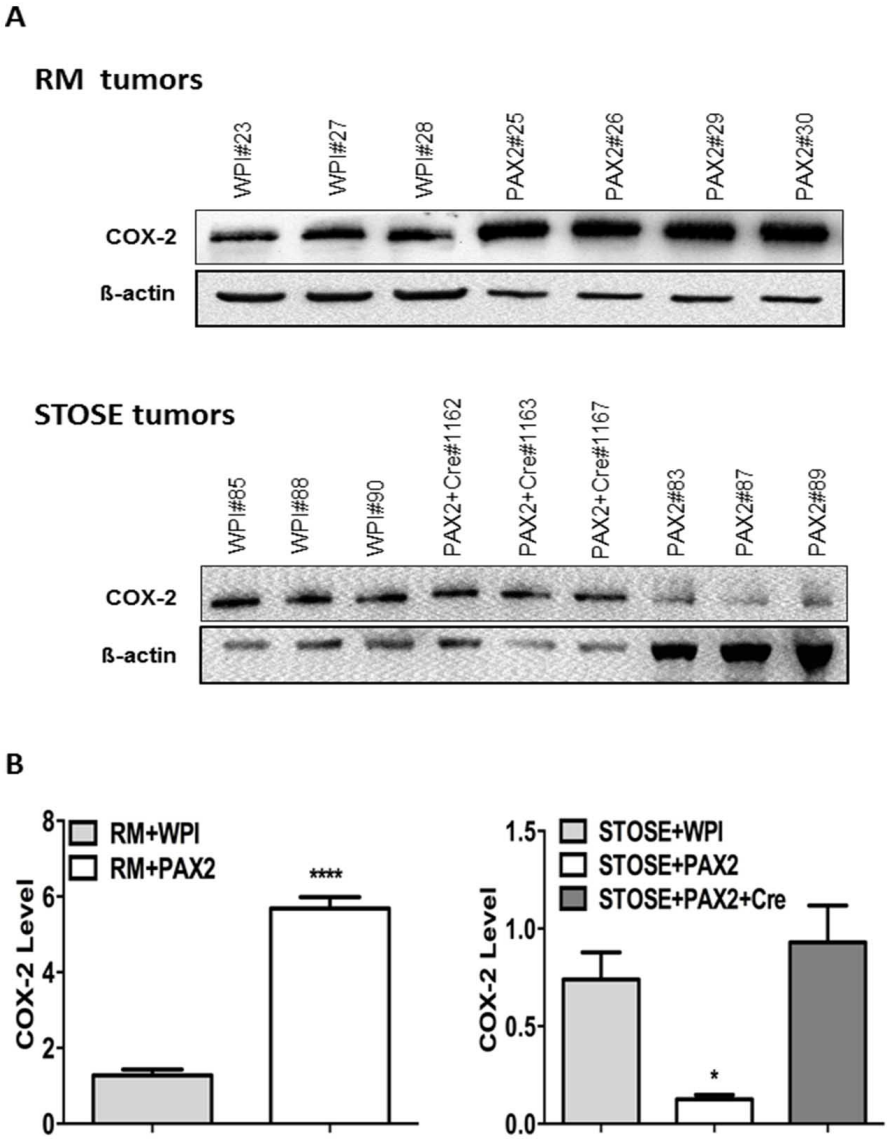

Figure 33: PAX2 regulates COX-2 differently in different tumor model systems. A: Western blot analysis showing increased COX-2 expression in RM tumors expressing PAX2 (top), whereas PAX2 tumors from STOSE cells show a reduction in COX-2 (bottom). B: Histograms represent densitometric analysis of the COX-2 levels that were normalized to β-actin. Level of COX-2 in different tumors (RM; left and STOSE; right) was analyzed using t-test for RM tumors and using one-way ANOVA for STOSE tumors. *$p<0.05$, ****$p<0.0001$.

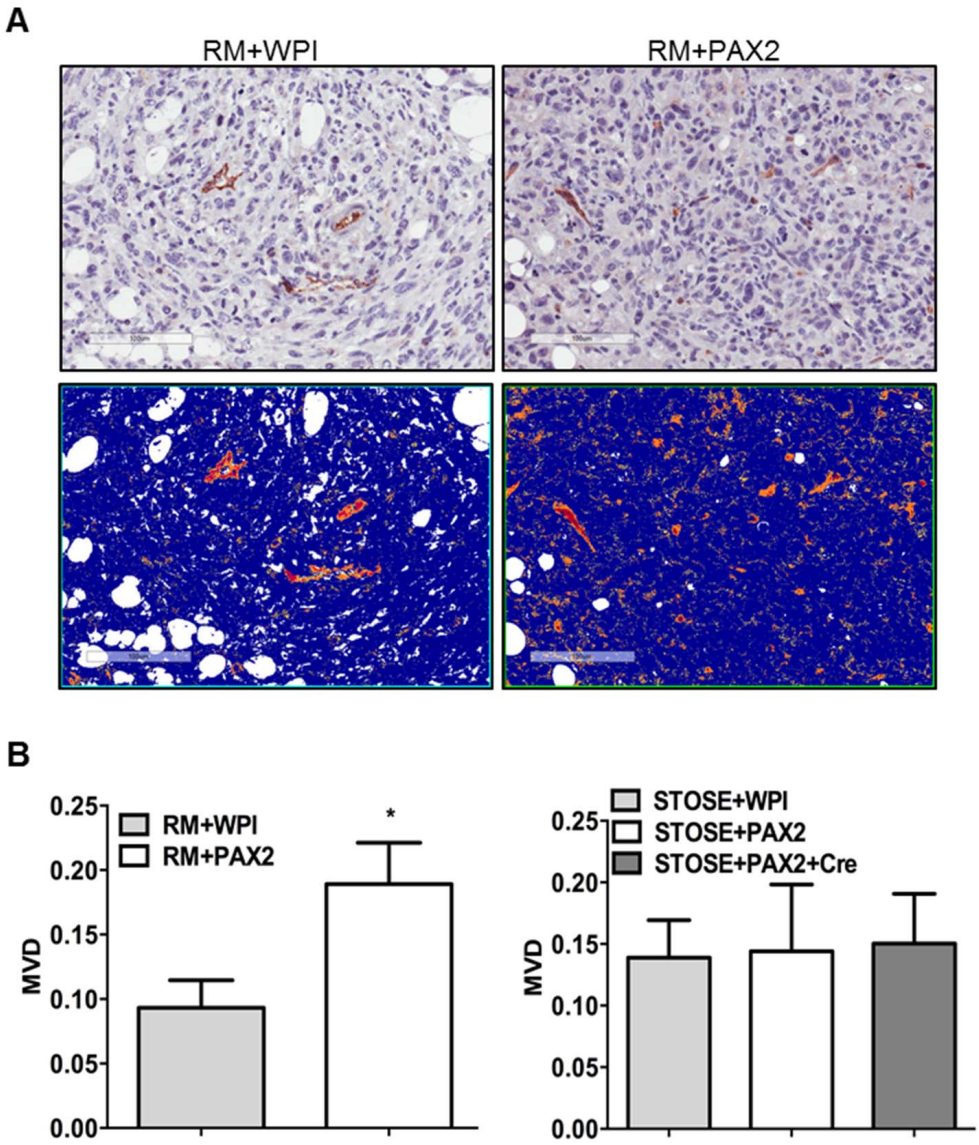

Figure 34: PAX2 enhances the microvessels density (MVD) in RM , but not STOSE tumors. A: Immunohistochemical analysis for CD31, as an indicator of MVD, in RM tumors (top sections). Sections at the bottom show positive pixel selection (red/orange) of CD31 staining performed using AperioImageScope Positive Pixel Count algorithm (scale bar is 100µm). B: Histograms represent areas of CD31 staining (positive pixels) taken from five random areas of at least 3 different tumors per group. Areas of CD31 expression in RM tumors was compared using unpaired t-test, while in STOSE tumors, one-way ANOVA was used for analysis, *$p<0.05$.

3.2 PAX2 and MET

3.2.1 PAX2 reduces cellular motility

Because PAX2 induces a more epithelial phenotype in mOSE cells, we investigated whether it might activate the MET process in these cells. One of the major phenotypic features of cells undergoing MET is reduced motility. To identify the effect of PAX2 on cellular motility of mOSE cells, wound-healing assays were performed on cells with and without PAX2. As seen in Figure 35A and B, PAX2 inhibited cell migration significantly in both normal and P53-null mOSE cells. The data indicate that cells positive for PAX2 have lower motility as compared to their controls.

These observations were strongly supported by the microarray analysis performed on the M0505 cells. The IPA showed changes in the targets of PAX2 are genes involved in cellular assembly and movement (Table 3). The analysis showed a significant decrease in cellular movement and migration as shown in Fig. 36. Therefore, PAX2 is a negative modulator for cellular motility in mOSE cells (41).

3.2.2 PAX2 targets genes involved in the process of MET in mOSE cells

As mentioned above, PAX2 induction in mOSE cells results in enhancement of a more epithelial morphology, including smaller cell diameters, and reduced cellular motility, both of which are phenotypic markers for MET transition. Therefore, we further investigated whether PAX2 activates the expected gene expression changes associated with the MET

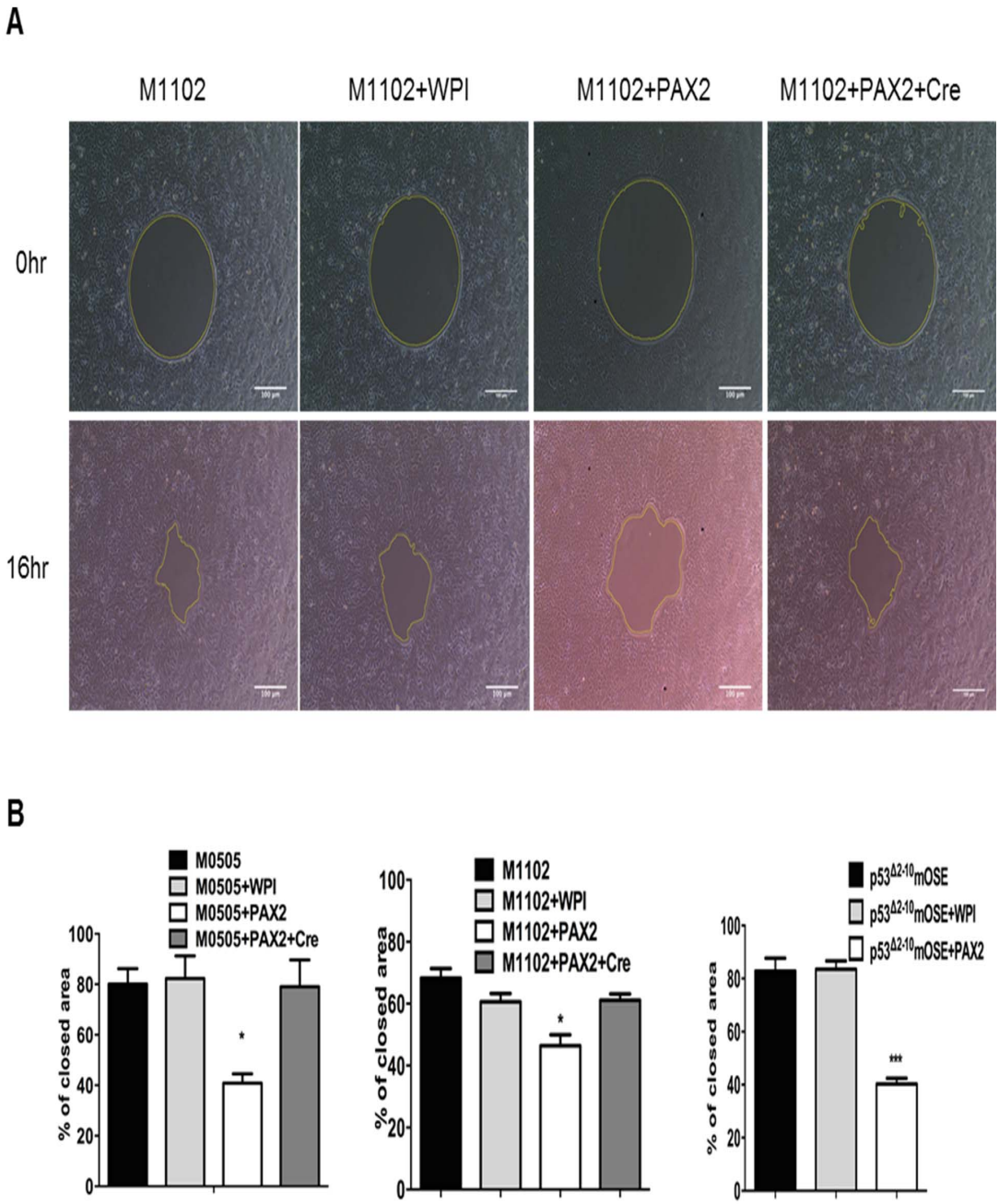

Figure 35: PAX2 induction results in a reduced cellular motility in mOSE cells (with and without P53). A: Migration Assay was performed utilizing the Radius™ 24-Well Cell Migration Assay (scale bar represents 100 μm). B: Histograms represent the percentage of area covered by cells (Image J software) for M0505 lines at 22hrs (left), M1102 lines at 16hrs (middle) and p53$\Delta^{2\text{-}10}$ mOSE lines at 16hrs (right). Statistical analysis was done using one-way ANOVA. *p<0.05, **p<0.01

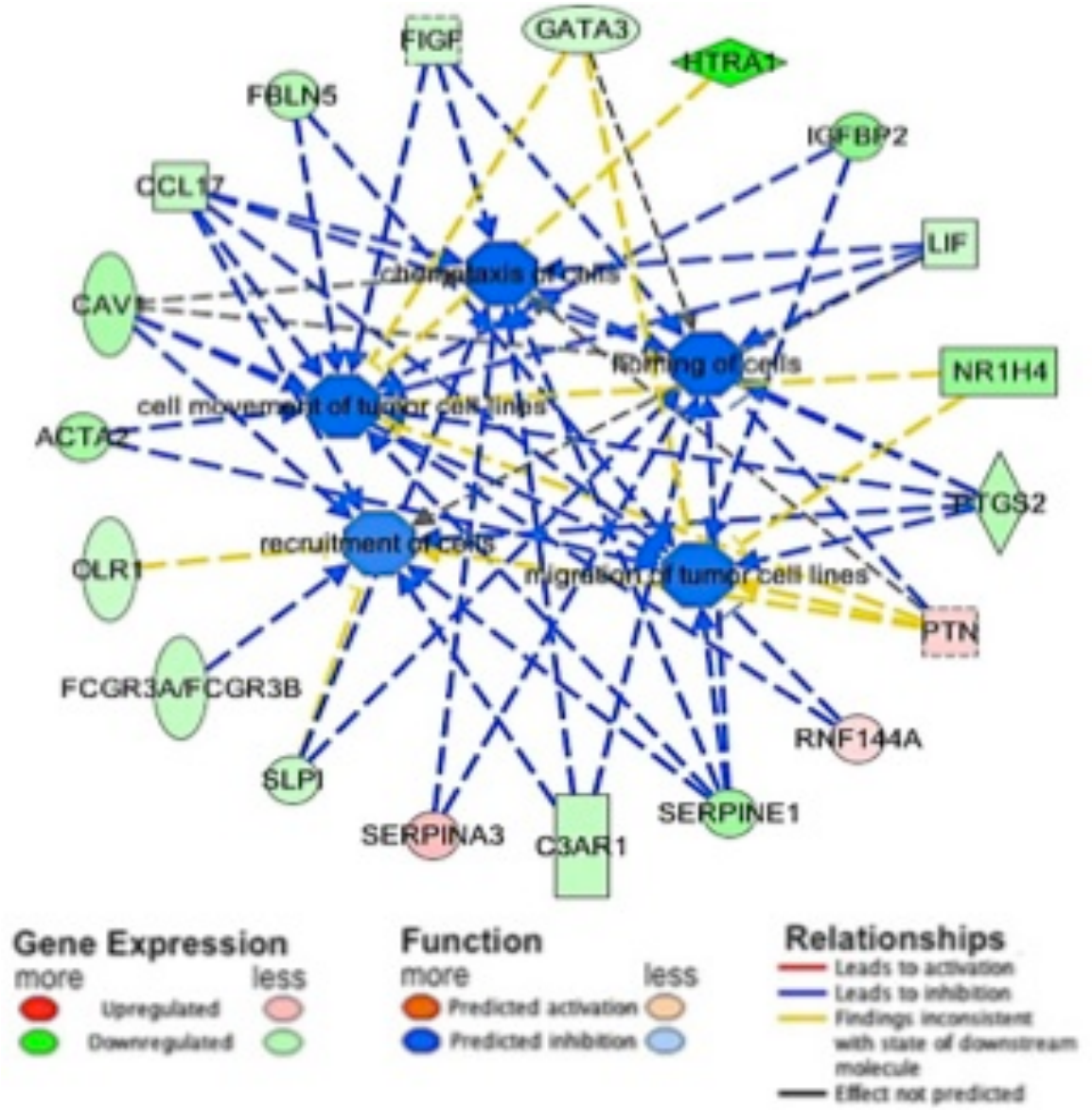

Figure 36: IPA analysis showing genes regulated by PAX2 expression that are associated with decreased cell movement and migration. Ingenuity Pathways Analysis database was used to assign genes to biological functions and determine functions that were enriched, based on statistical significance. The relationship (lines between regulators) and the node themselves (genes) are color-coded based on the predicted relationship as indicated in the legend.

program in these cells. Interestingly, none of the commonly reported markers of MET (N-cadherin, Vimentin, Snail, CK-19) was regulated by PAX2 as shown by microarray and western blot analysis (Fig. 37A). However, the microarray analysis did identify two important targets regulated by PAX2 and known to be associated with the MET program. The EMT marker, smooth muscle actin-alpha *(SMA-α)* was significantly decreased by PAX2 and was validated by immunoblot analysis (Fig. 37A). *COX-2* was another EMT marker shown to be reduced by microarray analysis. COX-2 expression was strongly reduced by PAX2 at the protein level (Fig. 37A). To determine whether this relationship between PAX2 and SMA-α and COX-2 extends to another cell type, we used oviductal epithelial cell lines, OVE-4 and OVE-16, that endogenously express PAX2. After PAX2 knockdown, using shRNA constructs (performed by another student in the lab), we hypothesized that the cells will retain less epithelial phenotype and levels of both SMA-α and COX-2 would increase. Surprisingly, reduced expression of PAX2 did not affect morphology of the cells and did not result in any changes in the levels of either protein (Fig. 37B).

3.2.3 TGF-β1-induced EMT in mOSE cells is inhibited by PAX2 induction

The data so far indicates that PAX2 induced a more epithelial phenotype in mOSE cells and markedly repressed EMT drivers such as SMA-α and COX-2. In addition, we found that when oviductal cells that normally express PAX2 were treated with the EMT-driver, TGF-β1, their PAX2 levels dropped significantly (Fig. 38A). To determine whether reduced PAX2 expression is a prerequisite for the induction of EMT by TGF-β1, we investigated whether the expression of PAX2 would inhibit the induction of EMT by TGF-β1 in mOSE cells. mOSE are known to be a poorly differentiated epithelium, which is supported by co-

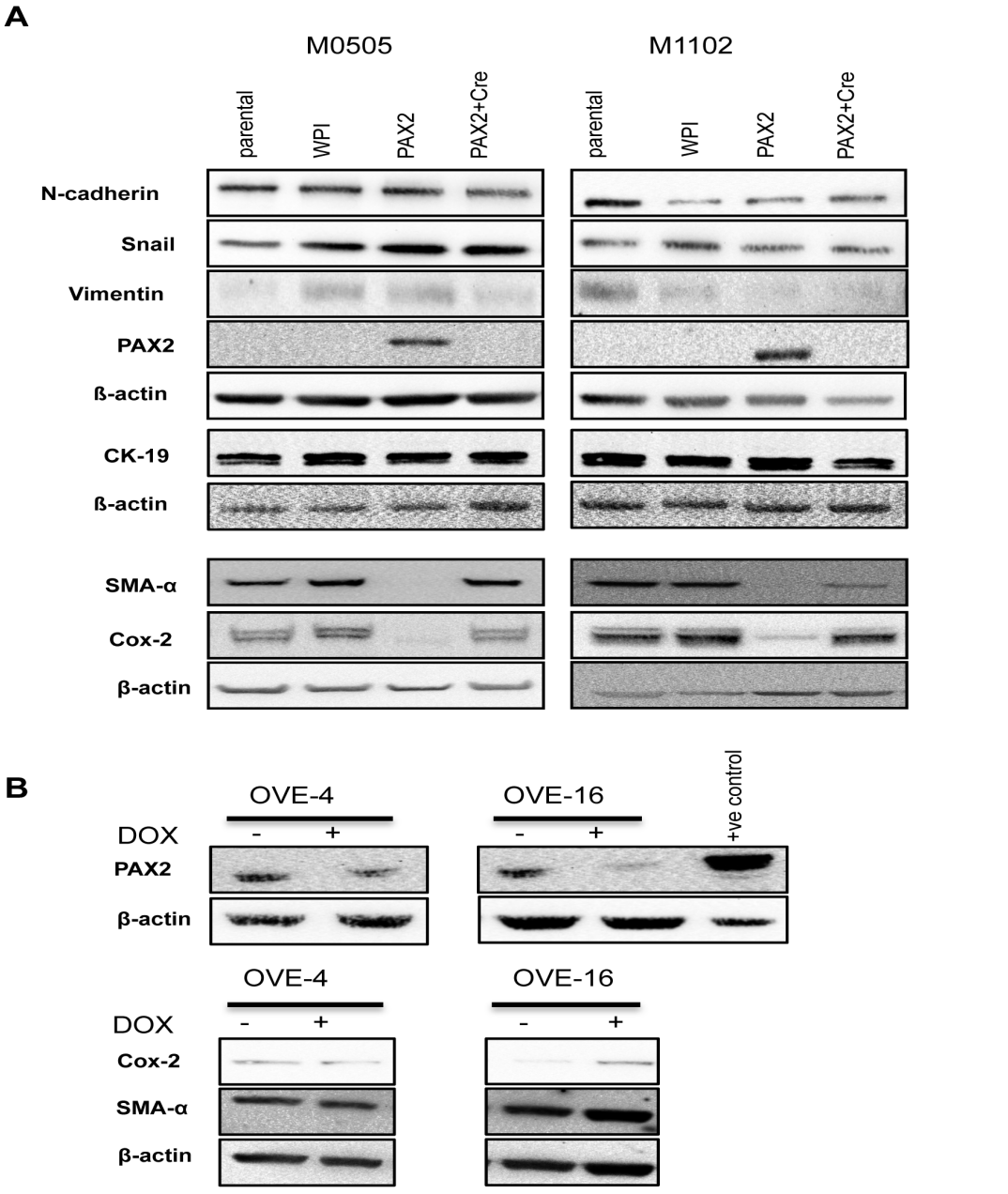

Figure 37: Modulation of markers of EMT by PAX2. A: Western blot analysis showing the expression of markers of EMT in MOSE lines M0505 and M1102. B: Doxycycline inducible knockdown of PAX2 in oviductal epithelial cell lines (OVE-4 and OVE-16) (top panel) and expression of COX-2 and SMA-α.

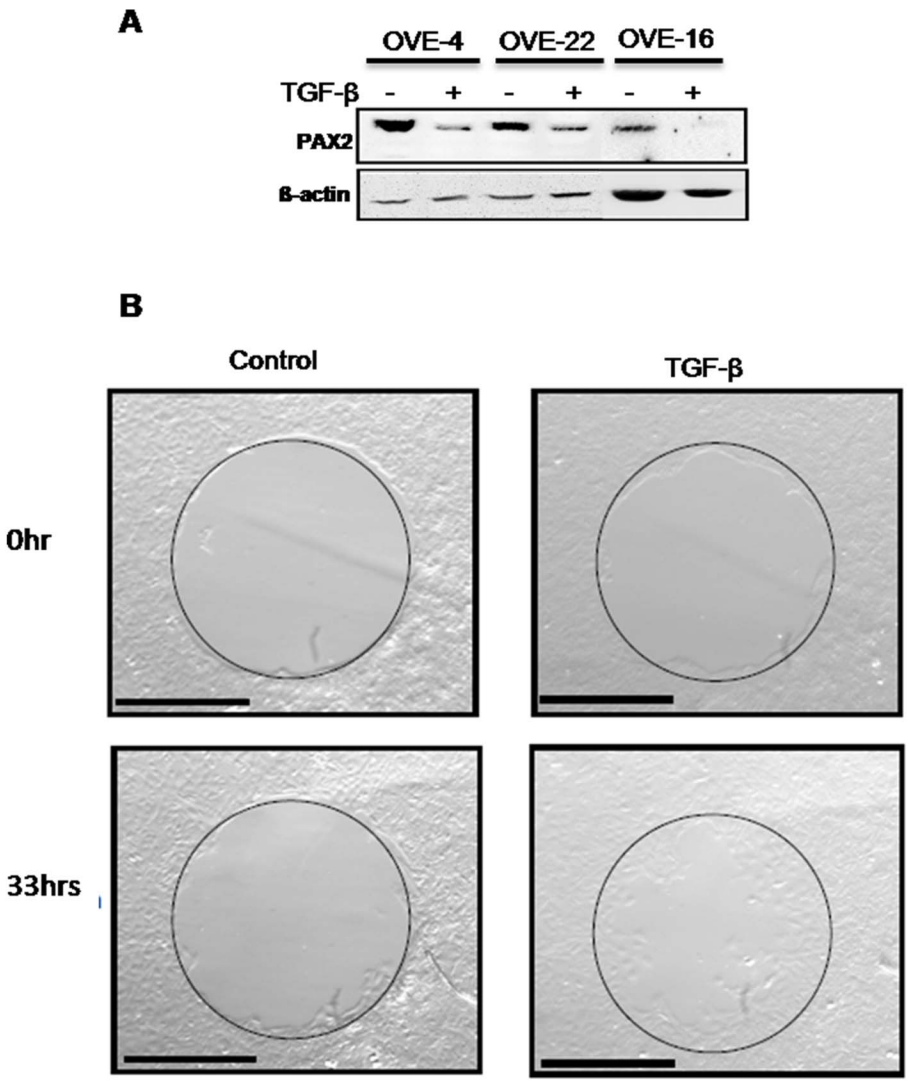

Figure 38: TGF-β induces reduced PAX2 expression in OVE cells and EMT in mOSE. A: Western blot analysis shows that treatment with TGF-β for 7 days resulted in reduced levels of PAX2 in oviductal epithelial cell lines (OVE-4, OVE-22 and OVE-16).Treatment with TGF-β induced migrationin mOSE cells (B), a phenotypic marker of EMT. Figure 38A courtesy of Kholoud Alwosaibai, while Figure 38B courtesy of Olga Colins.

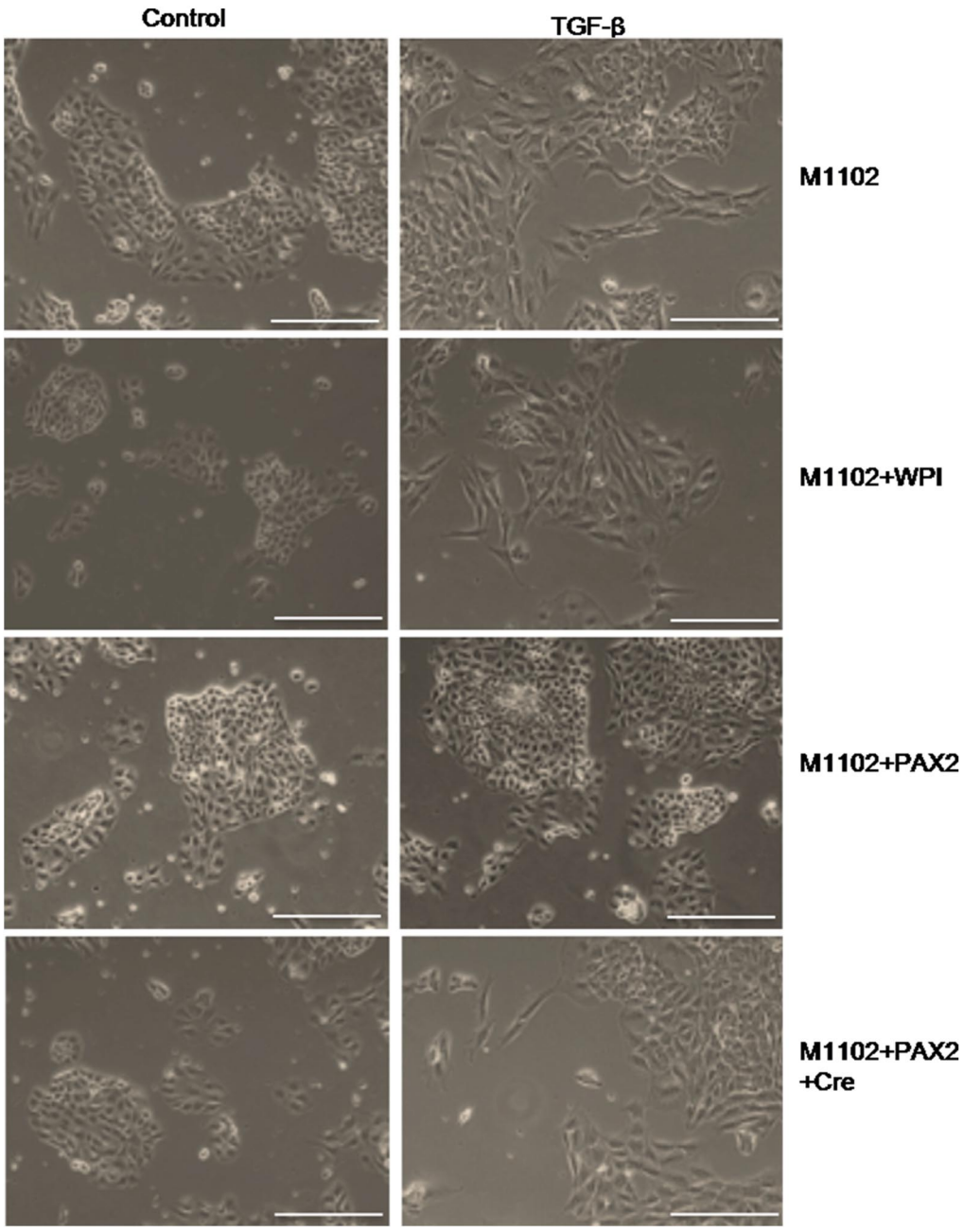

Figure 39: Treatment with TGF-β induced spindle-shape morphology, a phenotypic marker of EMT. PAX2 inhibited the TGF-β-induced EMT morphology in mOSE cell.

expression of epithelial markers (cytokeratin) and the mesenchymal proteins N-cadherin, Snail and SMA-α (as seen in Fig. 37A). When mOSE cells were treated with 10 ng/ml of TGF-β1, the cells showed higher migratory ability (Fig. 38B) and developed an elongated-spindle shape morphology (Fig. 39). However, the acquired mesenchymal morphology following TGF-β1 treatment was not evident in mOSE cells expressing PAX2 (Fig. 39).

At the molecular level, cells showed significant upregulation of Snail, Vimentin and COX-2 following treatment with TGF-β1 for 24 hrs (Fig. 40). Surprisingly, TGF-β1 resulted in significant changes in the level of SMA-α only after extended exposure for 10 days (Fig. 40B and C).The presence of PAX2 did not inhibit the TGF-β1-mediated induction of Vimentin or Snail, while it completely repressed COX-2 (Fig. 40A and D) and inhibited the induction SMA-α (Fig. 40C and E). Therefore, we intended to confirm our observations in oviductal epithelial cells. When oviductal cells were treated with TGF-β1, the levels of COX-2 and SMA-α did not change (Fig. 41A), although Vimentin and Snail were upregulated and E-cadherin was downregulated (Fig. 41B). Hence, in oviductal epithelium, TGF-β1-mediated downregulation of PAX2 and PAX2 knockdown does not seem to affect the levels of COX-2 and SMA-α, although PAX2 induction in mOSE cells results in marked reduction of both proteins.

Since COX-2 was significantly induced by TGF-β1 and completely inhibited by PAX2 in mOSE cells, we examined the regulation of COX-2 in more detail. mOSE cells were pretreated with SB-421542, an inhibitor of SMAD2 and SMAD3 phosphorylation, which are both mediators of the canonical TGF-β1 signaling pathway, and then the cells were exposed to TGF-β1. Confirmation of SMAD2 and SMAD3 inhibition is shown in Figure 42A.

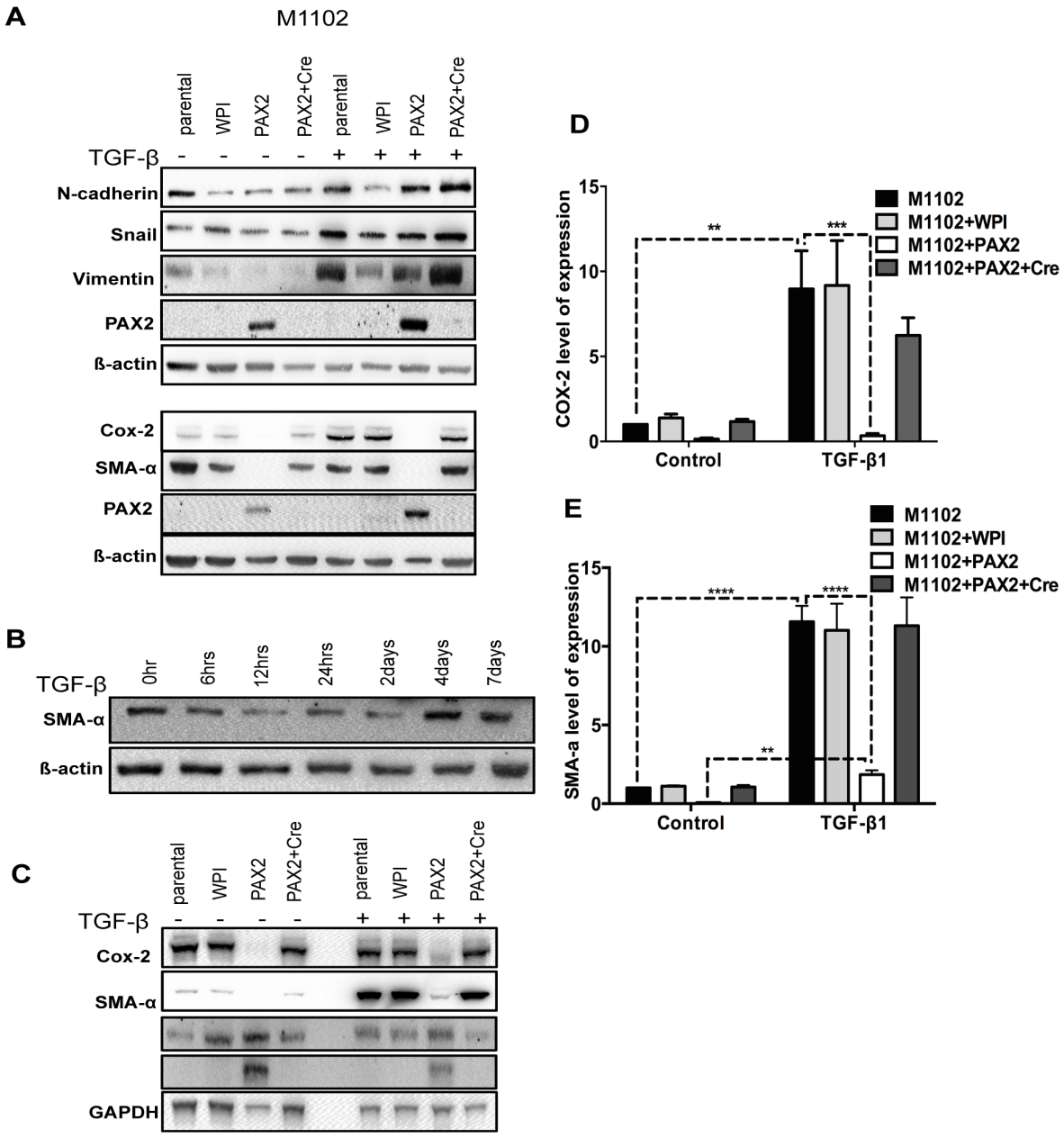

Figure 40: Effects of TGF-β on mOSE lines (with and without PAX2). A: Western blot analysis of markers of EMT before and afterTGF-β treatment in M1102 cells(with and without PAX2 expression). B and C: western blots show that TGF-β induces SMA-α expression, only after 10 days. PAX2-expression inhibits the TGF-β induction of COX-2 (D) and SMA-α (E) in M1102 as quantitated by densitometry. Bands were normalized to bands of β-actin (N=3) and stats were done using one-way ANOVA and two-way ANOVA.

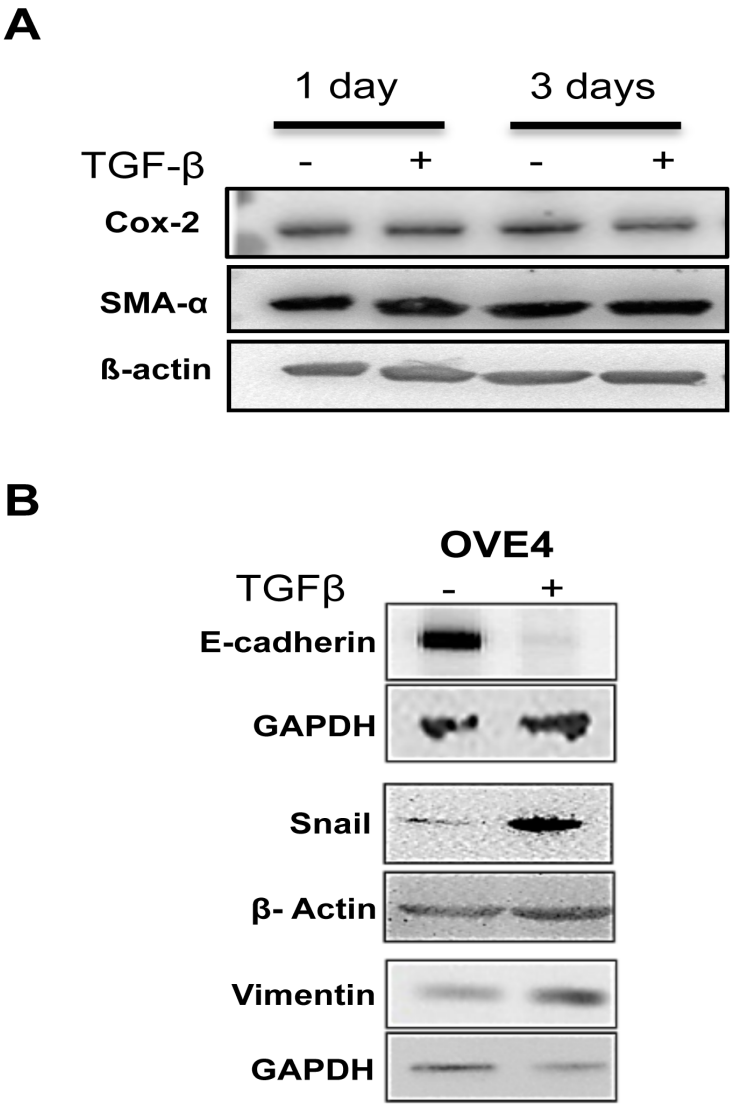

Figure 41: Expression COX-2 and SMA-α is not stimulated by TGF-β is oviductal epithelial cells, as shown by western blot analysis (A). B: Western blot analysis shows that TGF-β treatment resulted in induction of EMT shown by reduced expression of E-cadherin and enhanced expression of Snail and Vimentin in oviductal epithelium.

Stimulation of COX-2 was completely inhibited in the presence of SB-421542, as seen in Figure 42B. Therefore, it appears that TGF-β1 induces COX-2 through the upregulation of phosphorylated SMADs 2 and 3. Although PAX2 overexpression inhibited the induction of COX-2 by TGF-β1, it did not inhibit the TGFβ1-mediated phosphorylation of SMAD2 and SMAD3 (Fig. 42C). Hence, it seems that PAX2 downregulates COX-2 through pathways other than the canonical SMAD2/3 pathway, or the PAX2-COX-2 relationship could be downstream of SMAD2/3 phosphorylation. In summary, PAX2 seems sufficient to inhibit theinduction of EMT by TGF-β1, and it is also able to suppress the induction of COX-2, an important mediator of tumorigenicity.

3.2.4 Estrogen reduces PAX2 level in human ovarian cancer cell lines

Estrogen was found to induce EMT in ovarian cancer cell lines (184). In addition, it was suggested that estrogen treatment induces PAX2 expression in endometrial cancer. The presence of an ER-α-binding sequence within the *PAX2* upstream regulatory region was evident following estrogen treatment. Furthermore, data from this investigation showed that PAX2 is a key mediator of cell proliferation in response to estrogen in endometrial cancer cells (123). Considering data from our lab showing that estrogen promotes ovarian tumor growth(145)and the pro-proliferative role of PAX2 in ovarian cancer cells (104), we hypothesized that in ER-α positive ovarian cancer cell lines, estrogen induces PAX2 expression.

To determine if PAX2 is induced by estrogen, we used two different ovarian cancer cell lines that express ER-α (OVCAR-3 (185) and OVCA-432 (186). Consistent with others, we

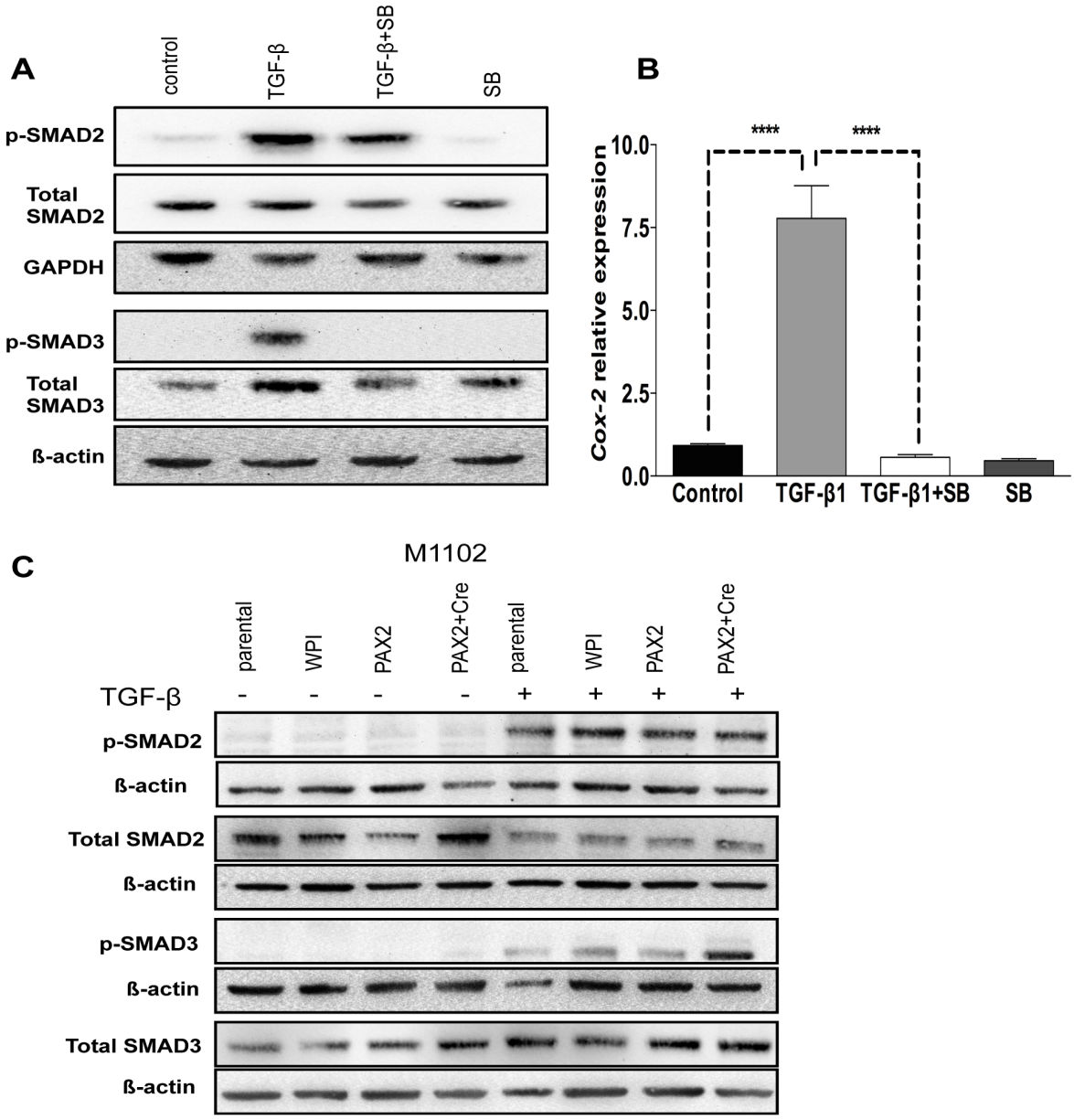

Figure 42: COX-2 stimulation by TGF-β is mediated by phosphorylation of SMAD2/3. mOSE cells were pretreated with an inhibitor of phosphorylation of SMAD2/3 (SB-421542; labeled as SB) for 30 minutes and then treated with TGF-β for 6hrs. Confirmation of the p-SMAD2/3 inhibition is shown by western blot (A). Stimulation of COX-2 was completely inhibited when phosphorylation of SMAD2/3 was inhibited as shown by Q-PCR analysis (B). (C) Western blot analysis shows that TGF-β treatment resulted in induction of phosphorylation of SMAD2/3 in mOSE cells, independent of PAX2 status.

found the two cells lines are positive for ER-α (Fig. 43A). Also, both cell lines express PAX2, as shown in Figure 43B. Cells were treated with different concentrations of estradiol and collected after 4 and 24hrs. Protein analysis shows that 4hrs of exposure to 100 nM estrogen resulted in a significant reduction of PAX2 levels in both cell lines (Fig. 43C and D). This was further confirmed by RNA analysis, as shown in Figure 44A. Expression of PAX2 returned to normal levels by 24 hours.

To more closely examine the time course of PAX2 repression by estrogen, cells were treated with 100nM of estrogen and RNA was collected at 2, 4, 8, 16 and 24hrs. As shown in Figure 44B, 4 and 8 hrs of exposure to estrogen resulted in a significant reduction of PAX2 levels in both cell lines. The data indicate that estrogen treatment results in PAX2 inhibition is both time- and dose-dependent manners in ER-α-expressing ovarian cancer cells. However, results from this experiment could have limited interpretation since the experiment was not done in estrogen-free media.

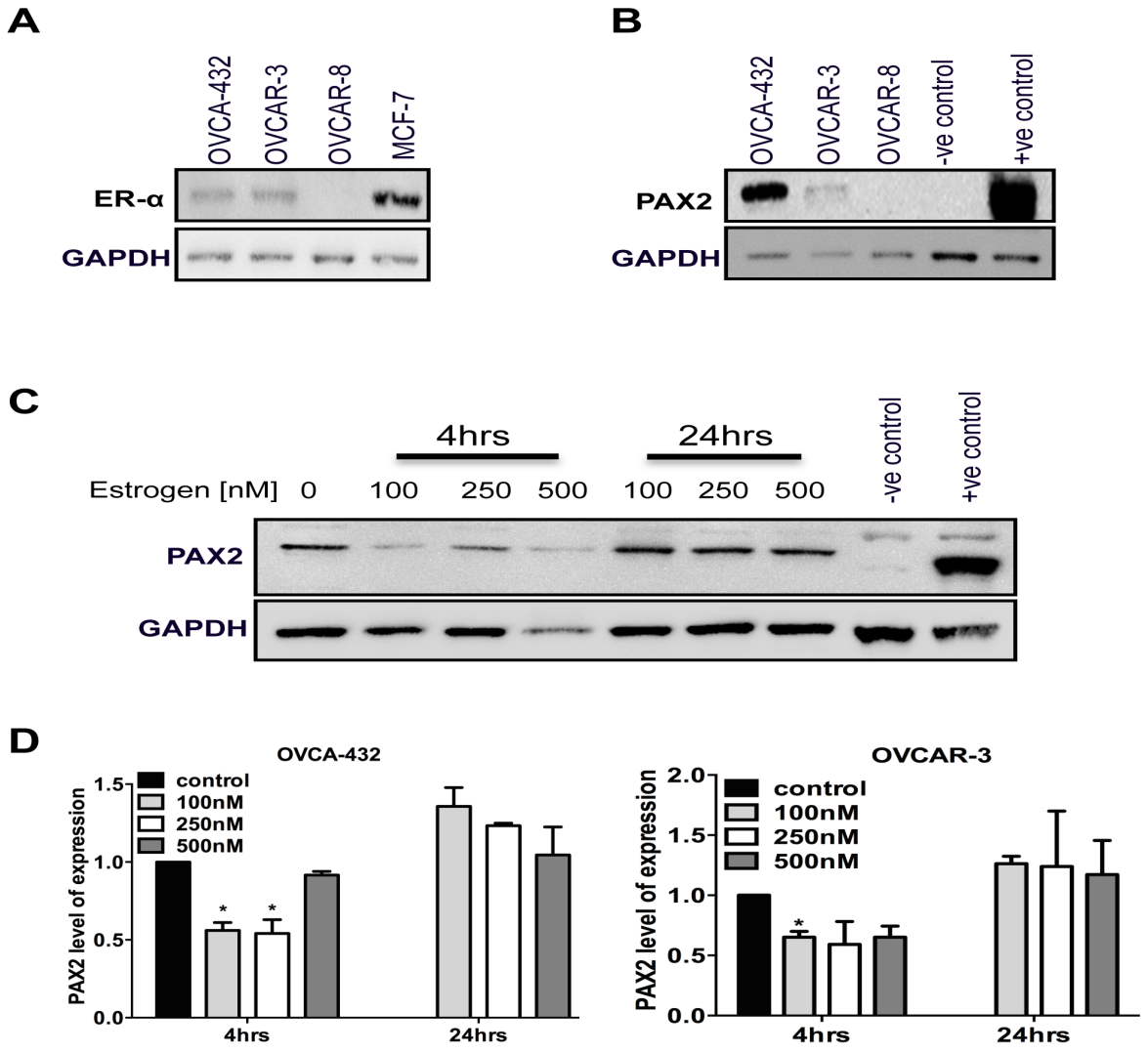

Figure 43: Estrogen treatment results in a decrease in PAX2 levels in human ovarian cancer cell lines. A: Western blot analysis showing expression of ER-α in OVCA-432 and OVCAR-3 cells. OVCAR-8 and MCF-7 are negative and positive controls for ER-α expression, respectively. B: Western blot analysis shows expression of PAX2 in OVCA-432 and OVCAR-3, but not OVCAR-8. C: Western blot analysis shows that estrogen treatment results in reduction of PAX2 levels in the OVCA-432 human ovarian cancer cell line. Cells were treated with the indicated concentrations of estradiol for the indicated period of time, while 0 indicates no treatment. D: Histograms represent densitometric analysis of PAX2 expression from western blots normalized to β-actin (N=2) in two different mOSE cell lines (OVCA-432; left and OVCAR-3; right).

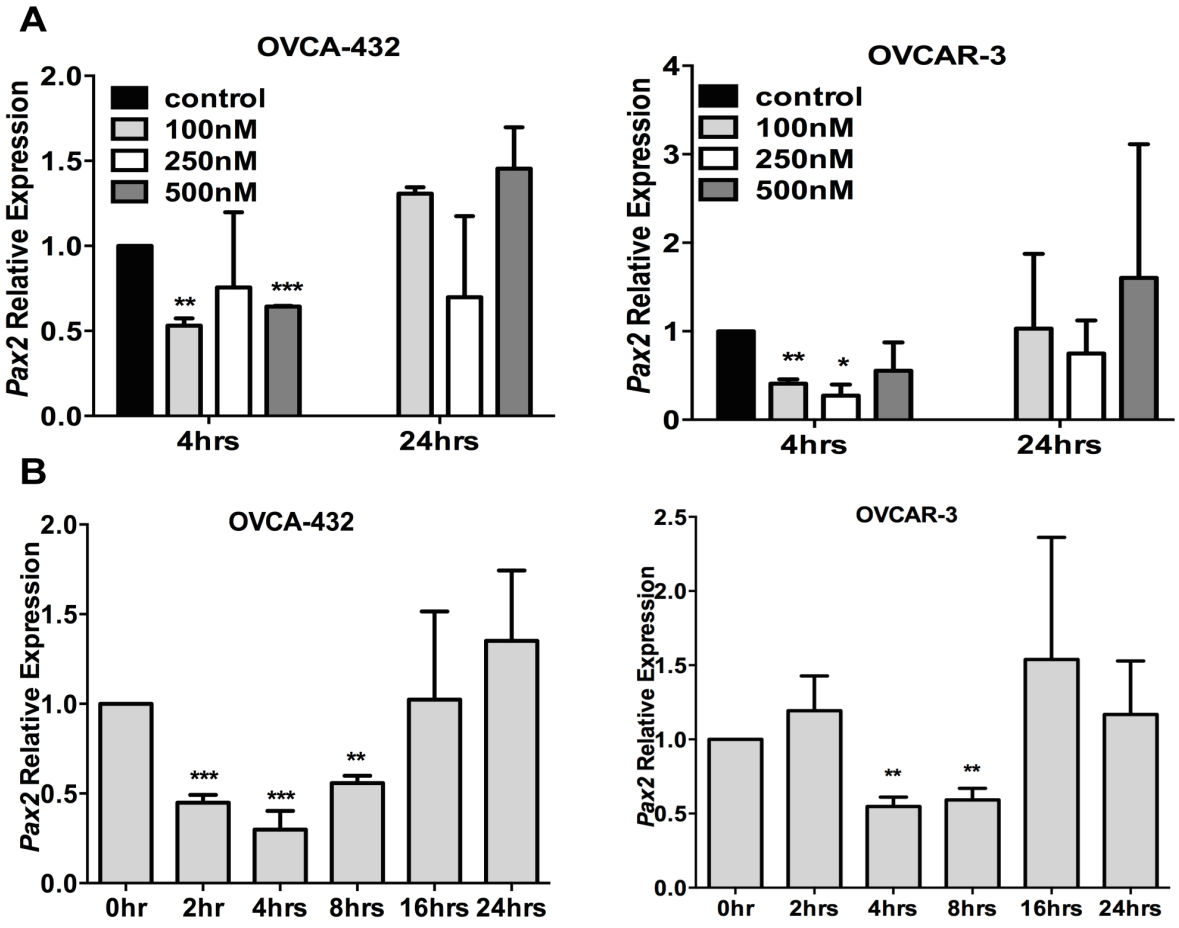

Figure 44:Q-PCR analysis shows that estrogen treatment results in a decrease in PAX2 expression in human ovarian cancer cell lines. (A: 100 nM of estrogen consistently decreased the levels of *Pax2* transcripts. B: Q-PCR analysis showing that estrogen downregulates Pax2 in time-dependent manner. *Pax2* level was normalized to PPIA (N=3) in two different human ovarian cancer cell lines (OVCA-432; left and OVCAR-3; right).

DISCUSSION

PAX2 and tumorigenicity

The overall aim of this study was to determine the roles of PAX2 in the etiology and progression of ovarian cancer, using models of normal ovarian epithelium and defined genetic models of ovarian cancer. Although PAX2 has been suggested previously to be a potential oncogene in fibroblast cells (119), its oncogenic potential has yet to be demonstrated in normal cells from which tumors arise. As a preliminary step to understanding the role of PAX2 in ovarian cancer, we expressed it in mOSE cells, which are potential precursor cells to ovarian cancer. Although PAX2 was an enhancer of cell survival and proliferation in normal and cancerous cells, it was not sufficient to induce tumorigenicity, unless combined with loss of P53. Using two murine ovarian tumor models, we showed that PAX2 can accelerate or inhibit the progression of tumors, and appears to regulate cell signaling differentially depending on tumor context.

Based on histological and molecular characteristics, recent studies have suggested that cells of the Müllerian system are the sites of origin of some high-grade serous EOC (6, 40). However, OSE or inclusion cysts that arise from OSE cells are the probable and most widely accepted origin of several subtypes of EOCs. OSE cells form a poorly differentiated epithelium that covers the surface of the ovary and arises from the same, but distinct, coelomic epithelial cells that give rise to the Müllerian system (reviewed in (3). Because the OSE is not of Müllerian duct origin, a central theme of the debate questioning OSE as the origin of EOCs is that EOCs show Müllerian-like epithelial histotypes and presumably must be derived from Müllerian precursors (5, 14). This challenging paradigm disregards the observation that, in culture, OSE cells have been shown to retain the potential to differentiate

into epithelia similar to that of the Müllerian system (24). We have also found that OSE cells in culture can spontaneously transform into cancer cells that form tumors sharing the Müllerian characteristics of high-grade serous cancers, including expression of the Müllerian marker, PAX8 (25). As importantly, *in vivo* analysis shows that OSE cells acquire Müllerian-like epithelial differentiation as a pre-requisite to their transformation, possibly explaining the variant histological subtypes observed in EOCs (12, 16, 17). Interestingly, some of the heterogeneity of EOCs has been explained by aberrant expression of *HOX* genes. *HOX* genes are regulators of Müllerian duct differentiation and are not expressed normally in OSE cells but are expressed in different EOC subtypes. When *HOX* genes are expressed in OSE-derived cancer cells, the cells undergo distinct pathways of differentiation with acquisition of Müllerian-like features(187).

In addition to *HOX* genes, *PAX* genes (notably, *PAX2* and *PAX8*) are also required for Müllerian epithelial differentiation and are expressed in a subset of EOCs (80, 92). The fact that PAX2 is not expressed in OSE cells, but is highly expressed in ciliated inclusion cysts, low-malignant potential and low-grade ovarian tumors (92) indicates that gain of PAX2 expression in OSE cells might be an early step toward their transformation. Indeed, expression of *Pax2* led to transformation of the fibroblast 280 rat cells, as evident by tumor formation after injection in mice (119). PAX2 overexpressing transgenic mice suffer cyst formation in kidneys with a higher proliferative index, but with no evidence of tumor (79).

In the current study, we showed that expression of PAX2 in normal mOSE cells induced a more differentiated epithelial phenotype. In addition, PAX2 induction in mOSE cells resulted in a significant increase in cell proliferation, even when the cells were deprived of growth factors. PAX2 also enhanced evasion of cell death when cells were exposed to cisplatin. Increased proliferation, self-sufficiency in growth signals and apoptotic evasion

can all serve as a platform for tumor formation as identified by Hanahan and Weinberg (120).

In addition to its biological effects, microarray analysis showed that PAX2 activates signaling pathways involved in cancer and reproductive diseases, as well as stimulation of cellular proliferation. All of this is consistent with PAX2 expression playing a role in early events during malignant transformation of OSE cells. Although cancer is a multi-step process (177), we considered that induction of PAX2 might be sufficient to initiate tumorigenicity given that PAX2 inhibits P53 induction, a potential second hit towards tumorigenesis. Our data indicate that PAX2 expression in normal mOSE was not sufficient to induce transformation; however, it resulted in a gain of cancer-related characteristics.

Previous studies showed that loss of *Trp53* is required to initiate ovarian tumorigenicity in mOSE with combined alterations in *K-Ras*, *Myc* and/or *Akt* (32). Because null mutations in *TP53* have been found in (24%) of ovarian cancers (141), we expressed PAX2 in P53-null mOSE cells. P53-null cells that express PAX2 showed enhanced proliferation, as compared to P53-null PAX2-non-expressing cells. In addition, a subset of animals (2/4) injected with P53-null and PAX2-expressing cells formed tumors, while there was no evidence of tumor in mice that received P53-null cells. This suggests that deletion of P53 promotes the tumorigenic potency of PAX2, even though PAX2 itself leads to a reduction of P53 expression. In agreement with others (32), we showed that deficiency of P53 is not sufficient to induce tumorigenicity but, instead, predisposes ovarian epithelial cells to transformation by another initiating event (i.e. PAX2 induction). Similarly, PAX2 expression is not sufficient to cause ovarian epithelial cell transformation, but sensitizes the cells to become tumorigenic following *Trp53* mutation (Fig. 45).

Because PAX2 induction in mOSE cells seems to be an early step toward their

transformation, we anticipated that TAg, is a positive regulator of PAX2 in our TAg-based transgenic models (33, 188). However, using mOSE cells that harbor a temperature-permissive TAg transgene, there was no induction of PAX2 following induction of TAg (see Appendix).

In cancerous cells, several *in vitro* analyses strongly support the oncogenic behavior of PAX2 as an enhancer of cell proliferation, survival and migration(104, 121, 125). In tumor-derived endothelial cells, *PAX2* expression is associated with enhanced angiogenesis, adhesion, invasion, proliferation and survival (124). In addition, silencing PAX2 in human endometroid and colon carcinoma cells resulted in decreased tumor volume in xenograft models (122, 127). Hueber et al. showed that although PAX2 knockdown did not affect the survival of animals injected with renal cancer cells, it resulted in enhanced tumor regression when accompanied with cisplatin (125). Although these different models of cancer have undoubtedly improved our knowledge of the role of PAX2 in carcinogenesis, we have no direct evidence for its contribution to ovarian tumorigenicity, especially since the available reports on the role of PAX2 in ovarian cancer are limited and conflicting. PAX2 has been shown to enhance or inhibit the growth of different human ovarian cancer cell lines (104, 110). This difference could be associated with tumor subtype and/or *TP53* status. It could be that PAX2 acts as a tumor suppressor in serous tumors that harbor *TP53* mutation, while it induces an oncogenic effect when it is expressed in clear cell, mucinous and edometroid tumors with wild type *TP53*.

To understand the role of PAX2 in ovarian tumor progression, we used two different murine cancer models reflecting low-grade and high-grade ovarian cancers. The RM model was developed by expression of mutant *K-RAS*^{G12D} and *MYC* in immortalized mOSE cells.

Activating mutations in K-RAS, or one of its downstream mediators, B-RAF, are present in two-thirds of low-grade serous ovarian carcinomas (178). Overexpression of c-MYC has been found in about 70% of ovarian cancers (179).

Due to the limited availability of human low-grade serous ovarian cancer cell lines and murine modesl (189, 190), the RM cells were considered to be a model for low-grade serous ovarian cancer due to their dependency on K-RAS mutation. Although the genetic alterations in this model resemble what is found in low-grade ovarian serous cancers, when RM cells are injected into nude mice, they form highly aggressive disease that kills mice within 3-4 weeks after engraftment. This is in contrast to the natural disease progression of low-grade ovarian cancer in women.Tumors developed from these cells show stable expression of P53, since those tumors did not have TAg (Fig. 29), induction of P53 could be explained by mutant *K-RAS* and *MYC* as mutant RAS or increased levels of c-MYC, stimulate the p19ARF–MDM2 complex formation and thereby causes a sequestration of MDM2 and subsequent stabilization of P53 (191, 192).

As summarized in Figure 45, after expressing PAX2 in RM cells, the cells became more proliferative in culture and more aggressive *in vivo*, as seen by shorter animal survival. Molecular analysis showed that PAX2 expression was associated with complete ablation of P53 expression, the loss of caspase-3 cleavage and the induction of phosphorylated AKT and ERK1/2. In addition, PAX2-expressing RM tumors showed increased microvessel density, as compared to their control. Therefore, it appears that enhanced angiogenesis and reduced apoptosis, but not increased proliferation, in the RM+PAX2 tumors may account for the accelerated tumor growth and shorter survival.

The STOSE ovarian cancer model mimics many features of human high-grade serous

ovarian carcinoma. STOSE cells are tumorigenic in both SCID and syngeneic FVB/N mice with median endpoints of 47 and 48 days, respectively. Based on immunohistochemical staining, the tumors show marker expression (cytokeratin+, WT1+, inhibin- and PAX8+) that is consistent with the human ovarian high-grade serous cancer histotype (31). It is worth mentioning that PAX8 is a regulator of Müllerian differentiation and expressed in Müllerian-derived epithelia but not OSE cells (193, 194), including the M0505 cells from which this tumor arose. In addition, since *TP53* mutation is a hallmark for high-grade ovarian serous carcinomas (10), exons 2, 5-11 of *Trp53* were sequenced; however, no mutations were detected (31).It is also worth mentioning that STOSE cells have a high degree of aneuploidy with increased expression of cyclinD1 and potential upregulation of the NF-κB pathway (31).

In both immune-deficient and -competent mice injected with STOSE cancerous cells, expression of PAX2 improved survival and reduced tumor mass, which indicates that PAX2 could be a negative regulator of some aspects of ovarian tumorigenicity. Ki67 staining showed that STSOE+PAX2 tumors are less proliferative than their controls. Furthermore, PAX2-carrying STOSE tumors were mainly restricted to the abdominal wall with limited dissemination into the peritoneal cavity, indicating a potentially less metastatic disease.

The microarray analysis identified the *Htra1*gene as the most downregulated by PAX2 in mOSE cells. *Htra1* is a putative tumor suppressor gene that is downregulated in ovarian cancers (171, 172) and enhances sensitivity to cisplatin in ovarian cancer cell lines by targeting the anti-apoptotic protein, XIAP for degradation (180). Downregulation of HTRA1 resulted in enhanced peritoneal dissemination in a xenograft study through enhancement of EGFR phosphorylation and activation of AKT and MAPK 44/42 (ERK1/2)(181).

Interestingly, we found that *Htra1* transcripts were more abundant in STOSE+PAX2 tumors, but lower in RM+PAX2 tumors, as compared to the corresponding controls. In STOSE tumors, PAX2 induction did not alter the low levels of apoptosis (as evident by cleavage of caspase-3) or phosphorylation of ERK1/2. However, expression of PAX2 in RM tumors showed an enhanced phosphorylation of AKT and a robust increase in the level ERK1/2, as compared to controls. This was likely not due to the upregulation of HTRA1 and the subsequent activation of the EGFR pathway, as EGFR was not detected in those tumors. Therefore, the activation of ERK1/2 by PAX2 is either through modulators other than HTRA1 or through an HTRA1 pathway that has not yet been identified. To our knowledge, this is the first report that identifies HTRA1 as a downstream target for PAX2.

Interestingly, we found that PAX2 expression in RM tumors downregulates PTEN expression significantly. Since PTEN isa negative regulator of the PI3K pathway (195), dwonregulation of PTEN might explain the activation of the AKT and ERK1/2 pathways.

Another novel target for PAX2 identified in this study is PTGS2 or COX-2, with asecond distinction in PAX2 function in RM vs. STOSE tumors in its ability to regulate expression of *Cox-2.* Aberrant upregulation of *COX-2* has been found in ovarian tumors and associated with chemoresistance (183). In a xenograft study, treatment with the selective COX-2 inhibitor, celecoxib, suppressed ovarian tumor growth accompanied with reduction in the tumor microvessel density and an increase in apoptotic rate (182). In the current study, PAX2 enhanced COX-2 expression in RM tumors, but reduced its expression in STOSE tumors. Therefore, we suspect that PAX2 may confer or inhibit tumor progression, at least partially, through differential regulation of COX-2, depending on the tumor context. Both the apoptotic rate and microvessel density were altered by PAX2 in RM tumors, but not STOSE

tumors. Further investigations are required to determine if PAX2 acts conclusively via COX-2. Future experiments should include an animal model where RM cells (with and without PAX2) are injected and then the animals are continuously exposed to celecoxib. This will determine if inhibition of COX-2 slows tumor progression in PAX2-expressing RM cells. Another model, where STOSE cells ectopically express both PAX2 and COX-2 and are injected into mice, would identify the effects of combination of these two potential oncogenes. In addition, it might be interesting to examine the expression profiles for PAX2, COX-2 and CD31 in human ovarian cancers, in correlation with tumor grade and overall survival for the patients from whom the tumors were taken (Fig. 45).

Interestingly, the observed changes in COX-2 expression may reflect a modulation of TGF-β1 signaling within the tumors by HTRA1, as summarized in Figure 45. COX-2 is induced by TGF-β1 [our data and (196)] and HTRA1 is a protease that has been reported to degrade TGF-β receptors, and, in turn, has an inhibitory action on TGF-β signaling (197). TGF-β1 expression in human ovarian tumors is associated with poor prognosis, suggesting a role for the tumor microenvironment in the biology of those tumors (164). Therefore, we speculate that TGF-β in the microenvironment of STOSE tumors might modulate tumor metastatic potential. In STOSE+PAX2 tumors, where *Htra1* is upregulated, the effect of TGF-β1might be decreased due to degradation of the receptors, resulting in less metastatic potential. Therefore, examining expression of TGF-β receptors in STOSE tumors is a reasonable future direction. If PAX2-carrying tumors show lower levels of the receptors, then a more rigorous experiment could be done by injecting STOSE cells (with and without PAX2) under the ovarian bursa to evaluate the metastatic potential of those tumors. Although results from the current study indicate that PAX2-carrying STOSE tumors seem to have less

metastatic potential as shown by limited dissemination, i.p. injection is not the best method to evaluate tumor metastasis (Fig. 45).

This investigation identified novel molecular targets dysregulated by PAX2 (i.e. COX-2 and HTRA1) in STOSE tumors, both of which are involved in cell proliferation (198, 199). IHC analysis shows that PAX2 inhibits proliferation of STOSE tumors. Although apoptotic induction was enhanced by PAX2 in STOSE cells, no apparent apoptosis (shown by cleavage of caspase-3) was evident in STOSE tumors. Interestingly, STOSE+PAX2 cells form fewer coloniesin soft agar than their controls, indicating a higher rate of anoikis. This may be attributed to the induction of HTRA1 as it has been shown that HTRA1 prevents metastasis by inducing anoikis (181). Thus, the induction of HTRA1 might contribute to the ability of PAX2 to suppress metastasis in STOSE tumors.

This study raises the question of how PAX2 could cause both anti- and pro-tumor functions. The anti-tumor role of PAX2 in ovarian cancer has been suggested previously by Song et al., where PAX2 has tumor suppressor function in serous and *TP53* mutant ovarian cancer cell lines (110). Compelling evidence that PAX2 might act as a tumor suppressor in well-differentiated epithelia comes from studies reporting that PAX2 is completely lost or markedly reduced in the early stages of tubal and endometrial intraepithelial carcinomas (114, 200). Furthermore, high-grade serous ovarian cancers have a low incidence of PAX2 expression (92). One could argue that, since STOSE cells form tumors resembling high-grade serous ovarian cancers, forced expression of PAX2 may allow the demonstration of its tumor suppressive function. In contrast, expression of K-RAS (as in RM cells) and PAX2 are both associated with low-grade serous cancers (92, 178), and induction of PAX2 in this model enhanced tumor aggressiveness.

In summary, it appears that PAX2 induces carcinogenic features in normal ovarian epithelial cells and it positively modulates their sensitivity to transformation. Interestingly, in ovarian cancer cells, PAX2 could confer or inhibit their aggressiveness *in vivo*. Furthermore, the molecular pathways associated with PAX2 induction in different tumor models are distinct and might be activated or repressed in a manner dependent on the molecular environment that leads to high-grade vs. low-grade serous ovarian cancers (Fig. 45).

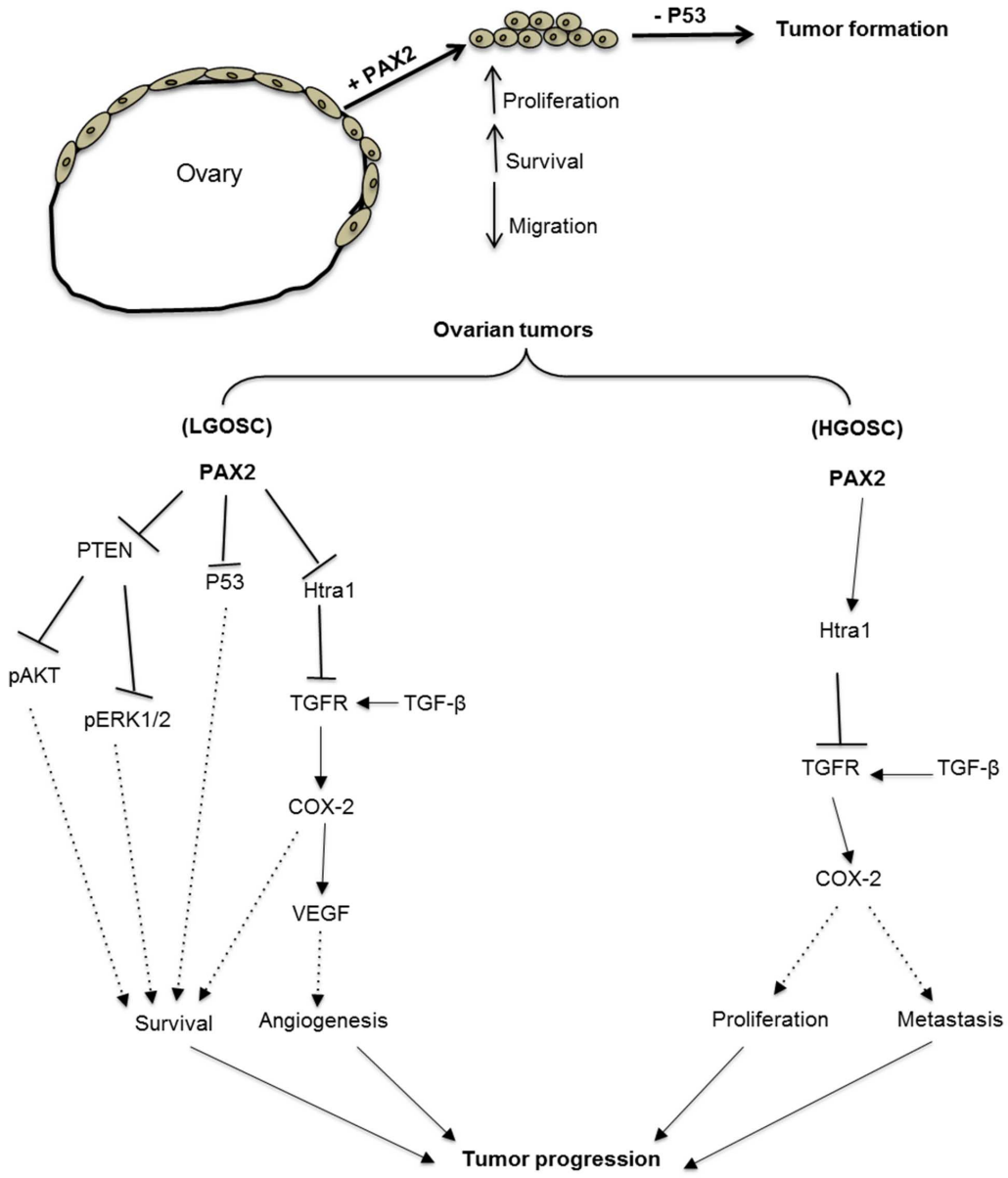

Figure 45: The proposed model for PAX2 actions in both normal and cancerous ovarian cells. PAX2 induction in normal mOSE enhances their epithelial morphology, proliferation, and survival and inhibits migration; however, it is not tumorigenic, unless combined with loss of P53. When PAX2 is induced in low-grade ovarian cancer (LGOSC) it enhances survival, through dwonregulation of PTEN, induction of pAKT and pERK1/2 and/or loss of P53, while it seems to enhance angiogenesis through COX-2 induction. On the other hand, PAX2 induction in low-grade ovarian cancer (HGOSC)ovarian carcinoma may inhibit tumor progression through less metastatic and proliferative capacity, likely via downregulation of COX-2. Dotted lines indicate the predicted effect of the indicated proteins on the biological behavior of tumor cells.

PAX2 and MET

Many publications have highlighted the multipotential nature of OSE. The uncommitted OSE cells can differentiate into mesenchymal cells to heal ovulatory-associated trauma (201, 202) and can adopt aberrant epithelial phenotypes when trapped in inclusion cysts (16, 21, 25). Our lab has shown that TGF-β1 is a component of the follicular fluid that is released during ovulation and inhibits mOSE cell proliferation (18), while enhancing EMT (unpublished data; Gamwell and Collins). The TGF-β1-mediated induction of EMT was shown by the induction of a mesenchymal morphology and enhanced motility. At the molecular level, TGF-β1 treatment resulted in enhancement of expression of the EMT proteins Snail, Vimentin and COX-2. In this context, it is interesting to note that only with prolonged (10 days) exposure to TGF-β1 did mOSE cells increase expression of SMA-α, which is a major EMT driver known to be induced by TGF-β1 (203).

Herein, we showed that PAX2 stimulates proliferation and promotes MET in mOSE cells. At the phenotypic level, PAX2-expressing mOSE cells looked more epithelial, were more attached to each other and smaller in size, and had lower motility than cells that did not express PAX2. Furthermore, PAX2 induction ablated the expression of SMA-α and COX-2 in mOSE cells. COX-2 is an enzyme induced only during inflammation (204) and its expression is induced by TGF-β1 (196). Interestingly, in well-differentiated OVE cells, knockdown of PAX2 was not sufficient to induce the expression of these two EMT markers and did not assume a less epithelial phenotype.

Since TGF-β1 and PAX2 seem to have opposite effects on mOSE cells, there might be ainverse correlation between both proteins. In agreement with others (165), results from our lab have shown that TGF-β1 inhibits PAX2 expression in oviductal epithelium (Alwosaibai;

unpublished data). Activation of TGF-β receptors results in induction of several pathways, including phosphorylation of SMAD2/3. SMAD4 then binds to the phosphorylated SMAD2/3, forming a complex that translocates into the nucleus and regulates transcription of target genes (205). Although a 0.4 kb fragment of the upstream region of *Pax2* has consensus binding sites for Smad transcription factors (206) and unpublished work from a recent PhD thesis by Gagandeep Kaur (Otago University)shows that the SMAD2/3 complex can directly bind to the promoter of PAX2 (207), Liu et al. have suggested that TGF-β1 inhibits PAX2 at the post-transcriptional level (165). It is of course possible that both mechanisms are used to regulate PAX2 levels.

The above-mentioned observations from our lab and others raised the question of whether PAX2 reverses or blocks TGF-β1 signaling in mOSE cells, at least in terms of the EMT process. Findings from this study show that, although PAX2 inhibits the mesenchymal phenotype triggered by TGF-β1, it does not inhibit the TGF-β1-mediated induction of the known EMT markers, Snail and Vimentin. However, PAX2 inhibited the strong upregulation of COX-2 and SMA- α following TGF-β1 treatment. To our knowledge, COX-2 is a novel downstream target of PAX2 (See Figure 46).

Interestingly, although TGFβ is an enhancer of invasion and metastasis in the context of more advanced carcinoma cells, it is found to bea powerful tumor suppressor in the context of pre-malignant cells (208, 209).Interruption of TGF-β signaling has been shown frequently during early steps offormation of gastrointestinal and pancreatic tumors, and this indeed, in accordance with the potential oncogenic role of PAX2 in OSE cells (208-210).

Because TGF-β1 inhibits PAX2 in oviductal cells and PAX2 inhibits the TGF-β1-mediated induction of COX-2 and SMA-α in mOSE cells, we thought that TGF-β1 might induce COX-2 and SMA-α in oviductal cells via the downregulation of PAX2. However, the

results show that neither treatment with TGF-β1 nor knockdown of PAX2 results in enhanced levels of both proteins in oviductal epithelia (Fig. 46).

OSE is subject to cyclical ovulatory ruptures (50), which creates a local inflammatory microenvironment in which TGF-β1 is produced (18, 211), and COX-2 is an inflammatory enzyme that is necessary for ovulation to occur (212). Therefore, it might be of significance to study the TGF-β1-COX-2-PAX2 relationship in greater detail. Using inhibitors of phosphorylated SMAD2/3, we found that TGF-β1 induced COX-2 through the canonical SMAD pathway. However, although PAX2 inhibited COX-2 induction by TGF-β1, phosphorylation of SMADs was not inhibited by PAX2. This indicated that PAX2 might either act downstream of phosphorylated SMADs or act through a non-canonical pathway. PAX2 could also potentially be binding directly to the *Cox-2* promoter. Although numerous PAX2 binding sites in the *Cox-2* promoter can be identified using factor binding site algorithms (213), evidence for functional PAX2 binding would need to be assessed using ChIP analysis.

Estrogen is known to be central to normal ovarian functions and plays a significant role in the etiology of ovarian, endometrial and breast carcinoma (143). Park et al. found that estrogen induces EMT in ovarian cancer cell lines (184). Herein, we showed that estrogen inhibits PAX2 in two different ovarian cancer cell lines. This indicates that estrogen may induce EMT via downregulation of PAX2 in ovarian cancer.

In summary, this work shows that in poorly differentiated ovarian epithelial cells (mOSE), PAX2 promotes epithelial morphology by suppressing COX-2 and SMA-α. In addition, PAX2-expressing mOSE cells retain their epithelial phenotype when exposed to TGF-β1 and PAX2 blocks the TGF-β-mediated induction of COX-2 and SMA-α (Fig. 32), suggesting that PAX2 is a novel inhibitor for some of TGF-β actions. These findings might

help to explain the changes that occur in early preneoplastic lesions associated with human ovarian cancer, where PAX2 appears when surface epithelial cells become trapped within inclusion cysts lined by a well-differentiated epithelium (92). Furthermore, PAX2 induces oncogenic characteristics in mOSE cells, including enhanced proliferation, survival and independence of growth signals. Therefore, this study confirms the oncogenic potential of PAX2 and indicates gain of its expression might be an early step toward OSE transformation, when another mutation (i.e. loss of P53) is present. On the other hand, once a tumor is developed, PAX2 may act as an oncogene or a tumor suppressor, depending on the tumor context. PAX2 seems to enhance tumor progression, at least in part, via inhibition of apoptosis and enhancement of angiogenesis. However, in models that mimic high-grade ovarian serous cancers, PAX2 might inhibit tumor progression through inhibition of proliferation and dissemination. Different pathways could be induced by PAX2 in different tumor contexts, and these include ERK1/2, HTRA1 and COX-2. To our knowledge, COX-2 and HTRA1 are novel targets for PAX2 that were revealed in the current study (see Fig. 46 for the proposed model).

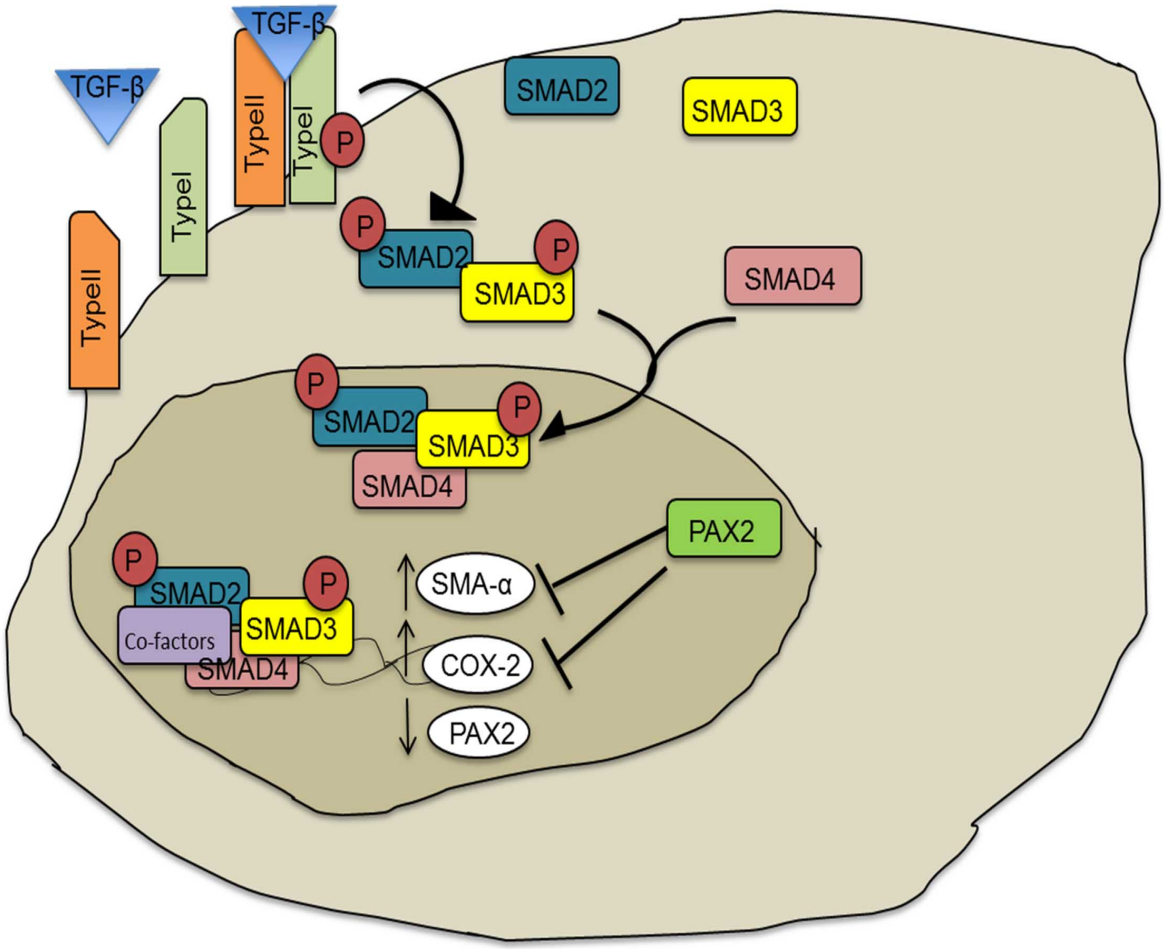

Figure 46: Schematic representation of the proposed model for PAX2 and TGF-β action in mOSE cells. Activation of TGF-β receptors following binding to the ligand (TGF-β1), results in phosphorylation of SMAD-2/3, which enhances affinity to SMAD4. The SMAD complex then translocates to the nucleus, where it activates transcription of SMA-α and COX-2 (214-216) and suppresses PAX2. In the presence of elevated levels of PAX2both SMA-α and COX-2 are inhibited. Rectangles in the schematic represent proteins, while ovals indicate transcripts.

REFERENCES

1. Vaughan, S., et al., *Rethinking ovarian cancer: recommendations for improving outcomes.* Nat Rev Cancer, 2011. **11**(10): p. 719-25.
2. Romero, I. and R.C. Bast, Jr., *Minireview: human ovarian cancer: biology, current management, and paths to personalizing therapy.* Endocrinology, 2012. **153**(4): p. 1593-602.
3. Auersperg, N., *The origin of ovarian cancers--hypotheses and controversies.* Front Biosci (Schol Ed), 2013. **5**: p. 709-19.
4. Coleman, R.L., et al., *Latest research and treatment of advanced-stage epithelial ovarian cancer.* Nat Rev Clin Oncol, 2013. **10**(4): p. 211-24.
5. Kurman, R.J. and M. Shih Ie, *The origin and pathogenesis of epithelial ovarian cancer: a proposed unifying theory.* Am J Surg Pathol, 2010. **34**(3): p. 433-43.
6. Kurman, R.J. and M. Shih Ie, *Molecular pathogenesis and extraovarian origin of epithelial ovarian cancer--shifting the paradigm.* Hum Pathol, 2011. **42**(7): p. 918-31.
7. Malpica, A., *Grading of ovarian cancer: a histotype-specific approach.* Int J Gynecol Pathol, 2008. **27**(2): p. 175-81.
8. Shih Ie, M. and R.J. Kurman, *Ovarian tumorigenesis: a proposed model based on morphological and molecular genetic analysis.* Am J Pathol, 2004. **164**(5): p. 1511-8.
9. Nik, N.N., et al., *Origin and pathogenesis of pelvic (ovarian, tubal, and primary peritoneal) serous carcinoma.* Annu Rev Pathol, 2014. **9**: p. 27-45.
10. Cancer Genome Atlas Research, N., *Integrated genomic analyses of ovarian carcinoma.* Nature, 2011. **474**(7353): p. 609-15.
11. Bell, D.A., *Origins and molecular pathology of ovarian cancer.* Mod Pathol, 2005. **18 Suppl 2**: p. S19-32.
12. Okamura, H. and H. Katabuchi, *Pathophysiological dynamics of human ovarian surface epithelial cells in epithelial ovarian carcinogenesis.* Int Rev Cytol, 2005. **242**: p. 1-54.
13. Scully, R.E., *Pathology of ovarian cancer precursors.* J Cell Biochem Suppl, 1995. **23**: p. 208-18.
14. Dubeau, L., *The cell of origin of ovarian epithelial tumors and the ovarian surface epithelium dogma: does the emperor have no clothes?* Gynecol Oncol, 1999. **72**(3): p. 437-42.
15. Landen, C.N., Jr., M.J. Birrer, and A.K. Sood, *Early events in the pathogenesis of epithelial ovarian cancer.* J Clin Oncol, 2008. **26**(6): p. 995-1005.
16. Auersperg, N., et al., *Ovarian surface epithelium: biology, endocrinology, and pathology.* Endocr Rev, 2001. **22**(2): p. 255-88.
17. Auersperg, N., *Ovarian surface epithelium as a source of ovarian cancers: unwarranted speculation or evidence-based hypothesis?* Gynecol Oncol, 2013. **130**(1): p. 246-51.
18. Gamwell, L.F., O. Collins, and B.C. Vanderhyden, *The mouse ovarian surface epithelium contains a population of LY6A (SCA-1) expressing progenitor cells that are regulated by ovulation-associated factors.* Biol Reprod, 2012. **87**(4): p. 80.

19. Szotek, P.P., et al., *Normal ovarian surface epithelial label-retaining cells exhibit stem/progenitor cell characteristics.* Proc Natl Acad Sci U S A, 2008. **105**(34): p. 12469-73.
20. Bowen, N.J., et al., *Gene expression profiling supports the hypothesis that human ovarian surface epithelia are multipotent and capable of serving as ovarian cancer initiating cells.* BMC Med Genomics, 2009. **2**: p. 71.
21. Okamoto, S., et al., *Mesenchymal to epithelial transition in the human ovarian surface epithelium focusing on inclusion cysts.* Oncol Rep, 2009. **21**(5): p. 1209-14.
22. Farghaly, S.A., *Current diagnosis and management of ovarian cysts.* Clin Exp Obstet Gynecol, 2014. **41**(6): p. 609-12.
23. Maines-Bandiera, S.L. and N. Auersperg, *Increased E-cadherin expression in ovarian surface epithelium: an early step in metaplasia and dysplasia?* Int J Gynecol Pathol, 1997. **16**(3): p. 250-5.
24. Auersperg, N., et al., *E-cadherin induces mesenchymal-to-epithelial transition in human ovarian surface epithelium.* Proc Natl Acad Sci U S A, 1999. **96**(11): p. 6249-54.
25. Pothuri, B., et al., *Genetic analysis of the early natural history of epithelial ovarian carcinoma.* PLoS One, 2010. **5**(4): p. e10358.
26. Salazar, H., et al., *Microscopic benign and invasive malignant neoplasms and a cancer-prone phenotype in prophylactic oophorectomies.* J Natl Cancer Inst, 1996. **88**(24): p. 1810-20.
27. Kobel, M., et al., *Ovarian carcinoma subtypes are different diseases: implications for biomarker studies.* PLoS Med, 2008. **5**(12): p. e232.
28. Liu, J., et al., *A genetically defined model for human ovarian cancer.* Cancer Res, 2004. **64**(5): p. 1655-63.
29. Zheng, J., et al., *Induction of papillary carcinoma in human ovarian surface epithelial cells using combined genetic elements and peritoneal microenvironment.* Cell Cycle, 2010. **9**(1): p. 140-6.
30. Sasaki, R., et al., *Oncogenic transformation of human ovarian surface epithelial cells with defined cellular oncogenes.* Carcinogenesis, 2009. **30**(3): p. 423-31.
31. McCloskey, C.W., et al., *A new spontaneously transformed syngeneic model of high-grade serous ovarian cancer with a tumor-initiating cell population.* Front Oncol, 2014. **4**: p. 53.
32. Orsulic, S., et al., *Induction of ovarian cancer by defined multiple genetic changes in a mouse model system.* Cancer Cell, 2002. **1**(1): p. 53-62.
33. Connolly, D.C., et al., *Female mice chimeric for expression of the simian virus 40 TAg under control of the MISIIR promoter develop epithelial ovarian cancer.* Cancer Res, 2003. **63**(6): p. 1389-97.
34. Przybycin, C.G., et al., *Are all pelvic (nonuterine) serous carcinomas of tubal origin?* Am J Surg Pathol, 2010. **34**(10): p. 1407-16.
35. Carcangiu, M.L., et al., *Atypical epithelial proliferation in fallopian tubes in prophylactic salpingo-oophorectomy specimens from BRCA1 and BRCA2 germline mutation carriers.* Int J Gynecol Pathol, 2004. **23**(1): p. 35-40.

36. Crum, C.P., et al., *Lessons from BRCA: the tubal fimbria emerges as an origin for pelvic serous cancer.* Clin Med Res, 2007. **5**(1): p. 35-44.
37. Kuhn, E., et al., *TP53 mutations in serous tubal intraepithelial carcinoma and concurrent pelvic high-grade serous carcinoma--evidence supporting the clonal relationship of the two lesions.* J Pathol, 2012. **226**(3): p. 421-6.
38. Karst, A.M., K. Levanon, and R. Drapkin, *Modeling high-grade serous ovarian carcinogenesis from the fallopian tube.* Proc Natl Acad Sci U S A, 2011. **108**(18): p. 7547-52.
39. Perets, R., et al., *Transformation of the fallopian tube secretory epithelium leads to high-grade serous ovarian cancer in Brca;Tp53;Pten models.* Cancer Cell, 2013. **24**(6): p. 751-65.
40. Piek, J.M., et al., *BRCA1/2-related ovarian cancers are of tubal origin: a hypothesis.* Gynecol Oncol, 2003. **90**(2): p. 491.
41. Auersperg, N., *The origin of ovarian carcinomas: a unifying hypothesis.* Int J Gynecol Pathol, 2011. **30**(1): p. 12-21.
42. Martin, D.C., *Cancer and endometriosis: do we need to be concerned?* Semin Reprod Endocrinol, 1997. **15**(3): p. 319-24.
43. Veras, E., et al., *Cystic and adenofibromatous clear cell carcinomas of the ovary: distinctive tumors that differ in their pathogenesis and behavior: a clinicopathologic analysis of 122 cases.* Am J Surg Pathol, 2009. **33**(6): p. 844-53.
44. Rosenblatt, K.A. and D.B. Thomas, *Reduced risk of ovarian cancer in women with a tubal ligation or hysterectomy. The World Health Organization Collaborative Study of Neoplasia and Steroid Contraceptives.* Cancer Epidemiol Biomarkers Prev, 1996. **5**(11): p. 933-5.
45. McLemore, M.R., et al., *Epidemiological and genetic factors associated with ovarian cancer.* Cancer Nurs, 2009. **32**(4): p. 281-8; quiz 289-90.
46. Salehi, F., et al., *Risk factors for ovarian cancer: an overview with emphasis on hormonal factors.* J Toxicol Environ Health B Crit Rev, 2008. **11**(3-4): p. 301-21.
47. Godwin, A.K., et al., *Spontaneous transformation of rat ovarian surface epithelial cells: association with cytogenetic changes and implications of repeated ovulation in the etiology of ovarian cancer.* J Natl Cancer Inst, 1992. **84**(8): p. 592-601.
48. Fathalla, M.F., *Incessant ovulation--a factor in ovarian neoplasia?* Lancet, 1971. **2**(7716): p. 163.
49. Owen, J.A., Jr., *Physiology of the menstrual cycle.* Am J Clin Nutr, 1975. **28**(4): p. 333-8.
50. Murdoch, W.J. and A.C. McDonnel, *Roles of the ovarian surface epithelium in ovulation and carcinogenesis.* Reproduction, 2002. **123**(6): p. 743-50.
51. van Niekerk, C.C., et al., *Marker profile of different phases in the transition of normal human ovarian epithelium to ovarian carcinomas.* Am J Pathol, 1991. **138**(2): p. 455-63.
52. Kodaman, P.H. and H.R. Behrman, *Endocrine-regulated and protein kinase C-dependent generation of superoxide by rat preovulatory follicles.* Endocrinology, 2001. **142**(2): p. 687-93.

53. Murdoch, W.J. and J.F. Martinchick, *Oxidative damage to DNA of ovarian surface epithelial cells affected by ovulation: carcinogenic implication and chemoprevention.* Exp Biol Med (Maywood), 2004. **229**(6): p. 546-52.

54. Gruss, P. and C. Walther, *Pax in development.* Cell, 1992. **69**(5): p. 719-22.
55. Eccles, M.R., *The role of PAX2 in normal and abnormal development of the urinary tract.* Pediatr Nephrol, 1998. **12**(9): p. 712-20.
56. Dressler, G.R. and A.S. Woolf, *Pax2 in development and renal disease.* Int J Dev Biol, 1999. **43**(5): p. 463-8.
57. Dahl, E., H. Koseki, and R. Balling, *Pax genes and organogenesis.* Bioessays, 1997. **19**(9): p. 755-65.
58. Chi, N. and J.A. Epstein, *Getting your Pax straight: Pax proteins in development and disease.* Trends Genet, 2002. **18**(1): p. 41-7.
59. Blake, J.A. and M.R. Ziman, *Pax genes: regulators of lineage specification and progenitor cell maintenance.* Development, 2014. **141**(4): p. 737-51.
60. Eccles, M.R., et al., *PAX genes in development and disease: the role of PAX2 in urogenital tract development.* Int J Dev Biol, 2002. **46**(4): p. 535-44.
61. Ward, T.A., et al., *Alternative messenger RNA forms and open reading frames within an additional conserved region of the human PAX-2 gene.* Cell Growth Differ, 1994. **5**(9): p. 1015-21.
62. Bower, M., et al., *Update of PAX2 mutations in renal coloboma syndrome and establishment of a locus-specific database.* Hum Mutat, 2012. **33**(3): p. 457-66.
63. Dressler, G.R. and E.C. Douglass, *Pax-2 is a DNA-binding protein expressed in embryonic kidney and Wilms tumor.* Proc Natl Acad Sci U S A, 1992. **89**(4): p. 1179-83.
64. Lechner, M.S. and G.R. Dressler, *Mapping of Pax-2 transcription activation domains.* J Biol Chem, 1996. **271**(35): p. 21088-93.
65. Cai, Y., et al., *Phosphorylation of Pax2 by the c-Jun N-terminal kinase and enhanced Pax2-dependent transcription activation.* J Biol Chem, 2002. **277**(2): p. 1217-22.
66. Robson, E.J., S.J. He, and M.R. Eccles, *A PANorama of PAX genes in cancer and development.* Nat Rev Cancer, 2006. **6**(1): p. 52-62.
67. Singh, J., G. Kelloff, and B. Reddy, *Modulation of alterations in p53 tumor suppressor gene and its association with activation of ras proto-oncogenes during chemoprevention of colon cancer.* Int J Oncol, 1997. **10**(3): p. 449-56.
68. Schimmenti, L.A., *Renal coloboma syndrome.* Eur J Hum Genet, 2011. **19**(12): p. 1207-12.
69. Patel, S.R., et al., *The BRCT-domain containing protein PTIP links PAX2 to a histone H3, lysine 4 methyltransferase complex.* Dev Cell, 2007. **13**(4): p. 580-92.
70. Shilatifard, A., *Molecular implementation and physiological roles for histone H3 lysine 4 (H3K4) methylation.* Curr Opin Cell Biol, 2008. **20**(3): p. 341-8.
71. Cai, Y., et al., *Groucho suppresses Pax2 transactivation by inhibition of JNK-mediated phosphorylation.* EMBO J, 2003. **22**(20): p. 5522-9.
72. Abraham, S., et al., *The Groucho-associated Phosphatase PPM1B Displaces Pax Transactivation Domain Interacting Protein (PTIP) to Switch the Transcription Factor*

Pax2 from a Transcriptional Activator to a Repressor. J Biol Chem, 2015. **290**(11): p. 7185-94.
73. Patel, S.R., et al., *Epigenetic mechanisms of Groucho/Grg/TLE mediated transcriptional repression.* Mol Cell, 2012. **45**(2): p. 185-95.
74. Torres, M., et al., *Pax-2 controls multiple steps of urogenital development.* Development, 1995. **121**(12): p. 4057-65.
75. Torres, M., E. Gomez-Pardo, and P. Gruss, *Pax2 contributes to inner ear patterning and optic nerve trajectory.* Development, 1996. **122**(11): p. 3381-91.
76. Keller, S.A., et al., *Kidney and retinal defects (Krd), a transgene-induced mutation with a deletion of mouse chromosome 19 that includes the Pax2 locus.* Genomics, 1994. **23**(2): p. 309-20.
77. Favor, J., et al., *The mouse Pax2(1Neu) mutation is identical to a human PAX2 mutation in a family with renal-coloboma syndrome and results in developmental defects of the brain, ear, eye, and kidney.* Proc Natl Acad Sci U S A, 1996. **93**(24): p. 13870-5.
78. Pfeffer, P.L., et al., *The activation and maintenance of Pax2 expression at the mid-hindbrain boundary is controlled by separate enhancers.* Development, 2002. **129**(2): p. 307-18.
79. Dressler, G.R., et al., *Deregulation of Pax-2 expression in transgenic mice generates severe kidney abnormalities.* Nature, 1993. **362**(6415): p. 65-7.
80. Mansouri, A., M. Hallonet, and P. Gruss, *Pax genes and their roles in cell differentiation and development.* Curr Opin Cell Biol, 1996. **8**(6): p. 851-7.
81. Porteous, S., et al., *Primary renal hypoplasia in humans and mice with PAX2 mutations: evidence of increased apoptosis in fetal kidneys of Pax2(1Neu) +/- mutant mice.* Hum Mol Genet, 2000. **9**(1): p. 1-11.
82. Torban, E., et al., *PAX2 suppresses apoptosis in renal collecting duct cells.* Am J Pathol, 2000. **157**(3): p. 833-42.
83. Burton, Q., et al., *The role of Pax2 in mouse inner ear development.* Dev Biol, 2004. **272**(1): p. 161-75.
84. Silberstein, G.B., G.R. Dressler, and K. Van Horn, *Expression of the PAX2 oncogene in human breast cancer and its role in progesterone-dependent mammary growth.* Oncogene, 2002. **21**(7): p. 1009-16.
85. Dziarmaga, A., et al., *Ureteric bud apoptosis and renal hypoplasia in transgenic PAX2-Bax fetal mice mimics the renal-coloboma syndrome.* J Am Soc Nephrol, 2003. **14**(11): p. 2767-74.
86. Li, H., et al., *Correlation of Pax-2 expression with cell proliferation in the developing chicken inner ear.* J Neurobiol, 2004. **60**(1): p. 61-70.
87. Bouchard, M., et al., *Nephric lineage specification by Pax2 and Pax8.* Genes Dev, 2002. **16**(22): p. 2958-70.
88. Rothenpieler, U.W. and G.R. Dressler, *Pax-2 is required for mesenchyme-to-epithelium conversion during kidney development.* Development, 1993. **119**(3): p. 711-20.
89. Soofi, A., I. Levitan, and G.R. Dressler, *Two novel EGFP insertion alleles reveal unique aspects of Pax2 function in embryonic and adult kidneys.* Dev Biol, 2012. **365**(1): p. 241-50.
90. Stoykova, A. and P. Gruss, *Roles of Pax-genes in developing and adult brain as suggested by expression patterns.* J Neurosci, 1994. **14**(3 Pt 2): p. 1395-412.

91. Chu, Y., S. Hughes, and T. Chan-Ling, *Differentiation and migration of astrocyte precursor cells and astrocytes in human fetal retina: relevance to optic nerve coloboma.* FASEB J, 2001. **15**(11): p. 2013-5.
92. Tung, C.S., et al., *PAX2 expression in low malignant potential ovarian tumors and low-grade ovarian serous carcinomas.* Mod Pathol, 2009. **22**(9): p. 1243-50.
93. Tong, G.X., et al., *Expression of PAX2 in papillary serous carcinoma of the ovary: immunohistochemical evidence of fallopian tube or secondary Mullerian system origin?* Mod Pathol, 2007. **20**(8): p. 856-63.
94. Cai, Q., et al., *Pax2 expression occurs in renal medullary epithelial cells in vivo and in cell culture, is osmoregulated, and promotes osmotic tolerance.* Proc Natl Acad Sci U S A, 2005. **102**(2): p. 503-8.
95. Chen, Q., D.J. DeGraff, and R.A. Sikes, *The developmental expression profile of PAX2 in the murine prostate.* Prostate, 2010. **70**(6): p. 654-65.
96. Cohen, T., et al., *PAX2 is reactivated in urinary tract obstruction and partially protects collecting duct cells from programmed cell death.* Am J Physiol Renal Physiol, 2007. **292**(4): p. F1267-73.
97. Li, C.G. and M.R. Eccles, *PAX Genes in Cancer; Friends or Foes?* Front Genet, 2012. **3**: p. 6.
98. Ning, G., et al., *The PAX2-null immunophenotype defines multiple lineages with common expression signatures in benign and neoplastic oviductal epithelium.* J Pathol, 2014.
99. Jiang, Y., et al., *Cell atavistic transition: Paired box 2 re-expression occurs in mature tubular epithelial cells during acute kidney injury and is regulated by Angiotensin II.* PLoS One, 2014. **9**(4): p. e93563.
100. Sanyanusin, P., et al., *Mutation of the PAX2 gene in a family with optic nerve colobomas, renal anomalies and vesicoureteral reflux.* Nat Genet, 1995. **9**(4): p. 358-64.
101. Amiel, J., et al., *PAX2 mutations in renal-coloboma syndrome: mutational hotspot and germline mosaicism.* Eur J Hum Genet, 2000. **8**(11): p. 820-6.
102. Stayner, C., et al., *Pax2 gene dosage influences cystogenesis in autosomal dominant polycystic kidney disease.* Hum Mol Genet, 2006. **15**(24): p. 3520-8.
103. Winyard, P.J., et al., *The PAX2 tanscription factor is expressed in cystic and hyperproliferative dysplastic epithelia in human kidney malformations.* J Clin Invest, 1996. **98**(2): p. 451-9.
104. Muratovska, A., et al., *Paired-Box genes are frequently expressed in cancer and often required for cancer cell survival.* Oncogene, 2003. **22**(39): p. 7989-97.
105. Khoubehi, B., et al., *Expression of the developmental and oncogenic PAX2 gene in human prostate cancer.* J Urol, 2001. **165**(6 Pt 1): p. 2115-20.
106. Buttiglieri, S., et al., *Role of Pax2 in apoptosis resistance and proinvasive phenotype of Kaposi's sarcoma cells.* J Biol Chem, 2004. **279**(6): p. 4136-43.
107. Gnarra, J.R. and G.R. Dressler, *Expression of Pax-2 in human renal cell carcinoma and growth inhibition by antisense oligonucleotides.* Cancer Res, 1995. **55**(18): p. 4092-8.
108. Daniel, L., et al., *Pax-2 expression in adult renal tumors.* Hum Pathol, 2001. **32**(3): p. 282-7.

109. Gokden, N., et al., *The utility of PAX-2 in distinguishing metastatic clear cell renal cell carcinoma from its morphologic mimics: an immunohistochemical study with comparison to renal cell carcinoma marker.* Am J Surg Pathol, 2008. **32**(10): p. 1462-7.
110. Song, H., et al., *PAX2 Expression in Ovarian Cancer.* Int J Mol Sci, 2013. **14**(3): p. 6090-105.
111. Chivukula, M., et al., *PAX 2: a novel Mullerian marker for serous papillary carcinomas to differentiate from micropapillary breast carcinoma.* Int J Gynecol Pathol, 2009. **28**(6): p. 570-8.
112. Sharma, S.G., et al., *The utility of PAX-2 and renal cell carcinoma marker immunohistochemistry in distinguishing papillary renal cell carcinoma from nonrenal cell neoplasms with papillary features.* Appl Immunohistochem Mol Morphol, 2010. **18**(6): p. 494-8.
113. Quick, C.M., et al., *PAX2-null secretory cell outgrowths in the oviduct and their relationship to pelvic serous cancer.* Mod Pathol, 2012. **25**(3): p. 449-55.
114. Roh, M.H., et al., *High-grade fimbrial-ovarian carcinomas are unified by altered p53, PTEN and PAX2 expression.* Mod Pathol, 2010. **23**(10): p. 1316-24.
115. Chen, E.Y., et al., *Secretory cell outgrowth, PAX2 and serous carcinogenesis in the Fallopian tube.* J Pathol, 2010. **222**(1): p. 110-6.
116. Ordonez, N.G., *Value of PAX2 immunostaining in tumor diagnosis: a review and update.* Adv Anat Pathol, 2012. **19**(6): p. 401-9.
117. Laury, A.R., et al., *Fallopian tube correlates of ovarian serous borderline tumors.* Am J Surg Pathol, 2011. **35**(12): p. 1759-65.
118. Mehra, K., et al., *STICS, SCOUTs and p53 signatures; a new language for pelvic serous carcinogenesis.* Front Biosci (Elite Ed), 2011. **3**: p. 625-34.
119. Maulbecker, C.C. and P. Gruss, *The oncogenic potential of Pax genes.* EMBO J, 1993. **12**(6): p. 2361-7.
120. Hanahan, D. and R.A. Weinberg, *Hallmarks of cancer: the next generation.* Cell, 2011. **144**(5): p. 646-74.
121. Gibson, W., et al., *Inhibition of PAX2 expression results in alternate cell death pathways in prostate cancer cells differing in p53 status.* Cancer Lett, 2007. **248**(2): p. 251-61.
122. Zhang, H.S., et al., *PAX2 protein induces expression of cyclin D1 through activating AP-1 protein and promotes proliferation of colon cancer cells.* J Biol Chem, 2012. **287**(53): p. 44164-72.
123. Wu, H., et al., *Hypomethylation-linked activation of PAX2 mediates tamoxifen-stimulated endometrial carcinogenesis.* Nature, 2005. **438**(7070): p. 981-7.
124. Fonsato, V., et al., *Expression of Pax2 in human renal tumor-derived endothelial cells sustains apoptosis resistance and angiogenesis.* Am J Pathol, 2006. **168**(2): p. 706-13.
125. Hueber, P.A., et al., *In vivo validation of PAX2 as a target for renal cancer therapy.* Cancer Lett, 2008. **265**(1): p. 148-55.
126. Hurtado, A., et al., *Regulation of ERBB2 by oestrogen receptor-PAX2 determines response to tamoxifen.* Nature, 2008. **456**(7222): p. 663-6.
127. Zhang, L.P., et al., *RNA interference of pax2 inhibits growth of transplanted human endometrial cancer cells in nude mice.* Chin J Cancer, 2011. **30**(6): p. 400-6.

128. Muenyi, C.S., et al., *Sodium arsenite +/- hyperthermia sensitizes p53-expressing human ovarian cancer cells to cisplatin by modulating platinum-DNA damage responses.* Toxicol Sci, 2012. **127**(1): p. 139-49.
129. Mizuarai, S., et al., *Discovery of gene expression-based pharmacodynamic biomarker for a p53 context-specific anti-tumor drug Wee1 inhibitor.* Mol Cancer, 2009. **8**: p. 34.
130. Chen, X.P., et al., *MicroRNA-370 suppresses proliferation and promotes endometrioid ovarian cancer chemosensitivity to cDDP by negatively regulating ENG.* Cancer Lett, 2014. **353**(2): p. 201-10.
131. Perego, P., et al., *Association between cisplatin resistance and mutation of p53 gene and reduced bax expression in ovarian carcinoma cell systems.* Cancer Res, 1996. **56**(3): p. 556-62.
132. Stuart, E.T., et al., *Loss of p53 function through PAX-mediated transcriptional repression.* EMBO J, 1995. **14**(22): p. 5638-45.
133. Yuan, S.S., Y.T. Yeh, and E.Y. Lee, *Pax-2 interacts with RB and reverses its repression on the promoter of Rig-1, a Robo member.* Biochem Biophys Res Commun, 2002. **296**(4): p. 1019-25.
134. Poznic, M., *Retinoblastoma protein: a central processing unit.* J Biosci, 2009. **34**(2): p. 305-12.
135. McConnell, M.J., et al., *Differential regulation of the human Wilms tumour suppressor gene (WT1) promoter by two isoforms of PAX2.* Oncogene, 1997. **14**(22): p. 2689-700.
136. Kudoh, T., et al., *G1 phase arrest induced by Wilms tumor protein WT1 is abrogated by cyclin/CDK complexes.* Proc Natl Acad Sci U S A, 1995. **92**(10): p. 4517-21.
137. Dziarmaga, A., et al., *Neuronal apoptosis inhibitory protein is expressed in developing kidney and is regulated by PAX2.* Am J Physiol Renal Physiol, 2006. **291**(4): p. F913-20.
138. Bose, S.K., et al., *PAX2 oncogene negatively regulates the expression of the host defense peptide human beta defensin-1 in prostate cancer.* Mol Immunol, 2009. **46**(6): p. 1140-8.
139. Zhou, T.B., *Signaling pathways of PAX2 and its role in renal interstitial fibrosis and glomerulosclerosis.* J Recept Signal Transduct Res, 2012. **32**(6): p. 298-303.
140. Corney, D.C., et al., *Role of p53 and Rb in ovarian cancer.* Adv Exp Med Biol, 2008. **622**: p. 99-117.
141. Sood, A.K., et al., *Distant metastases in ovarian cancer: association with p53 mutations.* Clin Cancer Res, 1999. **5**(9): p. 2485-90.
142. Saifudeen, Z., et al., *A p53-Pax2 pathway in kidney development: implications for nephrogenesis.* PLoS One, 2012. **7**(9): p. e44869.
143. Cunat, S., P. Hoffmann, and P. Pujol, *Estrogens and epithelial ovarian cancer.* Gynecol Oncol, 2004. **94**(1): p. 25-32.
144. Glud, E., et al., *Hormone therapy and the impact of estrogen intake on the risk of ovarian cancer.* Arch Intern Med, 2004. **164**(20): p. 2253-9.
145. Laviolette, L.A., et al., *17beta-estradiol upregulates GREB1 and accelerates ovarian tumor progression in vivo.* Int J Cancer, 2014. **135**(5): p. 1072-84.

146. Persson, I., *Estrogens in the causation of breast, endometrial and ovarian cancers - evidence and hypotheses from epidemiological findings.* J Steroid Biochem Mol Biol, 2000. **74**(5): p. 357-64.
147. Shang, Y., et al., *Cofactor dynamics and sufficiency in estrogen receptor-regulated transcription.* Cell, 2000. **103**(6): p. 843-52.
148. Lavoie, J.L. and C.D. Sigmund, *Minireview: overview of the renin-angiotensin system--an endocrine and paracrine system.* Endocrinology, 2003. **144**(6): p. 2179-83.
149. Suganuma, T., et al., *Functional expression of the angiotensin II type 1 receptor in human ovarian carcinoma cells and its blockade therapy resulting in suppression of tumor invasion, angiogenesis, and peritoneal dissemination.* Clin Cancer Res, 2005. **11**(7): p. 2686-94.
150. Uemura, H., et al., *Angiotensin II receptor blocker shows antiproliferative activity in prostate cancer cells: a possibility of tyrosine kinase inhibitor of growth factor.* Mol Cancer Ther, 2003. **2**(11): p. 1139-47.
151. Bose, S.K., et al., *Angiotensin II up-regulates PAX2 oncogene expression and activity in prostate cancer via the angiotensin II type I receptor.* Prostate, 2009. **69**(12): p. 1334-42.
152. Zhang, S.L., B. Moini, and J.R. Ingelfinger, *Angiotensin II increases Pax-2 expression in fetal kidney cells via the AT2 receptor.* J Am Soc Nephrol, 2004. **15**(6): p. 1452-65.
153. Psyrri, A., et al., *Effect of epidermal growth factor receptor expression level on survival in patients with epithelial ovarian cancer.* Clin Cancer Res, 2005. **11**(24 Pt 1): p. 8637-43.
154. Niikura, H., et al., *Expression of epidermal growth factor-related proteins and epidermal growth factor receptor in common epithelial ovarian tumors.* Int J Gynecol Pathol, 1997. **16**(1): p. 60-8.
155. Wakeling, A.E., et al., *ZD1839 (Iressa): an orally active inhibitor of epidermal growth factor signaling with potential for cancer therapy.* Cancer Res, 2002. **62**(20): p. 5749-54.
156. Chong, C.R. and P.A. Janne, *The quest to overcome resistance to EGFR-targeted therapies in cancer.* Nat Med, 2013. **19**(11): p. 1389-400.
157. Harris, R.C., E. Chung, and R.J. Coffey, *EGF receptor ligands.* Exp Cell Res, 2003. **284**(1): p. 2-13.
158. Shen, W., et al., *Akt and Mammalian target of rapamycin regulate separate systems of proteolysis in renal tubular cells.* J Am Soc Nephrol, 2006. **17**(9): p. 2414-23.
159. Grande, J.P., *Role of transforming growth factor-beta in tissue injury and repair.* Proc Soc Exp Biol Med, 1997. **214**(1): p. 27-40.
160. Knight, P.G. and C. Glister, *TGF-beta superfamily members and ovarian follicle development.* Reproduction, 2006. **132**(2): p. 191-206.
161. Berchuck, A., et al., *Regulation of growth of normal ovarian epithelial cells and ovarian cancer cell lines by transforming growth factor-beta.* Am J Obstet Gynecol, 1992. **166**(2): p. 676-84.
162. Wrana, J.L., *TGF-beta receptors and signalling mechanisms.* Miner Electrolyte Metab, 1998. **24**(2-3): p. 120-30.

163. Fried, G. and H. Wramsby, *Increase in transforming growth factor beta1 in ovarian follicular fluid following ovarian stimulation and in-vitro fertilization correlates to pregnancy.* Hum Reprod, 1998. **13**(3): p. 656-9.
164. Komiyama, S., et al., *Expression of TGFss1 and its receptors is associated with biological features of ovarian cancer and sensitivity to paclitaxel/carboplatin.* Oncol Rep, 2011. **25**(4): p. 1131-8.
165. Liu, S., et al., *Transforming growth factor-beta 1 regulates the expression of Pax-2, a developmental control gene, in renal tubule cells.* Exp Nephrol, 1997. **5**(4): p. 295-300.
166. Yang, S.P., et al., *Potential biological role of transforming growth factor-beta1 in human congenital kidney malformations.* Am J Pathol, 2000. **157**(5): p. 1633-47.
167. Yao, D.S., et al., *[The mouse ovarian surface epithelium cells (MOSE) transformation induced by c-myc/K-ras in].* Zhonghua Zhong Liu Za Zhi, 2006. **28**(12): p. 881-5.
168. Yoshihara, K., et al., *Gene expression profiling of advanced-stage serous ovarian cancers distinguishes novel subclasses and implicates ZEB2 in tumor progression and prognosis.* Cancer Sci, 2009. **100**(8): p. 1421-8.
169. Sellar, G.C., et al., *OPCML at 11q25 is epigenetically inactivated and has tumor-suppressor function in epithelial ovarian cancer.* Nat Genet, 2003. **34**(3): p. 337-43.
170. Toler, C.R., D.D. Taylor, and C. Gercel-Taylor, *Loss of communication in ovarian cancer.* Am J Obstet Gynecol, 2006. **194**(5): p. e27-31.
171. Chien, J., et al., *A candidate tumor suppressor HtrA1 is downregulated in ovarian cancer.* Oncogene, 2004. **23**(8): p. 1636-44.
172. Narkiewicz, J., et al., *Changes in mRNA and protein levels of human HtrA1, HtrA2 and HtrA3 in ovarian cancer.* Clin Biochem, 2008. **41**(7-8): p. 561-9.
173. Lancaster, J.M., et al., *High expression of insulin-like growth factor binding protein-2 messenger RNA in epithelial ovarian cancers produces elevated preoperative serum levels.* Int J Gynecol Cancer, 2006. **16**(4): p. 1529-35.
174. Cody, N.A., et al., *Characterization of the 3p12.3-pcen region associated with tumor suppression in a novel ovarian cancer cell line model genetically modified by chromosome 3 fragment transfer.* Mol Carcinog, 2009. **48**(12): p. 1077-92.
175. Koensgen, D., et al., *Overexpression of the plasminogen activator inhibitor type-1 in epithelial ovarian cancer.* Anticancer Res, 2006. **26**(2C): p. 1683-9.
176. Yan, X., et al., *Increased expression of annexin A3 is a mechanism of platinum resistance in ovarian cancer.* Cancer Res, 2010. **70**(4): p. 1616-24.
177. Knudson, A.G., Jr., *Mutation and cancer: statistical study of retinoblastoma.* Proc Natl Acad Sci U S A, 1971. **68**(4): p. 820-3.
178. Singer, G., et al., *Mutations in BRAF and KRAS characterize the development of low-grade ovarian serous carcinoma.* J Natl Cancer Inst, 2003. **95**(6): p. 484-6.
179. Chen, C.H., et al., *Overexpression of cyclin D1 and c-Myc gene products in human primary epithelial ovarian cancer.* Int J Gynecol Cancer, 2005. **15**(5): p. 878-83.
180. He, X., et al., *HtrA1 sensitizes ovarian cancer cells to cisplatin-induced cytotoxicity by targeting XIAP for degradation.* Int J Cancer, 2012. **130**(5): p. 1029-35.
181. He, X., et al., *Downregulation of HtrA1 promotes resistance to anoikis and peritoneal dissemination of ovarian cancer cells.* Cancer Res, 2010. **70**(8): p. 3109-18.

182. Li, W., et al., *Effects of combining Taxol and cyclooxygenase inhibitors on the angiogenesis and apoptosis in human ovarian cancer xenografts.* Oncol Lett, 2013. **5**(3): p. 923-928.
183. Ferrandina, G., et al., *Increased cyclooxygenase-2 (COX-2) expression is associated with chemotherapy resistance and outcome in ovarian cancer patients.* Ann Oncol, 2002. **13**(8): p. 1205-11.
184. Park, S.H., et al., *Estrogen regulates Snail and Slug in the down-regulation of E-cadherin and induces metastatic potential of ovarian cancer cells through estrogen receptor alpha.* Mol Endocrinol, 2008. **22**(9): p. 2085-98.
185. Brasseur, K., et al., *ERalpha-targeted therapy in ovarian cancer cells by a novel estradiol-platinum(II) hybrid.* Endocrinology, 2013. **154**(7): p. 2281-95.
186. Lau, K.M., S.C. Mok, and S.M. Ho, *Expression of human estrogen receptor-alpha and -beta, progesterone receptor, and androgen receptor mRNA in normal and malignant ovarian epithelial cells.* Proc Natl Acad Sci U S A, 1999. **96**(10): p. 5722-7.
187. Cheng, W., et al., *Lineage infidelity of epithelial ovarian cancers is controlled by HOX genes that specify regional identity in the reproductive tract.* Nat Med, 2005. **11**(5): p. 531-7.
188. Garson, K., et al., *Generation of tumors in transgenic mice expressing the SV40 T antigen under the control of ovarian-specific promoter 1.* J Soc Gynecol Investig, 2003. **10**(4): p. 244-50.
189. Anglesio, M.S., et al., *Correction: Type-Specific Cell Line Models for Type-Specific Ovarian Cancer Research.* PLoS One, 2013. **8**(9).
190. Fan, H.Y., et al., *Cell type-specific targeted mutations of Kras and Pten document proliferation arrest in granulosa cells versus oncogenic insult to ovarian surface epithelial cells.* Cancer Res, 2009. **69**(16): p. 6463-72.
191. Lowe, S.W., *Activation of p53 by oncogenes.* Endocr Relat Cancer, 1999. **6**(1): p. 45-8.
192. Zindy, F., et al., *Myc signaling via the ARF tumor suppressor regulates p53-dependent apoptosis and immortalization.* Genes Dev, 1998. **12**(15): p. 2424-33.
193. Kobayashi, A. and R.R. Behringer, *Developmental genetics of the female reproductive tract in mammals.* Nat Rev Genet, 2003. **4**(12): p. 969-80.
194. Ozcan, A., et al., *PAX 8 expression in non-neoplastic tissues, primary tumors, and metastatic tumors: a comprehensive immunohistochemical study.* Mod Pathol, 2011. **24**(6): p. 751-64.
195. Carracedo, A. and P.P. Pandolfi, *The PTEN-PI3K pathway: of feedbacks and cross-talks.* Oncogene, 2008. **27**(41): p. 5527-41.
196. Shao, J., et al., *Coordinate regulation of cyclooxygenase-2 and TGF-beta1 in replication error-positive colon cancer and azoxymethane-induced rat colonic tumors.* Carcinogenesis, 1999. **20**(2): p. 185-91.
197. Graham, J.R., et al., *Serine protease HTRA1 antagonizes transforming growth factor-beta signaling by cleaving its receptors and loss of HTRA1 in vivo enhances bone formation.* PLoS One, 2013. **8**(9): p. e74094.
198. Xia, J., et al., *Elevated serine protease HtrA1 inhibits cell proliferation, reduces invasion, and induces apoptosis in esophageal squamous cell carcinoma by blocking the nuclear factor-kappaB signaling pathway.* Tumour Biol, 2013. **34**(1): p. 317-28.

199. Wang, R., et al., *shRNA-targeted cyclooxygenase (COX)-2 inhibits proliferation, reduces invasion and enhances chemosensitivity in laryngeal carcinoma cells.* Mol Cell Biochem, 2008. **317**(1-2): p. 179-88.
200. Monte, N.M., et al., *Joint loss of PAX2 and PTEN expression in endometrial precancers and cancer.* Cancer Res, 2010. **70**(15): p. 6225-32.
201. Ahmed, N., E.W. Thompson, and M.A. Quinn, *Epithelial-mesenchymal interconversions in normal ovarian surface epithelium and ovarian carcinomas: an exception to the norm.* J Cell Physiol, 2007. **213**(3): p. 581-8.
202. Salamanca, C.M., et al., *Effects of epidermal growth factor/hydrocortisone on the growth and differentiation of human ovarian surface epithelium.* J Soc Gynecol Investig, 2004. **11**(4): p. 241-51.
203. Desmouliere, A., et al., *Transforming growth factor-beta 1 induces alpha-smooth muscle actin expression in granulation tissue myofibroblasts and in quiescent and growing cultured fibroblasts.* J Cell Biol, 1993. **122**(1): p. 103-11.
204. Hales, D.B., et al., *Cyclooxygenases expression and distribution in the normal ovary and their role in ovarian cancer in the domestic hen (Gallus domesticus).* Endocrine, 2008. **33**(3): p. 235-44.
205. Derynck, R. and Y.E. Zhang, *Smad-dependent and Smad-independent pathways in TGF-beta family signalling.* Nature, 2003. **425**(6958): p. 577-84.
206. Kuschert, S., et al., *Characterization of Pax-2 regulatory sequences that direct transgene expression in the Wolffian duct and its derivatives.* Dev Biol, 2001. **229**(1): p. 128-40.
207. Kaur, G. *Regulation of human PAX2 in cancer cells by Transforming Growth Factor-beta (TGF-β)*
. 2012; Available from: http://otago.ourarchive.ac.nz/handle/10523/2428.
208. Heldin, C.H., M. Landstrom, and A. Moustakas, *Mechanism of TGF-beta signaling to growth arrest, apoptosis, and epithelial-mesenchymal transition.* Curr Opin Cell Biol, 2009. **21**(2): p. 166-76.
209. Levy, L. and C.S. Hill, *Alterations in components of the TGF-beta superfamily signaling pathways in human cancer.* Cytokine Growth Factor Rev, 2006. **17**(1-2): p. 41-58.
210. Guasch, G., et al., *Loss of TGFbeta signaling destabilizes homeostasis and promotes squamous cell carcinomas in stratified epithelia.* Cancer Cell, 2007. **12**(4): p. 313-27.
211. Richards, J.S., et al., *Ovulation: new dimensions and new regulators of the inflammatory-like response.* Annu Rev Physiol, 2002. **64**: p. 69-92.
212. Lim, H., et al., *Multiple female reproductive failures in cyclooxygenase 2-deficient mice.* Cell, 1997. **91**(2): p. 197-208.
213. Mathelier, A., et al., *JASPAR 2014: an extensively expanded and updated open-access database of transcription factor binding profiles.* Nucleic Acids Res, 2014. **42**(Database issue): p. D142-7.
214. Hu, B., et al., *Gut-enriched Kruppel-like factor interaction with Smad3 inhibits myofibroblast differentiation.* Am J Respir Cell Mol Biol, 2007. **36**(1): p. 78-84.
215. Hu, B., Z. Wu, and S.H. Phan, *Smad3 mediates transforming growth factor-beta-induced alpha-smooth muscle actin expression.* Am J Respir Cell Mol Biol, 2003. **29**(3 Pt 1): p. 397-404.

216. Matsumura, T., et al., *Regulation of transforming growth factor-beta-dependent cyclooxygenase-2 expression in fibroblasts.* J Biol Chem, 2009. **284**(51): p. 35861-71.

APPENDIX

T-antigen (TAg) does not induce PAX2 in mOSE cells

Our data indicate that TGF-ß1 and estrogen both downregulate PAX2 in normal oviductal and ovarian cancer cells, respectively. In search for factors that may regulate PAX2 expression and taking in consideration PAX2 seems to be one of the earlier events toward ovarian transformation, we anticipated that TAg, is a positive regulator of PAX2 in our TAg based transgenic models. To test our hypothesis, we used mOSE cells obtained from Immortomice, which harbor a temperature-permissive TAg transgene. Following TAg-induction (Fig. 34), protein extracts were PAX2-immunoperecipated and then immunblotted for PAX2 expression. As seen in Figure 34, TAg did not induce PAX2 expression in mOSE cells. Taken together, we identified two factors (TGF-ß1 and estrogen) that regulate PAX2 expression and we omitted TAg as a potential regulator for PAX2 expression.

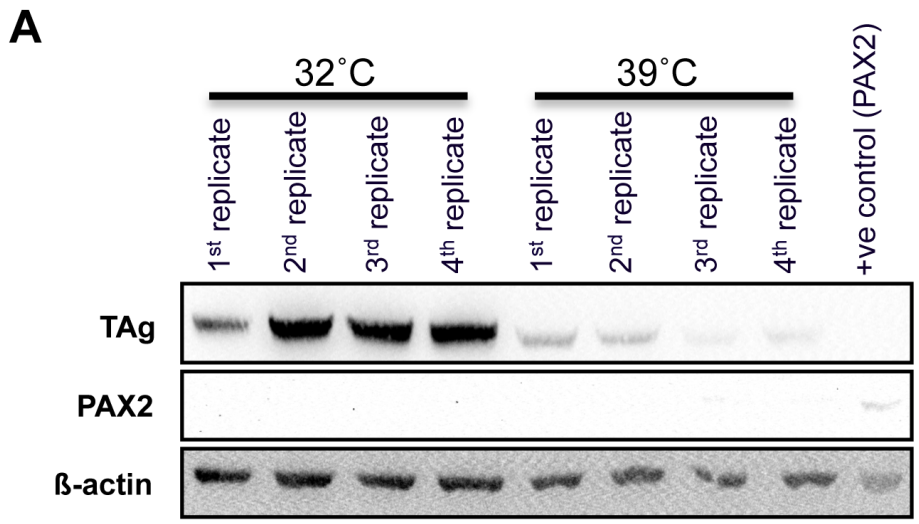

Figure 47:T-antigen does not induce PAX2 in mOSE cells. Western blot analysis shows induction of SV40 T-antigen (TAg) in mOSE cells derived from Immortomice, which harbor a temperature-permissive (32˚C) TAg transgene. Proteins were extracted from cells incubated at the permissive temperature or incubated at the non-permissive temperature (39˚C).